Assessing the Carbon Dynamics in Natural and Human-Perturbed Boreal Aquatic Systems

Alexandre Ouellet

A Thesis

in the Department

of

Chemistry and Biochemistry

Presented in Partial Fulfillment of the Requirements
For the Degree of Doctor of Philosophy at
Concordia University
Montreal, Quebec, Canada

July 2010

Your file Votre référence
ISBN: 978-0-494-71129-3
Our file Notre référence
ISBN: 978-0-494-71129-3

Abstract

Assessing the Carbon Dynamics in Natural and Human-Perturbed Boreal Aquatic Systems

Alexandre Ouellet, Ph.D.
Concordia University, 2010

Most lakes and reservoirs worldwide are supersaturated with respect to water concentrations of carbon dioxide (CO_2) and methane (CH_4), two potent greenhouse gases (GHG). Although surface water GHG concentrations have been measured for more than three decades in lakes and reservoirs around the globe, the mechanisms leading to GHG supersaturation are still obscure, with the relative contributions of the different GHG producing processes hotly debated. In this study, we evaluated the terrestrial organic matter (OM) exports from land to aquatic systems, followed by its degradation and contribution to the surface freshwaters GHG concentrations.

Natural lakes, reservoirs as well as lakes and reservoirs with a wood harvested watershed were sampled in the summer of 2007 and analyzed for a broad variety of bulk water chemical parameters and OM molecular proxies. In order to collect sufficient quantities of OM for the amino acid (AA) and lipid molecular analyses, a tangential flow filtration reverse osmosis systems (TFF-RO) was used following the evaluation of its performance for total OM possible molecular fractionation and recoveries using FTIR, stable carbon isotope signatures ($\delta^{13}C$) and total organic carbon (TOC) concentrations. No significant sample fractionation or carry over was obtained with recoveries ranging between 94.6 and 106.9 % using the TFF-RO system.

All lakes and reservoirs sampled in this study were supersaturated in CO_2 and CH_4, with wood harvested water bodies and the reservoir having significantly higher water surface

CO_2 concentrations and emissions to the atmosphere compared to the natural lakes. The bulk water and OM chemical and isotopic analyses showed that the increase in terrestrial dissolved organic carbon and total nitrogen concentrations positively influenced bacterial OM degradation, which drove CO_2 production. Molecular analyses showed a direct relationship between the increases in bacterial biomarker abundances in the dissolved and sedimentary OM fractions, and higher water CO_2 concentrations. This result suggests that OM bacterial oxidation is the most important process leading to GHG production in freshwater aquatic systems.

Acknowledgements

This project was proposed and initiated by a multidisciplinary team; Marc Michel Lucotte, Yves Gélinas, Changhui Peng and Éric Duchemin are kindly acknowledged for their efforts in designing this project. Nicolas Soumis, a research manager working with M. M. Lucotte, is thanked for his help in coordinating and organizing seasonal field campaigns as well as for compiling a huge amount of data in a standardized database. Haibin Wu is acknowledge for his discussions and inputs as for modeling and coupling terrestrial and aquatic systems. I am especially grateful to Jean-Baptiste Plouhinec, a close UQAM collaborator and partner in leading all seven sampling missions; he became my friend as well as a very good and diversified environmental scientist; I admire his work and contributions to the field of photo-oxidation. I am thankful to anonymous reviewers of the already published Chapter (2) but also to Robert Panetta, Karine Lalonde, Mina Ibrahim and Denis Brion for helpful discussions and constructive comments on the research design and manuscripts. We extend our thanks to B. Ghaleb (GEOTOP), V. P. Nguyen and L.-H. Bourgoin (Université de Moncton), as well as A. Tessier (CBAMS – Concordia) and Jean-François Hélie for their help with the ^{210}Pb, amino acid, Fe and dissolved inorganic carbon isotopic analyses, respectively. This study was funded through grants (YG and MML) and scholarships (AO and JBP) from BIOCAP-Canada, FQRNT and NSERC, as well as a grant from the Canadian Foundation for Innovation (YG) and GEOTOP. Unrelated to this research, there are key personalities that need to be thanked for daily support; my so loved wife and my son are both acknowledged for their respective positivism and time sacrifice during the last years of this doctorate. My parents

always believed in and supported me during all six years of my graduate studies. It is also worth mentioning that Yves Gélinas is one of the best research supervisors that a graduate student can dream of, he always inspired me. Yves equally had good intuitions, great suggestions and truthful criticisms during the realization of this project. Thank you Yves, these last six years were terrific.

Table of content

List of Figures

List of Tables

Glossary and Definitions

δ: Difference of the stable isotope ratio of a sample versus that of a reference standard in per mil (‰)

$\delta^{13}C$: Carbon 13 stable isotope signature

$\delta^{15}N$: Nitrogen 15 stable isotope signature

AA: Amino acids

Alk: Alkanes

Allochthonous: Coming from the surroundings of an aquatic system (*e.g.*, soil matter)

Autochthonous: Produced within the aquatic system (*e.g.*, algal production)

$(C:N)_a$: Carbon to Nitrogen atomic ratio

C: Carbon

CAR: Continental to Aquatic Ratio

CPI: Carbon Preference Index

DIC: Dissolved Inorganic Carbon

DN: Dissolved Nitrogen

DOC: Dissolved Organic Carbon

DOM: Dissolved Organic Matter

EA: Elemental Analyzer

Epilimnion: water that resides above the thermocline associated with higher temperature

FA: Fatty acids

FID: Flame Ionization Detector

FLOM: Flocculate Organic Matter

FPOC: Particulate Organic Carbon

FPOM: Particulate Organic Matter

FPN: Particulate Nitrogen

FTIR: Fournier Transform Infrared Spectroscopy

GC: Gas Chromatography

GHG: Greenhouse Gas

Hypolimnion: water that resides under the thermocline associated with lower temperature

IPCC: Intergovernmental Panel on Climate Change

IRMS: Isotope Ratio Mass Spectroscopy

MUFA: Mono Unsaturated Fatty Acid

N: Nitrogen

OM: Organic Matter

PUFA: Poly Unsaturated Fatty Acid

RO: Reverse Osmosis

SEOM: Sedimentary Organic Matter

TAR: Terrigenous to Aquatic Ratio

TCD: Thermal Conductivity Detector

TFF: Tangential flow filtration

THAA: Total Hydrolyzable Amino Acids

Thermocline or metalimnion: Water layer between the epilimnion and the hypolimnion characterized by a steep change in temperature

TN: Total Nitrogen

TOM: Terrestrial Organic Matter

TP: Total Phosphorus

%T_{AA}C: Percentage of AA that compose the total organic carbon in a given OM fraction

%T_{AA}N: Percentage of AA that compose the total nitrogen in a given OM fraction

UCM: Unresolved Complex Mixture

Chapter 1

1 The study of aquatic freshwater ecosystems

Freshwater contains less than three grams of salt per liter. Because of its dilute nature, freshwater is particularly sensitive to natural and anthropogenic stress imposed by and on surrounding land, which often results in physical, chemical and biological alteration to freshwater ecosystems. Drainage basins, also referred to as watersheds or catchments, are defined as the total land area drained by one or several tributary streams that flow in a lake or a main channel. Watersheds ubiquitously influence freshwater ecosystems (Cole et al 1994; Wetzel 2001). An environmental biogeochemical study of a freshwater ecosystem intends to depict the relationships of a water body with the soil, biota and hydrological characteristics of its watershed. This thesis focuses on the study of watershed wood harvesting as well as on the long-term effects of man made reservoirs operation on the carbon cycle of aquatic systems located in the boreal forest of Quebec, Canada.

1.1 The carbon cycle in freshwater ecosystems

One of the principal means of studying the health of aquatic ecosystems in environmental biogeochemistry is to follow organic matter (OM) inputs, exchanges, degradation and outputs. There are several OM input pathways in lakes and reservoirs including streams, atmospheric deposition, sediments, and watershed run-offs. As OM enters water bodies, it is processed based on its quality, reactivity, degree of complexation with inorganic material, and size (Aufdenkampe et al. 2001; Houel et al. 2006; Soumis et al. 2007). For example, if a phospholipid is released into open water via

cell death, it is either biologically utilized, sorbs onto a mineral particle, or is degraded to carbon dioxide (CO_2), phosphate (PO_4^{3-}) and, for nitrogen-containing phospholipids, nitrate (NO_3^-). The organo-phosphorus functionality confers hydrophilicity and lability to phospholipids, which make these compounds easily degradable. Other compounds such as soot, which is hydrophobic and chemically more refractory owing to its poly-aromatic nature, are not easily degradable and can thus accumulate in the sediment.

Molecules comprising organic and inorganic carbon are dynamically transported and (bio)chemically altered within ecosystems following a wealth of pathways that form the global carbon cycle. An example of such representation for the terrestrial and aquatic carbon sub-cycle is shown in Figure 1, in which particulate and dissolved carbon (POC and DOC, respectively) are considered separately owing to differences in their chemical and physical behavior in the environment. Although carbon is the currency used to represent bulk OM in such representation, one needs to keep in mind that other important elements, such as nitrogen, are also abundant in OM and in this cycle, albeit sometimes in a disconnected fashion.

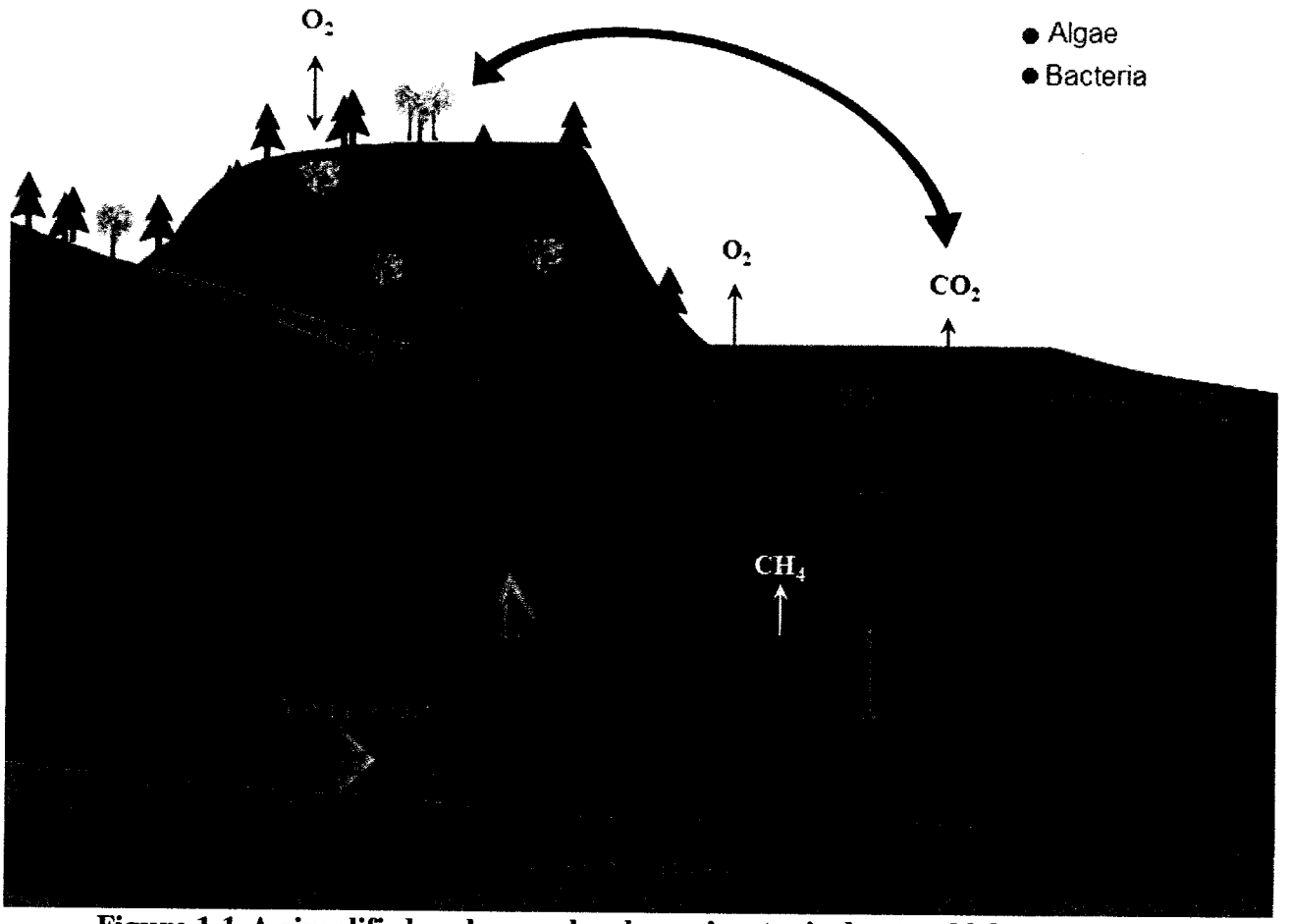

Figure 1-1. A simplified carbon cycle scheme in a typical natural lake
The epilimnion and hypolimnion are water masses of different temperature within a lake, represented here in light and dark blue, respectively. The black arrows represent the inorganic carbon exchanges while the red arrows show organic carbon pathways. Large blue arrows represent the groundwater flows.

Terrestrial POC and DOC (photosynthetically produced as well as material altered by fungi and bacteria) are introduced into streams and water bodies through the erosion of surface soil and percolation of water through deeper soil layers following precipitation or snow melting events (Stepanauskas et al. 2000; Kim et al. 2006). Terrestrial POC, estimated to contribute only one-sixth of total aquatic POC (Cole et al. 2002), adds to the autochthonous POC pool formed of a mix of algae, macrophyte, bacteria, zooplankton and non-living material (Planas et al. 2000; McCallister and del Giorgio 2008). Phytoplankton/algae and macrophytes are primary producers and are at the base of the

food web (lower trophic level). Heterotrophic bacteria and zooplankton (*e.g.* copepods, 1-2 mm long aquatic animals) feed on primary producers and thus belong to the second trophic level. Fishes (feeding on phyto- and zooplankton) and fish consumers, including humans, are of higher trophic levels. Thus, aquatic communities from all trophic levels are affected by changes in terrestrial and aquatic OC inputs and production, respectively (Pace et al. 2004). Terrestrial OC along with dead organisms of different trophic levels are continuously degraded by bacterial and photo-oxidative processes to produce small, generally soluble, organic molecules and CO_2 (as well as CH_4 in anoxic water columns). The residual POC eventually sinks to the benthic layer (water-sediment interface) where extensive bacterial degradation takes place. Dissolved or particulate organic matter (DOM or POM) escaping water column degradation or bio-utilization is eventually integrated into the sediment OM pool (SEOM; von Wachenfeldt and Tranvik 2008). Degradation of the OM in the sediment similarly results in small organic compounds, CO_2 and methane (CH_4). Carbon dioxide directly produced through oxic OM degradation processes or resulting from CH_4 oxidation joins the aquatic dissolved inorganic carbon (DIC) pool (Hélie 2004):

$$\mathbf{H_2O + CO_2 \leftrightarrow H_2CO_3 \leftrightarrow HCO_3^- + H^+ \leftrightarrow CO_3^{2-} + H^+}$$

In freshwater systems, the ultimate fate of dissolved CO_2 is to either be biologically or chemically precipitated as $CaCO_3$ (*e.g.* foraminifera or water pH >8.0, respectively), reused by primary producers in the photic zone or lost to the atmosphere through diffusion (Lehmann et al. 2004; Soumis et al. 2004; Tremblay et al. 2005). The low ionic strength and slightly acidic pH of freshwater in boreal ecosystems makes the precipitation of $CaCO_3$ unlikely; instead, a balance between primary production (CO_2 consumers) and

bacterial and/or photo oxidation (CO_2 producing pathways) is believed to control CO_2 exchanges at the air-water interface (Osburn et al. 2001; Marty et al. 2005; Soumis et al. 2007; McCallister and del Giorgio 2008). Organic matter that escapes oxic sediment degradation eventually accumulates in anoxic sediment, where it can be preserved or further degraded to CH_4, albeit at a much slower rate than in an oxic environment (Duchemin et al. 1995). As CH_4 is produced, it diffuses back into the water column where it is oxidized into CO_2 by methanotrophic bacteria (Striegl and Michmerhuizen 1998; Steinmann et al. 2008) or directly emitted to the atmosphere. Atmospheric fluxes of CH_4 are small but because CH_4 absorbs infrared radiation 23 times more efficiently compared to CO_2 (greater greenhouse effect; Tremblay et al. 2005), they remain significant. Owing to its hydrophobic nature, significant fluxes of CH_4 through bubble production in sediments are also observed (Duchemin et al. 2000).

1.2 Greenhouse gases supersaturation in lakes

Carbon dioxide and methane are greenhouse gases (GHG) that play a major role in determining the Earth's climate. The large increase in GHG concentrations in the atmosphere following industrialization has resulted in a global temperature increase estimated to be approximately 0.6 ± 0.2 C during the 20^{th} century (IPCC 2001). Cole et al. (1994) provided the first evidence for worldwide CO_2 supersaturation in lakes. In their study, they showed that 87% of worldwide lakes (n = 1835) sampled in autumn had a CO_2 partial pressure (pCO_2) that averaged up to three time atmospheric CO_2 levels. Furthermore, they found that the surface waters of arctic, boreal and tropical lakes were systematically supersaturated with CO_2 during the ice-free and stratification periods. As global oceanic waters represent a net sink for atmospheric CO_2, the discovery that global

freshwater systems were net emitters of GHG was surprising and led to a reassessment of their importance in the global hydrospheric and atmospheric GHG exchanges. Several hypotheses were proposed to explain the high pCO_2 levels in lakes and reservoirs (Cole et al. 1994; Osburn et al. 2001; Dubois et al. 2009). To date, the most widely accepted explanation pertains to the large inputs of terrestrial organic matter (TOM) through DOC leaching from soils (terrestrial DOC generally accounts for >90% of total DOC in freshwater systems), and its degradation to CO_2 through photochemical or bacterial processes (Cole et al. 1994, 2002; Prairie et al. 2002; Sobek et al. 2003; McCallister et al. 2008). More specifically, it was also shown that the pCO_2 measured in boreal lakes was correlated to DOC concentrations, which in turn, were governed by watershed characteristics such as the drainage ratio (watershed area *vs.* lake area) and the wetland area to total watershed area ratio (Sobek et al. 2003). Others have proposed an alternate explanation based on metabolic incubations or isotopic studies, which suggests that CO_2 supersaturation would be caused by direct inputs of CO_2 from external sources (*e.g.* groundwater; Carignan et al. 2000a; Dubois et al. 2009). Clearly, there is a need for studies assessing the major processes controlling CO_2 saturation levels using approaches allowing a mechanistic understanding of the carbon cycle in freshwater aquatic systems.

Diffusion of GHG to the atmosphere is also partially controlled by water column stratification, which results in a warmer and lighter water mass that is located above a colder and denser one (called epilimnion and hypolimnion, respectively; Figure 1). The diffusion of GHG from the bottom to the surface waters is slow owing to a sharp change in water density at the thermocline (the interface between the two water masses also called metalimnion). Therefore, because the bottom waters are not in open contact with

the atmosphere, greater GHG concentrations are found in the hypolimnion compared to the epilimnion at the beginning of the stratification in spring and until the water turnover in fall. Kim et al. (2006) have shown that DOC and POC can migrate through the thermocline. As the thermocline deepens from spring to summer (from ~1 to ~4 m in this work; data not shown), hypolimnic GHG are transferred to the epilimnion and diffuse to the atmosphere. Varying quantities of GHG are therefore stored in the hypolimnion during the stratified period; these accumulations only take place in deeper sections of the water bodies and therefore do not account for a significant fraction of the total yearly GHG emissions of the lakes. For example, in this study the hypolimnic GHG accumulation is estimated to account for less than 1.5 hours of the averaged daily emissions from the lake surface in the summer. (see Chapter 6, Table 6-1). This clearly demonstrates that the direct comparison of the summer CO_2 fluxes between systems with or without a thermocline (stratification) is valid and is not biased to a significant extent owing to GHG accumulation in the hypolimnion.

1.3 Anthropogenic effects on GHG fluxes

This section consists in an overview of published work on the effect of two anthropogenic perturbations, hydroelectric reservoir formation and operation as well as wood harvesting, on the carbon cycling in freshwater aquatic systems. Importantly, the relationship between the changes in aquatic bioprocesses upon watershed perturbation and air-water exchanges in GHG has never been directly studied.This is of particular importance when considering that most major aquatic bioprocesses are affected by changes in external OM inputs. Typical DOC concentrations in non-perturbed and natural boreal aquatic systems in Quebec typically range between 0.15 to 1.7 mmol L^{-1} (Prairie et

al. 2002; Houle et al. 1995; del Giorgio and Peters 1994; Chapters 2 and 3), whereas POC concentrations are about two orders of magnitude lower ranging from 10 to 90 μmol L^{-1} (Chapters 2 and 3). Given that the pCO_2 in surface waters is linked to the degradation of OM (Sobek et al. 2003), important variations in DOC concentrations are likely to modify the dissolved CO_2 concentrations and atmospheric fluxes. Therefore, anthropogenic perturbations of the watershed around freshwater systems, which in most cases increase DOC lixiviation and transfer to aquatic systems, should lead to an increase in GHG production.

1.3.1 Hydro-electric reservoirs

Reservoir formation and operation in Canada serves two major purposes: water flow regulation and hydropower production. Dissolved GHG concentrations and atmospheric emissions from Quebec hydroelectric reservoirs have been extensively examined in the past (Duchemin et al. 1995; Tremblay et al. 2005; Duchemin et al. 2006). More recently, an intensive GHG monitoring program was initiated by the main producer of hydroelectricity in Quebec, Hydro-Quebec, to estimate GHG emissions attributable to the flooding of a watershed upon the formation of new reservoirs (Demarty et al. 2009; Prairie 2009). It was reported that the dissolved GHG concentrations were very high during the first three years following impoundment but returned to values comparable to those measured in natural lakes after a maximum of 10 years (Tadonléké et al. 2005; Tremblay et al. 2005; Demarty et al. 2009). If true, such a conclusion would be particularly important in Quebec as it would support Hydro-Quebec's claim that a reservoir carbon imprint is low and that hydroelectricity is greener than other sources of energy (Duchemin et al. 1995; Tremblay et al. 2005). However, it is still controversial as

most direct comparison studies are directly linked to lakes rather than to the preexisting CO_2 balance with the forest before impoundment. Additionally, most studies focus on the quantification, rather than on the processes leading to, lakes and reservoirs GHG emissions. Recent studies showed that averaged atmospheric CO_2 fluxes are from 1.5 to 2.0 times higher in reservoirs than in lakes situated in the Canadian boreal forest (Tremblay et al. 2005; Tadonléké et al. 2005). Because GHG fluxes to the atmosphere are dependent on dissolved GHG concentrations in surface waters and on wind speed (which vary greatly on very short time scales), the standard deviations are often too large to get statistically significant differences in fluxes between lakes and reservoirs at the 95% confidence interval (Table 1-1).

Table 1-1: Welch's test investigating for CO_2 fluxes differences in lakes and reservoirs (values taken from Tremblay et al. 2005)

Province	Number of lakes - reservoirs	CO_2 fluxes in lakes (mg CO_2 m^{-2} d^{-1})	CO_2 fluxes in old reservoirs (mg CO_2 m^{-2} d^{-1})	$p <$
Quebec	21 - 18	1090 ± 1100	1370 ± 970	0.20
Newfoundland	6 - 8	760 ± 330	2010 ± 830	0.0025
Manitoba	12 - 6	1530 ± 2340	3840 ± 2760	0.1

Welch's test: Student t-test for groups with differing # of samples and standard deviations

Furthermore, comparisons between natural lakes and reservoirs always include averaged CO_2 fluxes from ice break up in the spring to ice build-up late in the fall. During this interval, CO_2 concentrations can vary from 20 to 70 µmol L^{-1} (Tremblay et al. 2005; Demarty et al. 2009); therefore, a year-round average CO_2 flux value is obtainable during constant monitoring. Seasonal variations within one system is the major contributor to the measured yearly standard deviations, therefore, seasonal rather than

yearly atmospheric CO_2 fluxes should be considered when comparing lakes and reservoirs.

Despite this controversy, a number of publications reporting plankton community responses upon land flooding and reservoir operation were recently published. It was shown for instance that recently flooded terrestrial OM was better degraded by bacteria under oxic conditions and warm temperatures (20 – 22°C) compared to colder temperatures and/or oxygen-limited conditions (Therrien and Morrison 2005). In addition, organisms from primary and secondary trophic levels proliferate upon impoundment owing to high inputs of phosphorus and labile OM. Upon long-term reservoir operation, the zooplankton biomass decreases most likely because of the lower water residence time in reservoirs compared to lakes. An increase in zooplankton abundance also appears to have a direct effect on lower plankton communities and on dissolved CO_2 concentrations (Marty et al. 2005). In a different study, bacterial activity was shown to increase with higher DOC concentrations, which explained, in part, the variance in CO_2 fluxes between the different systems (Tadonléké et al. 2005). Finally, Planas et al. (2005) have shown that there was no significant difference in phytoplankton primary production and planktonic respiration between old reservoirs and nearby lakes. However, planktonic respiration positively correlated the aquatic CO_2 fluxes, which suggests that bacterial activity plays an important role in modulating CO_2 concentrations and fluxes in freshwater aquatic systems. So far, no one has used molecular level approaches to systematically study the bioprocesses that control atmospheric GHG fluxes from lakes and reservoirs of the Quebec boreal region. Moreover, little interest has been given to modifications in sedimentary processes upon long-term reservoir operation,

which are key contributors to GHG production (Algesten et al. 2005). In addition, it was shown that from 1.5 to 2.0 times more autochthonous OM is delivered to the sediment of an old reservoir (70 y.o.) compared to lakes (Houel et al. 2006). Reservoirs are hydrologically more dynamic (Marty et al. 2005), leading to well-mixed water columns without a distinct thermocline in most locations, higher oxygen levels in the bottom waters and possibly leads to higher abundance of autochthonous bacteria in the sediments; these characteristics may be the major force driving atmospheric CO_2 fluxes in reservoirs.

1.3.2 Wood harvesting activities

Despites the importance of wood harvesting for the Canadian economy, little attention has been paid to the effect of these activities on boreal aquatic systems before the late 1990s. To date, several studies carried out in Finland and Canada have shown that forest harvesting leads to direct DOC, dissolved organic nitrogen (DON), total nitrogen and phosphorus (TN and TP, respectively) inputs from the watershed to the nearby aquatic systems, which unambiguously affect autochthonous populations (Ahtiainen and Huttunen 1999; Carignan et al. 2000b Piirainen et al. 2007; Winkler et al. 2009). Through continuous monitoring of algal populations in eleven boreal lakes two years before and after forest harvesting activities, Prepas et al. (2001) showed that phytoplankton and bacterial abundances were higher in the shallow zones of the lakes following wood harvesting. Common studies monitor changes in aquatic fauna populations upon wood harvesting in comparison to natural lakes within the same region. For instance, a three-year study showed that chlorophyll A and algal biomass increased significantly and correlated with TP concentrations following wood harvesting;

moreover, higher algal abundances were measured in the shallow photic zones of the perturbed compared to natural lakes (Planas et al. 2000). Wood harvesting also leads to higher zooplankton abundances with increasing algal populations, and in opoosite, to lower abundances with increasing cyanobacterial populations (owing to higher food supply and the presence of neurotoxins, respectively; Rask et al. 1998; Prepas et al. 2001).

When exports of terrestrial humic DOC from the watershed to boreal lakes upon wood harvesting are important, the thermocline depth decreases following the attenuation of light penetration which limits algal growth (Schindler et al. 1997; Turkia et al. 1998; Carignan and Steedman 2000; Karlsson et al. 2009). Although the effects of wood harvesting on OM cycling in aquatic systems have been extensively studied at the fauna and bulk level, with only partial success, these profound disturbances were never directly linked to processes controlling dissolved GHG concentrations and fluxes to the atmosphere (del Giorgio and Peters 1994; del Giorgio et al. 1999; Carignan et al. 2000a. For the reason that an increasing number of studies suggest that increases in water DOC concentrations lead to higher dissolved CO_2 concentrations (Sobek et al. 2003; Tadonléké et al. 2005; Chapter 3), important changes in CO_2 production and fluxes are therefore expected following forest harvesting.

1.4 Organic matter source studies

Until now, the effects of reservoir operation and wood harvesting on aquatic systems have only been assessed through biological, water chemical and GHG measurements. While some work has been done on the changes in OM sources in the water column and sediments upon long-term reservoir operation (Houel et al. 2006),

more studies are needed to more precisely apportion water column and sediment OM into allochthonous and autochthonous sources, as well as to pinpoint the relative importance of aquatic organisms to OM accumulating in sediments. The changes in the proportion and composition of terrestrial and aquatic DOM sources upon wood harvesting or reservoir impoundment, as well as the links between these changes and the resulting modifications in aquatic biomass populations, were never measured. Such information is pivotal for determining the controls that link OM composition and dissolved GHG concentrations and atmospheric fluxes.

The composition of aquatic OM can be assessed in several ways; bulk elemental (%C, %N, %H, %O) and isotopic ($\delta^{13}C$, $\delta^{15}N$, $\delta^{2}H$) analysis of the different OM fractions (DOM, POM and SeOM) are powerful enough to estimate OM sources based on simple mixing models (Meyers 1997; Perdue and Koprivnjak 2007). Unfortunately, when the differences in the bulk and isotopic signatures of the end-members are not large enough, or when there are too many potential sources, quantifying and discriminating between the different OM sources becomes exceedingly difficult. Then more powerful techniques, such as the determination of organic biomarkers including compound specific stable isotope signatures, are needed.

1.4.1 An elemental and isotopic approach

In this study, the elemental and isotopic composition of particulate and dissolved OM were first measured to evaluate OM sources and cycling, which complement the usual water chemical parameters (DOC, TN, TP, GHG) routinely measured in the field. The organic carbon to total nitrogen atomic ratio (C:N) is one of the most widely used bulk source proxy in organic geochemistry since it is relatively easy to measure and it

provides additional information on the whole sample (Perdue and Koprivnjak 2007). Because of their different growth environments, land plants contain high relative proportions of cellulose and lignin (C-rich biochemicals) while algae, phytoplankton, bacteria and zooplankton are enriched in protein (N-rich biochemicals). Therefore, land plants are characterized by a higher C:N ratio (20 and higher) compared to aquatic organisms (4 to 12; see Table 1-2). Using pre-determined values of the elemental composition for different end-members, one can thus evaluate the proportion of autochthonous and allochthonous OM in a given solid sample. However, the uncertainties related to such analysis are high and represent at best rough estimates of the relative contributions, which are dependent on watershed characteristics (*e.g.* peatland *vs.* mixed forest, slope of the drainage area, etc.), aquatic biomass characteristics, OM degradation, and bacterial contribution to total OM (Meyers 1997; Chapter 3). It is therefore important to use C:N ratios determined for end-members specific to the region under study.

Table 1-2: Carbon to nitrogen atomic ratios of different organisms

Organism	Atomic C:N	References
Bacteria	4 – 7	Kaiser and Benner 2008 Homblette et al. 2009
Zooplankton	5 – 6	del Giorgio and France 1996
Aquatic plants	8 – 12	Homblette et al. 2009 Chapter 3
Terrestrial plants	> 20	Meyers 1997

In freshwater systems, end-members sometimes have similar elemental composition, the determination of the OM stable carbon and nitrogen isotope ratios for organic ($\delta^{13}C_{org}$) carbon and total nitrogen ($\delta^{15}N_{tot}$) can help decipher the OM sources

(Meyer 2003; Lehmann et al. 2004). Primary producers use either atmospheric CO_2 (land plants) or dissolved inorganic carbon sources (DIC; aquatic organisms) as source material for the biosynthesis of OM. Because the stable isotope ratio (^{13}C *vs.* ^{12}C) of atmospheric CO_2 and DIC are different, OM produced on land and in aquatic systems will bear a different stable isotope signature. Stable isotope signatures are calculated using the isotopic ratio of a sample (SMP) compared to that of an international standard, and are expressed using the delta (δ) notation (Equation 1). The Pee Dee Belemnitella (PDB) and atmospheric N_2 standards are the global reference for $\delta^{13}C$ and $\delta^{15}N$ analyses, respectively:

$$\delta^{13}C_{(SMP/PDB)} = [(({}^{13}C/{}^{12}C)_{SMP} - ({}^{13}C/{}^{12}C)_{PDB})/({}^{13}C/{}^{12}C)_{PDB}] \times 10^3$$

Since the variations in ^{13}C isotope ratios are very small, the calculated difference between a sample and the standard is multiplied by 1000 and the units are expressed in parts per thousand, or *per mil* (‰; Meyer 1997). Using this formula, a sample is said to be depleted (negative value) or enriched (positive value) compared to the standard. Fractionation (*i.e.*, depletion or enrichment in the heavy isotope) is a kinetic process that occurs during enzymatic reactions (McSween et al. 2003). Fractionation is dependent on the biochemical pathway as well as on the isotopic signature of the substrate used to synthesize organic molecules. The vast majority of plants found in boreal lake and reservoir ecosystems exploit the C3 Calvin cycle to synthesize OM. Therefore, because the substrates are isotopically different, the resulting OM is characterized by contrasting stable isotope signatures (Meyers 1997; Lehmann et al. 2004; Marty and Planas 2008; Cole et al. 2002; Chapter 3):

Table 1-3: Stable isotope signatures of aquatic and terrestrial OM

Plants	Substrate	Substrate (‰)	Fractionation (‰)	OC produced (‰)	ON produced (‰)
Aquatic plants	DIC	-5 to -25	-6 to -20	-11 to -45	---
	Aquatic NO_3^-	7 to 10	0	---	7 to 10
Terrestrial C3 plants	CO_2 (atm)	-8	-20	-28	---
	Soils NO_3^-	0.4	0	---	0.4

Freshwater aquatic plants have a wide range of possible $\delta^{13}C$ signatures resulting from the highly variable $\delta^{13}C_{DIC}$ signature. The variability in the $\delta^{13}C_{DIC}$ is governed by two major processes, *(i)* OM respiration (photo and bacterial) introducing depleted CO_2 into the DIC pool (from the degradation of $\delta^{13}C$ depleted OM, ~ -28 ‰) and *(ii)* OM production by primary producers which preferentially use ^{12}C and thus enrich the DIC pool in $\delta^{13}C$. It was recently shown by Cole et al. (2002) that the fractionation induced by phytoplankton is lower (~ -6‰) than that induced by land plants (~ -20 ‰) upon OM biosynthesis. However, despite the high variability of $\delta^{13}C_{DIC}$ in freshwater systems, the $\delta^{13}C$ signatures of algal biomass isolated from boreal lakes and hydroelectric reservoirs in the summer were fairly constant at -32.7 ± 1.0 ‰ (Marty and Planas 2008). Those of bacteria and zooplankton vary a lot more and are dependent on the food sources (France and del Giorgio 1996, Cole et al. 2002).

Bulk elemental and isotopic signatures of a given OM fraction are measured using an elemental analyzer coupled to an isotopic ratio mass spectrometer (EA-IRMS). While data acquisition is rather simple, its interpretation is not as straightforward. As discussed for atomic C:N, isotopic results most often reflect a mix of varying proportions of all potential sources of OM in a system, with limited discriminating power. To differentiate

OM sources and alteration processes, complementary organic biomarkers measurements can be carried out on the same samples.

1.4.2 A biomarker approach

Biomarker measurements in biogeochemistry were initially developed to gain insight into the sources of OM fuelling sediments and thus being preserved on geological time scales. Biomarkers have been traditionally defined as molecular fossils of biochemicals that are specific to one or few living organisms and that are resistant to degradation (*e.g.* lignin, fatty acids, alkanes, etc.; Eglinton et al. 1964). Recently, it was more shown that more labile molecular compounds (*e.g.* amino acids, carbohydrates) could also be used as proxies for estimating OM freshness and recent processing (Cowie and Hedges 1994, Hedges et al. 1994). New biomarkers have been identified and used for determining the roles that biological organisms play in dissolved and particulate OM cycling in natural aquatic systems (Wakeham 1999, Meyers 2003, Tremblay and Benner 2009, Chapters 4 and 5).

Proteins and peptides are ubiquitous to all living organisms and comprise relatively similar proportions of the different amino acid (AA) constituents. Amino acids (AA) were first exploited by Cowie and Hedges (1992) as a proxy for the extent of OM degradation. For instance, the percentage of total organic nitrogen in a sample accounted for by AA is representative of OM freshness (higher percentages mean fresher OM). Also, several AA were found to be directly linked to bacteria in the environment, following their production through bacterial reworking of ubiquitous compounds. These AA are β-alanine and γ-aminobutyric acid that are derived from aspartic and glutamic acid, respectively as well as the D isomeric AA (D-AA) that are found mostly in

peptidoglycan, a major component of the bacterial cell walls (Cowie and Hedges 1994; Kaiser and Benner 2008). These bacterial biomarkers can therefore be used to monitor the response of bacterial communities and GHG to the varying conditions existing in natural lakes and perturbed systems.

The second category of biomarkers used in this study are lipids (defined broadly in this work as the compounds that are soluble in a mixture of non-polar solvents); more specifically, alkanes and fatty acids were used for estimating the relative contributions from algae, vascular land plants as well as microbial reworking (Meyers 1997). Also GC analysis of natural samples results in chromatograms that contain a broad peak corresponding to an unresolved complex mixture (UCM) of highly degraded aliphatic compounds including straight-chain, unsaturated, branched, alicyclic and aromatic hydrocarbons, including their numerous isomers. As resolvable biomarkers are indicative of mostly fresh organic materials from distinct sources, the UCM:biomarkers area ratio can thus be used as a molecular based biodegradation index of the bulk sample (Jeanneau 2006; Hautevelle et al. 2007).

Gas chromatography coupled to isotope ratio mass spectroscopy (GC-IRMS) combines the strengths of stable isotope measurements and molecular biomarkers to pinpoint very subtle changes in OM composition and processing. This approach is not only used for monitoring changes in the sources of sedimentary OM over time scales of up to 5,000-10,000 years (Hayes et al. 1990; Filley et al. 2001), but it also provides unique details on how source information and bioprocesses are linked. For instance, variations in the stable isotope signature of biomarkers that are specific to the bacterial biomass will reflect changes in the origin of the OM bio-utilized by the bacterial

community. As an example, the compound-specific ^{13}C analysis of anteiso C_{15} branched fatty acid (a universal bacterial biomarker; Meyers 2003) in a lake with a deforested watershed would most likely be different from the same analysis in a lake with an unperturbed watershed.

1.5 Thesis format, connecting text and co-author contributions

This manuscript-based thesis contains six chapters, four of which representing articles that are already published (Chapter 2), were, or that are to be submitted (Chapters 3, 4 and 5) to high profile scientific journals. Because this is a linear thesis with obvious relationships between the different chapters, the linking text between each chapter is recopied in this section.

First, the introduction provides the necessary background information for understanding the underlying context and scientific rationale of land use changes and freshwater ecosystems studies.

Chapter 2 (Ouellet, A., D. Catana, J.-B. Plouhinec, M. Lucotte and Y. Gélinas. 2008. Elemental, isotopic and spectroscopic assessment of chemical fractionation of dissolved organic matter sampled with a portable reverse osmosis system. *Environ. Sci. Technol.* **42:** 2490-2495) then describes the tangential flow filtration reverse osmosis system (TFF-RO) used for sampling fine POM (FPOM) and DOM in this study. The TFF-RO allows the sampling of a large quantity of OM and for the concentration of the DOM, in preparation for bulk and molecular analyses. Because sample recovery is not 100% using this approach, we evaluated OM losses and carry over effects through mass balance calculations, as well as OM fractionation and composition through spectroscopic analysis. I ran all the analyses in the laboratory and wrote the publication, with inputs

from my co-supervisors, Y. Gélinas and M. Lucotte. D. Catana and J.-B. Plouhinec took part in the sampling field trip and in the on-site OM collection using the TFF-RO system.

In Chapter 3 (Ouellet, A., J.-B. Plouhinec, N. Soumis, M. Lucotte, K. Lalonde and Y. Gélinas. Assessing the carbon dynamics and greenhouse gases production in natural and perturbed boreal aquatic systems: A bulk isotopic approach. Submitted to *Global Biogeochemical Cycles*), we present a study based on the exploitation of a wide array of water chemical parameters, as well as elemental and isotopic signatures of OM collected in the summer of 2007, to understand the main controls on OM cycling in lakes and reservoirs. We also evaluated how major biogeoprocesses are altered upon anthropogenic perturbation of the natural environment. I also wrote this publication with inputs from my co-supervisors, and ran most of the analyses except for the iron (partly done by Karine Lalonde), total nitrogen and phosphorus (analyzed by a technician, Sophie Chen, at UQAM). J.-B. Plouhinec and N. Soumis helped with sampling and on-site analysis (DOM, FPOM, water pH and temperature, nutrients, as well as dissolved CO_2, CH_4, and O_2 concentrations).

Because of the inherent limitations of bulk OM analyses, we also exploited the specificity of organic biomarkers to trace carbon inputs, transformations and sinks in these aquatic systems. In Chapter 4 (Ouellet, A., L. Tremblay, M. Lucotte and Y. Gélinas. Assessing carbon and nitrogen dynamics in natural and perturbed boreal aquatic systems: An amino acids approach. Submitted to *Limnology and Oceanography*), we present a study exploiting amino acid biomarkers analyzed in all of the OM fractions collected in the summer of 2007. Amino acid signatures allowed linking human perturbations to bacterial and phytoplanktonic responses, as well as bacterial biomass to

both perturbation and GHG concentrations. The amino acid data presented here were analyzed by Dr. Luc Tremblay, a collaborator from the Université de Moncton (NB). I wrote this manuscript with the inputs from the three co-authors.

Amino acids are especially good source indicators for bacterial biomass. In Chapter 5 (Ouellet, A., M. Lucotte and Y. Gélinas. The modulation of the carbon dynamics in natural and perturbed boreal aquatic ecosystems: A lipid biomarkers approach. To be submitted to *Limnology and Oceanography*), we report an exhaustive study based on the analysis of a broad series of lipid biomarkers, which were used to assess how terrestrial OM inputs affects the bacterial and primary producer communities in these water bodies, and to explain the changes in aquatic bioprocesses linked to GHG production pathways. I analyzed all the lipids reported in this work and wrote the manuscript, again with inputs from my co-supervisors.

Finally, an attempt to synthesize the data into presented in Chapters 2-5 is included in Chapter 6, together with the main conclusions and environmental implications reached in this study.

Chapter 2.

2 Elemental, isotopic and spectroscopic assessment of chemical fractionation of dissolved organic matter sampled with a portable reverse osmosis system

Published as :

Ouellet, A., D. Catana, J.-B. Plouhinec, M. Lucotte and Y. Gélinas. 2008. Environ. Sci. Technol. **42:** 2490-2495.

2.1 Abstract

Portable reverse osmosis (RO) systems are increasingly being used for isolating dissolved organic matter (DOM) from freshwater aquatic systems because of their high volume processing capacity and high absolute DOM recoveries. However, obtaining complete recoveries implies the rinsing of the reverse osmosis system with a solution of dilute NaOH and combining the rinse solution and the DOM concentrate. Because of the potential chemical alterations that can affect the integrity of the organic pool leached from the RO system at high pHs, this approach is not compatible with studies based on the molecular-level analysis of DOM. The potential for elemental, isotopic and chemical fractionation was thus evaluated on a series of freshwater DOM samples concentrated in the field with a portable RO system when the concentrate and the rinse solution are not combined. DOC recoveries in the concentrate varied between 81.6 and 88.8%, while total balance calculations showed total recoveries of dissolved and particulate organic carbon ranging between 96.4 and 106.9%. Despite similar $\delta^{13}C$ signatures, differences in N content and FTIR-based chemical composition between the concentrate and rinse DOM solutions suggest some degree of chemical fractionation.

2.2 Introduction

Dissolved organic matter (DOM) is one of the largest and most dynamic pools of organic carbon on Earth (Hansell and Carlson 2002). The number of studies on the bulk characteristics, chemical composition and biogeochemical cycling of DOM has grown exponentially in the last decade. With the recent advances in the development of sophisticated analytical instrumentation to probe the molecular composition of the complex mixtures of organic macromolecules found in DOM (*e.g.*, electrospray ionization mass spectrometry (Kujawinski et al. 2002); ion cyclotron resonance mass spectrometry (Hockaday et al. 2006); liquid chromatography coupled to mass spectrometry (Dittmar et al. 2007); two-dimentional gas chromatography (Adahcour et al. 2006); multi-dimensional nuclear magnetic resonance (Hertkorn et al. 2006); and others), an increasing emphasis is now being put on the collection of salt-free, chemically unaltered, and representative DOM samples. Different methods have been developed for this purpose, including resin adsorption chromatography (using synthetic polymeric resins such as polymethylmethacrylate or polyvinylpyrrolidone), tangential ultrafiltration (Benner et al. 1992), and more recently, solid-phase extraction disk (Kim et al. 2003) and reverse osmosis coupled to electrodialysis (Koprivnjak et al. 2006, Vetter et al. 2007). While these methodologies have been applied with varying success in numerous studies, they are either tedious to use, unsuitable for extracting large quantities of DOM, and/or lead to chemical fractionation owing to the incomplete recovery of DOM.

Reverse osmosis (RO) is the only method available to rapidly concentrate DOM from large volumes of water (hundreds of liters) with minimal DOM losses. The industrial use of reverse osmosis emerged in the early 1970s to produce large volumes of

clean water at a reasonable cost. Reverse osmosis has been exploited to concentrate freshwater DOM since the early 1980s and has since been used routinely in a broad range of freshwater environments (Ødegaard and Koottatep 1982, Clair et al. 1991, among others). In particular, Serkiz and Perdue (1990) have developed and commercialized a portable RO system that can be used in the field for concentrating large volumes of surface and ground water DOM samples. Total dissolved organic carbon (DOC) recoveries greater 90% are routinely reported with this system (Serkiz and Perdue 1990, Sun et al. 1995, Kitis et al. 2001, Kilduff et al. 2004, O'Driscoll et al. 2006), which make this approach the most attractive for the bulk and molecular characterization of freshwater DOM samples.

Depending on the study, these recoveries either correspond to the DOC recovered in the concentrate only, or they are calculated by combining the mass of DOC in the concentrated sample with the mass of carbon recovered upon rinsing the RO membranes following the concentration step, divided by the total mass of DOC in the initial, non-treated sample. The rinsing step is necessary because a fraction of the DOC pool, typically 10-20% of initial DOC, sorbs onto the membranes of the RO system and is not recovered in the permeate (water passing through the RO membranes) nor in the concentrate (volume of water containing the compounds rejected by the membrane). To completely recover this sorbed DOC fraction and eliminate problems associated with cross contamination of samples from carry over effects, the RO system is usually leached with a dilute NaOH leaching solution ($10^{-2} - 10^{-4}$ M), which is then neutralized and demineralized using an H^+-saturated cation exchange resin (Koprivnjak et al. 2006). While such harsh chemical treatment might not significantly alter the bulk reactivity

(Kitis et al. 2001, Kilduff et al. 2004) and trace metal complexation properties (De Schamphelaere et al. 2005) of the concentrated DOM pool, it might not be suitable when probing DOM dynamics through the analysis of specific molecular biomarkers. Such molecular-level studies hinge on the preservation of the chemical integrity of a sample as the slightest chemical alteration can result in the loss of a target molecule from the analytical window. It is thus important to evaluate the percentage of bulk DOM that remains sorbed onto the membranes of the RO system, and to know whether the composition of the sorbed DOM fraction differs from that of bulk DOM. Knowing whether the incomplete recovery of DOM leads to significant chemical fractionation upon sampling would also be useful in studies where only the DOM concentrate is used (see Gjessing et al. 1998 and Vogt et al 2004 for instance). Despite the fact that RO systems have been exploited for more than 15 years to collect and concentrate DOM from freshwaters, information on chemical fractionation still is not available in the literature.

This study was initiated with this major aim in mind. A commercial RO system was used to collect a series of samples from lakes and reservoirs of the boreal forest in Quebec, Canada. The samples were concentrated in the field, where no clean laboratory and organic-free water source were available, to estimate DOC recoveries of the RO system during routine field use. A complete carbon mass balance was calculated for each sample by analyzing the initial water for total organic carbon (TOC, which is the sum of dissolved and particulate organic carbon, DOC and POC, respectively), the POC fraction (>0.45 μm), DOC in the concentrate, DOC in the alkaline rinse solution, and the DOC in the permeate. Elemental, isotopic and chemical fractionation was assessed through mass balance calculations and spectroscopic characterization.

2.3 Materials and Methods

2.3.1 Field sampling

The samples were collected in different lakes and reservoirs of the boreal forest in the province of Quebec, Canada, at latitudes ranging between 46°10' and 47°46' N, and longitudes between 76°12' and 78°24' W between early spring 2006 and fall 2007. At each site, equal volumes of water sampled at regular intervals in the upper 10m of the lake or reservoir were collected in 50-L Nalgene carboys (total of 150 to 250 liters) using a drum transfer pump and pre-filtered online using a 63-µm nylon filter. The water at these sites is slightly acidic to slightly alkaline (pH 6.25-7.46), with DOC concentrations ranging between 2.7 and 7.7 mg C L^{-1}, and low total suspended solids concentration (<3 mg L^{-1}). Water column temperature at the time of sampling varied between 8.2 and 24.0°C.

2.3.2 Microfiltration-Reverse Osmosis (MF-RO) unit

The system includes a tangential flow filtration (TFF) unit equipped with a 0.45-µm polyvinylidene difluoride (PVDF) Pellicon 2 cassette filter (Millipore) coupled to the RealSoft PROS/2S RO system described in Serkiz and Perdue (1990) as well as Sun et al. (1995). A Chelex-100 resin (polystyrene-divinylbenzene iminodiacetate, Biorad) was installed upstream from the RO system to lower the concentration of dissolved cations in the feed solution. To separate the POM and DOM fractions, the sample was filtered on 0.45-µm membrane using a peristaltic pump and collected in a 50-L Nalgene® container while the retentate containing particulate organic matter (POM) was returned to the original sampling container. The DOM fraction was then concentrated using the approach described by Serkiz and Perdue (1990), and quantitatively recovered by completely emptying the RO system at the end of the concentration step. This last step was done by

applying a positive pressure using the high-pressure pump for air-flushing the system, and then opening the valve fitted at the bottom of the membrane casing. Because no organic-free water source was available at the time of sampling, a rinsing water solution at pH 12 (0.01M NaOH) was prepared from the RO permeate water; the dissolved organic carbon concentration in the permeate was consistently very low, with measured values ranging between 6.2 and 7.4 $\mu g\ C\ L^{-1}$. RO membranes were rinsed with 20L of this alkaline solution to avoid carry over of organic matter from sample to sample. Two 7-mL aliquots each of the 63µm-filtered water, RO concentrate, initial and final rinse pH 12 water were sub-sampled and acidified to pH <2 with clean 6M HCl for TOC measurements. Concentrated POM and DOM samples were doped with $HgCl_2$ to quench bacterial activity. Any residual water remaining in the RO system was then neutralized with diluted HCl. The TFF unit was then washed with 10 L of a sodium hypochlorite (Javel®) solution prepared with the RO permeate water and then rinsed once again with permeate water.

2.3.3 TOC measurement

A Shimadzu Total Organic Carbon (TOC) Analyzer model 5000A TOC-V_{CSH} was used throughout this work. The concentrated DOM samples were diluted 10-fold with milli-Q water (Barnstead EASYpure II) prior to analysis. Milli-Q water blanks were analysed each day to correct for instrumental background contribution to the measured intensities for the samples and potassium hydrogen phthalate standards. Each aliquot collected in the field was analysed in triplicate. Using the approach described here the precision was 3.6%.

2.3.4 EA-IRMS measurements

Bulk ^{13}C and elemental analyses were carried out on a EuroVector 3028-HT elemental analyzer coupled to an Isoprime isotope ratio mass spectrometer (EA-IRMS, GV Instruments, Manchester, England). The EA-IRMS was calibrated with an in-house pre-calibrated β-alanine standard ($\delta^{13}C = -25.98 \pm 0.23‰$ and $\delta^{15}N = -2.21 \pm 0.24‰$, n = 61), and the certified primary standards IAEA-C6 327 Sucrose ($\delta^{13}C = -10.45 \pm 0.03‰$) for both carbon and nitrogen quantitative and stable isotope measurements. Isotopic fractionation upon sampling was tested on three randomly selected reservoir water samples. A measured volume of the DOM concentrate and water rinse solutions were freeze-dried and analyzed in triplicate. Inorganic carbon (*i.e.*, carbonates) was removed from the freeze-dried samples prior to EA-IRMS measurement by exposing them to vapor-phase HCl overnight following the method of Hedges and Stern (*21*).

2.3.5 FTIR measurements

FTIR analyses were carried out on the same freeze-dried DOM concentrates and the corresponding freeze-dried rinsing solutions. About 0.5 mg of the concentrate and 1.5 mg of the rinse sample were homogenized with ~100 mg of potassium bromide. Approximately 50 mg of this homogenate was pressed into a pellet and analyzed using a N_2-purged Nicolet 6700 FTIR spectrophotometer.

2.4 Results and discussion

Working in the field often adds severe constraints on the procedures carefully developed in the laboratory when collecting high-quality samples from natural environments. The best compromise was thus established to optimize the number of DOM samples that could be collected during a sampling campaign without

compromising the quality of the samples. This was accomplished by systematically cleaning the RO system with an alkaline solution between samples to avoid carry-over of DOM from sample to sample, and by using the permeate water as a source of clean water for preparing the alkaline cleaning, bactericidal, and water rinsing solutions.

2.4.1 Carbon mass balance

Total carbon mass balances were calculated for water samples from nine lakes and reservoirs collected with the MF-RO system in the spring and summer of 2006, and in the fall of 2007 (Table 2-1). The initial TOC concentrations (sum of DOC and POC) ranged between 2.7 and 7.7 mg C L^{-1} in the non-treated water samples, while the DOC concentrations varied between 56 and 144 mg C L^{-1} in the final concentrates. DOC concentrations in the permeate were very close to the instrumental blank (and thus not quantitative at the 3σ level); therefore, they were not taken into account when calculating the total carbon mass balances. Because the initial DOC concentrations prior to RO concentration are not available (owing to the fact that the samples were water-column integrated and that the RO concentration step was initiated before the rate-limiting microfiltration step was completed), the yield of the RO system is calculated as the mass of DOC in the concentrate divided by the sum of the masses in the concentrate and in the rinse solution. Note that contrary to the values reported in some studies (Kilduff et al. 2004), these yields do not include the mass of carbon recovered in the alkaline water rinse, which was not combined in this work to allow assessing chemical fractionation between the concentrate and the rinse solution. The RO yields listed in Table 2-1 thus correspond to the true DOC recoveries of the RO system when collecting concentrated and chemically unaltered DOM from these aquatic systems. In all cases but one (n=8),

these DOC recoveries varied between 85.0 ± 2.5% and 88.8 ± 1.7% when consistently emptying the RO membrane casing, *i.e.* a volume of about 4 L of retentate, following the concentration step (Table 2-1). One sample had a slightly lower recovery at 81.6 ± 1.9%. The uncertainties associated with the above measurements represent the propagated error stemming from DOC concentration measurements in the concentrate and the rinsing solution. Although the small number of samples listed in Table 2-1 precludes the positive identification of statistically significant correlations, no trend was found between DOC recoveries and water temperature, pH, or with type of aquatic systems (lake or reservoir).

Table 2-1: Microfiltration-reverse osmosis organic carbon mass balance calculations on selected samples [a]

Sample	Initial TOC[b] (DOC + POC)		RO Concentrate (DOC)		RO Rinse (DOC)		RO Yield[c] (DOC)	MF Retentate[d] (POC)			Total Mass Balance[f]
	Volume (L)	Mass (mg)	Volume (L)	Mass (mg)	Volume (L)	Mass (mg)	Recovery (%)	Volume (L)	Mass (mg)	% of TOC (%)[e]	MF-RO (%)
Spring 2006											
Ellard-1	200	848 ± 32	7.88	664 ± 8	20.0	105 ± 2	86.3 ± 1.6	0.61	102.0	12.0	102.8 ± 4.0
Cabonga-3	245	1323 ± 18	8.00	1036 ± 13	20.0	183 ± 10	85.0 ± 1.8	0.65	88.6	6.7	98.9 ± 1.8
Decelles-2	200	1428 ± 40	7.92	1142 ± 43	20.0	144 ± 8	88.8 ± 5.0	0.44	132.9	9.3	99.4 ± 4.2
Summer 2006											
Mary-3	200	541 ± 2	7.30	407 ± 5	20.0	54 ± 2	88.8 ± 1.7	0.65	75.8	16.8	98.7 ± 1.2
Clair-2	200	1138 ± 8	7.74	827 ± 5	20.0	123 ± 4	87.0 ± 0.9	0.75	266.4	10.9	106.9 ± 1.1
Cabonga-3	200	1089 ± 11	8.00	797 ± 5	20.0	112 ± 4	87.7 ± 1.0	0.52	255.2	11.8	106.9 ± 1.4
Decelles-1	200	1339 ± 2	7.14	901 ± 11	20.0	204 ± 12	81.6 ± 1.9	0.71	257.2	10.2	101.8 ± 1.4
Decelles-2	200	1409 ± 13	7.72	1042 ± 20	20.0	134 ± 5	88.6 ± 2.7	0.55	226.0	9.6	99.5 ± 1.9
Decelles-9	150	1154 ± 14	7.51	806 ± 7	20.0	106 ± 2	88.4 ± 1.2	0.63	221.2	12.5	98.2 ± 1.5
Fall 2007											
Decelles-1	200	1090 ± 14	7.16	953 ± 12	20.0	82 ± 11	87.4 ± 2.0	0.40	49.1	4.5	99.4 ±1.9
Decelles-4	250	1494 ± 50	8.22	1270 ± 22	20.0	98 ± 9	85.0 ± 2.5	0.39	73.1	4.9	96.4 ± 3.7

[a] Uncertainty calculated using between 2 and 5 replicates

[b] 63-µm filtered sample containing POC (<63µm) and DOC (<0.45µm)

[c] The RO recovery is calculated using the initial DOC mass, which is assumed to be equal to the sum of the mass of DOC in the concentrate plus that in the rinse solution; percent recovery = 100 * $(\text{mass DOC})_{\text{concentrate}}$ / [$(\text{mass DOC})_{\text{concentrate}}$ + $(\text{mass DOC})_{\text{rinse}}$]

[d] Uncertainty smaller than 3.5% of the indicated values

[e] Contribution of POC to TOC, calculated using the formula 100 * (mass POC) / (mass TOC)

[f] Mass balance = 100 * [$(\text{mass DOC})_{\text{concentrate}}$ + $(\text{mass DOC})_{\text{rinse}}$ + (mass POC)] / (mass TOC)

A significant fraction of total DOC (11.2 ± 1.9% to 18.4 ± 2.5%) thus remained sorbed onto the surface of the membranes during the RO concentration step. Sun et al. (1995) showed that for samples with very high DOM concentrations, the use of a H^+-saturated cation exchange resin upstream from the membranes might results in the acidification of the solution followed by the precipitation of humic compounds in the RO system. More likely for our low-DOM samples, a pool of dissolved organic compounds might have a strong affinity for the functional groups present at the surface of the aromatic polyamide RO membranes. These two possibilities agree with our data and with the fact that the mass of DOC lost in the permeate amounted to only 1.1 ± 0.3% of the total initial mass of carbon.

Total carbon mass balances for each sample were calculated from the mass of the initial TOC in the unfiltered samples and the sum of the masses of organic carbon in each fraction (DOC in the concentrate, DOC in the rinse solution, and POC retained by microfiltration). The total recoveries of initial TOC vary between 96.4 ± 3.7% and 106.9 ± 1.4%, and could be underestimated by about 1% owing to the fact that the mass of carbon lost in the permeate was not included in this calculation. Mass balances for all samples are thus near or slightly above 100%, suggesting either a slight instrumental overestimation of the DOC concentrations, a low-level contamination of the vials and containers used to process and store the water samples, or the leaching of organic carbon from the RO system (tubing, pump, cation exchange resin and RO membranes) during the rinsing step at pH 12.

The high absolute carbon recoveries confirm the high potential of RO systems for collecting freshwater DOC (Serkiz and Perdue 1990). As also suggested by Kilduff et al.

(2004), systematically rinsing the RO membranes with a 0.01M NaOH solution completely eliminates DOC carry-over from sample to sample, which had been identified as a potential problem with RO systems used in the field (Sun et al. 1995). Without this rinsing step, cross-contamination between samples is likely given the relative proportion of initial DOC (between 11 and 18% of the initial mass of carbon) that sorbs on the surface of the RO membranes during the concentration step.

2.4.2 Sample fractionation

Sorption of a fraction of the DOM pool on the membranes of the RO system implies contrasting affinities, and thus contrasting chemical composition, between DOM sorbed to and DOM passing through the aromatic polyamide membranes. Chemical fractionation of the initial DOM pool is thus possible using RO systems. Whether such chemical fractionation is significant and whether chemical fractionation is accompanied by stable isotope fractionation must therefore be verified to confirm that the DOM concentrate is truly representative of the initial DOM pool. The DOM concentrate and alkaline rinse solution of three randomly selected samples were freeze-dried and quantitatively and isotopically analyzed for organic carbon (OC) and total nitrogen (TN) by EA-IRMS. These results are summarized in Table 2-2.

The OC concentration in the freeze-dried DOM concentrates reveals that inorganic materials account for roughly two-thirds of the total mass of the recovered DOC pool (assuming that 45% of DOM is DOC). Dissolved solids, most likely monovalent cations and anions as most of the divalent cations are removed by the Chelex-100 resin, as well as inorganic colloids, likely contribute to the inorganic fraction in these samples. The TN contents are lower, and the atomic C/N ratios are typical of

terrestrial DOM samples (Meyers 2003). Note that the contribution of dissolved nitrate accounts for less than 0.5% of total nitrogen in the freeze-dried concentrates (nitrate is assumed to behave conservatively during the RO concentration step, *i.e.*, the NO_3^- concentration in the filtrate is roughly the same as in the non-treated water sample; its contribution to total nitrogen in a freeze-dried filtrate sample can thus easily be calculated).

Table 2-2: Bulk analysis of a DOM concentrate and corresponding alkaline rinse solution

Sample	Organic C (wt%)	Total N (wt%)	$(C/N)_a$[a]	$\delta^{13}C$ (‰ vs PDB)
Decelles-2	18.11 ± 0.34	0.455 ± 0.002	46.5 ± 1.1	-27.4 ± 0.2
Decelles-2 rinse	0.52 ± 0.03	0.015 ± 0.000_2	39.2 ± 2.5	-27.1 ± 0.3
Decelles-2 rinse (nitrate-corrected)	0.52 ± 0.03	(0.006)	(>100)	-27.1 ± 0.3
Decelles-1	16.80 ± 0.22	0.598 ± 0.028	32.8 ± 1.9	-27.2 ± 0.1
Decelles-1 rinse	0.73 ± 0.05	0.021 ± 0.001	40.4 ± 5.0	-27.0 ± 0.0_4
Decelles-1 rinse (nitrate-corrected)	0.73 ± 0.05	(0.003)	(>100)	-27.0 ± 0.0_4
Decelles-4	18.31 ± 0.79	0.655 ± 0.054	32.6 ± 4.1	-27.2 ± 0.1
Decelles-4 rinse	0.94 ± 0.01	0.023 ± 0.001	48.6 ± 2.8	-27.1 ± 0.1
Decelles-4 rinse (nitrate-corrected)	0.94 ± 0.01	(0.001)	(>100)	-27.1 ± 0.1

[a] Atomic C/N ratio

Despite the similarity in $\delta^{13}C$ composition (Table 2-2), much lower OC concentrations are measured in the freeze-dried rinse solution. These lower concentrations reflect the high mass of salts generated when adjusting the pH of the rinse solution with HCl; ~99% of the total mass is inorganic. The atomic C/N ratio measured

for the rinse solutions are affected by the nitrates present in the water samples. Nitrates accounts in all cases for more than 60% of total N in the rinse solutions and artificially decreases the measured ratios; these ratios increase to more than 100 without the NO_3^- contribution and indicate that the chemical composition of the DOM fraction sorbed to the membranes is different from that of the initial DOM pool, at least with respect to N-containing functionalities.

To probe for chemical fractionation, the nature and relative abundances of the major chemical functionalities in the concentrated DOM fraction and in the rinse solution for three randomly selected samples were analyzed by FTIR spectroscopy (González et al. 2004, Peuravuori et al. 2005, Her et al. 2008). While the spectra collected for the concentrates are all similar (Figures 2-1A, -1C and -1E), those of the rinse solutions reveal important differences between samples (Figures 2-1B, -1D and -1F). The reasons for these differences could be linked to sample composition and/or working pressure of the RO system (which varied between 1000 and 1500 kPa in this work), but they are beyond the scope of this paper. All spectra show a broad peak between 3000 and 3500 cm^{-1} and corresponding to H-bonded OH stretching derived from a broad range of molecules, with possibly a small contribution from the N–H stretch absorption band of amines and amides. This band is sharper and more intense in the rinse solution of the first sample (Figure 2-1B) most likely because of the presence of residual water retained by the hydroscopic salts formed upon neutralization of the rinse solution. The absorption bands representing C–H stretching of methyl and aldehyde functional groups near 2960, 2920 and 2850 cm^{-1} contribute little to the total signal in most samples, except for the rinse solution of the last sample (Figure 2-1F). The stretching band of thiol groups (S–H)

near 2550 cm^{-1} is seen as a weak and broad peak on the spectra of the concentrates and rinse solutions collected in the fall (Figures 2-1 C–F). Absorption bands for C=O and C=C functionalities are intense in the 1750 to 1500 cm^{-1} region, although at varying relative contributions, in all concentrates and rinse solutions. The wavenumber region between 1470 and 1380 cm^{-1} is a significant contributor in all spectra and is attributed to CH_2 and CH_3 bending. The C–O stretch bands for the tertiary, secondary and primary alcohols at about 1150, 1120 and 1070 cm^{-1}, respectively, are also present on all spectra, albeit at a higher relative abundance in the DOM concentrates and in the rinse solution of the last sample. Other functional groups (Si–O and S=O) are also known to absorb in the same spectral window but their contribution is assumed to be small, particularly in the DOM concentrates. Although the series of peaks in the 700-1000 cm^{-1} region of some spectra (Figures 2-1 C–F) might be indicative of differences in alkene isomers and/or benzene substitution patterns, the associated alkene C–H stretch absorption normally seen at 3000-3100 cm^{-1} is absent from all spectra most likely because of the intensity of the O–H stretch band. A contribution from different mineral species also cannot be ruled out below 1000 cm^{-1}.

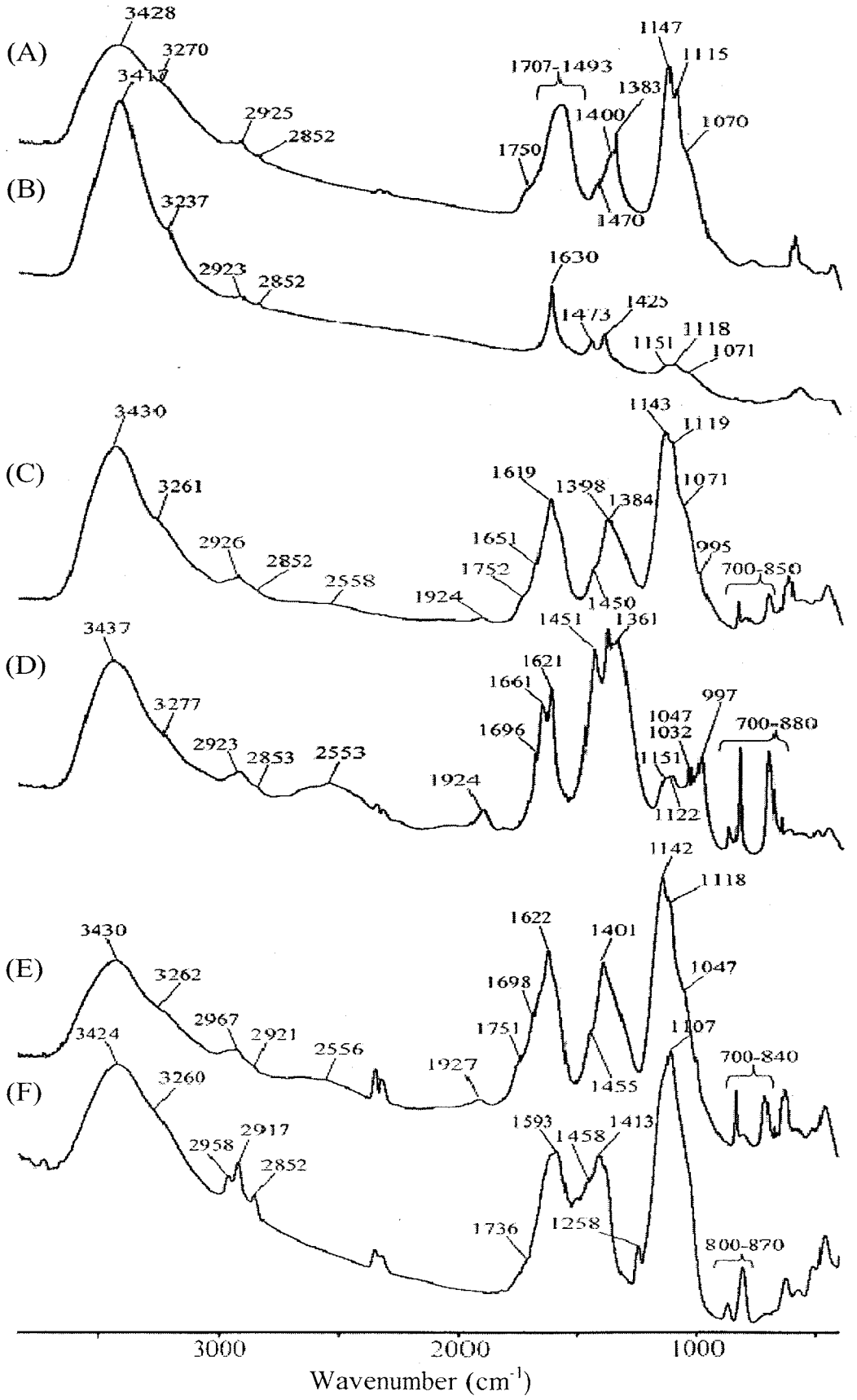
(A)
3428
3270
3417
2925
2852
1707
1493
1147
1115
1383
1400
1070
1750
1470
(B)
3237
2923
2852
1630
1473
1425
1151
1118
1071
(C)
3430
3261
2926
2852
2558
1924
1619
1398
1384
1651
1752
1450
1143
1119
1071
995
700-850
(D)
3437
3277
2923
2853
2553
1924
1621
1661
1696
1451
1361
997
1047
1032
1151
1122
700-880
(E)
3430
3262
2967
2921
2556
1927
1622
1698
1751
1401
1455
1142
1118
1047
1107
700-840
(F)
3424
3260
2958
2917
2852
1736
1593
1458
1413
1258
800-870
3000
2000
1000
Wavenumber (cm-1)

Figure 2-1. FTIR absorbance spectra of the lyophilized DOM concentrate and the rinse solutions from the Decelles Reservoir (Quebec, Canada).
(A) and (B) are the concentrate and rinse from station Decelles-2 (summer 2006); (C) and (D) are the concentrate and rinse from station Decelles-1 (fall 2007); and (E) and (F) are the concentrate and rinse from station Decelles-4 (fall 2007).

Important differences can be seen between the spectra of the concentrates and the rinse solutions, particularly for the first two samples (Figures 2-1 A-D). However, these differences are mostly linked to variations in the relative contributions from the four major regions of the spectrum, namely, (*i*) O–H/N–H stretching between 3000 and 3500 cm^{-1}, (*ii*) C=O and C=C stretching between 1500 and 1700 cm^{-1}, (*iii*) C–H bending between 1470 and 1380 cm^{-1}, and (*iv*) C–O stretching between 1170 and 1000 cm^{-1}. Within each one of these major groups, the relative intensities of the different contributing functionalities sometimes also varies between the concentrates and the rinse solutions. As an example, in the Decelle-2 DOM concentrate (Figure 2-1A), a broad band is observed between 1500-1700 cm^{-1}, flanked by a shoulder at 1750 cm^{-1}, indicating a combination of alkenes, aromatic C=C and amides C=O stretching, while the shoulder is assigned to ester C=O stretching. In the same spectral region, only a sharp band is observed at 1630 cm^{-1} for the rinse solution of the same sample (Figure 2-1B). This band could be associated to C=O stretching in amides, but given the low abundance of organic nitrogen in the rinse solution, it more likely corresponds to conjugated C=C with a ketone functional group. Coordination of the C=O functional groups with calcium or aluminum could also contribute to the signal at 1630 cm^{-1}. Bands indicative of methyl bending (1400 and 1383 cm^{-1}) and C=C stretching (1475 cm^{-1}) are present in the RO concentrate while only the C=C stretch can be observed in the rinse solution along with a new band occurring at 1425 cm^{-1}.

These differences between the concentrate and rinse solution for each sample indicate some degree of chemical fractionation upon concentrating DOM by RO, most likely stemming from differences in affinity of the sorbed DOM fraction for the aromatic polyamide membranes of the RO system through Van Der Walls interactions. However, the absence of a repeating pattern in the FTIR-based compositional differences between the concentrates and the rinse solutions prevents the confirmation of this hypothesis. The contribution of organic material leached from the RO system as the cause for these differences can be ruled out based on the variations in the chemical composition of the three rinse solutions and the OC recoveries of 96.4 to 99.5% measured for the samples analyzed by FTIR.

Given the fact that the DOC recovered in the rinse solution accounts for only 11 to 18% of the initial DOC pool, the impact of this fractionation on the bulk chemical characteristics of DOM is most likely small and could probably be neglected. Chemical fractionation could however introduce a bias in the results when targeting specific molecules present the DOM pool, as done in studies exploiting organic biomarkers. Owing to the composition of the ROM membranes, aromatic and aliphatic materials may preferentially be removed from the concentrate through sorption onto the membranes of the RO system. Such affinity-based fractionation could have an impact on the distribution of several families of aliphatic (lipids) and aromatic (lignin) biomarkers between the concentrates and the rinse solutions. This appears to have been the case with the last sample (Figures 2-1E and -1F) for which the relative abundance of the C–H stretching band, indicative of aliphatic molecules, is higher in the rinse solution than in the concentrate. Furthermore, the biogeochemical message carried by each biomarker or

family of biomarkers could be modified through the chemical alteration of individual molecules. As an example, fatty acids originating from neutral lipids (mostly di- or tri-glycerides) are often separated from those included in the polar lipids fraction (mostly phospholipids) as the latter originate mostly from living cells or from very recently living cells; the ratio between fatty acids from the two pools is thus an indicator for the living biomass. Raising the pH of the solution to 12 leads to the partial saponification (base hydrolysis) of the fatty acids from the parent molecule and thus, to a loss of information.

A series of precautions must thus be taken when collecting DOM samples from natural aquatic systems using the MF-RO system described above, particularly when working in the field. First, the system should systematically be rinsed with NaOH between each sample to eliminate sample-to-sample carry over effects. A significant fraction of the initial DOM pool is found in the rinse solution (11 to 18% in this study), but it can be recovered following the procedure outlined in Koprivnjak et al. (2006). Special care must be taken to completely empty the RO system when recovering the concentrate or the rinse solution. In previous work (Sun et al. 1995, Kilduff et al. 2004), this was done by flushing the system with permeate water, thus diluting the RO concentrate with ~4 L of flush water (void volume of the RO system; Sun et al. 1995). We took a different approach by applying a positive pressure using the high-pressure pump to avoid diluting the DOM concentrate, and obtained total recoveries ranging between 96.4 and 106.9%. Only about 1% of the initial DOC was not retained by the RO system and was thus lost in the permeate. As suggested previously (Sun et al. 1995), DOM lost in the permeate most likely comprised low molecular weight organic acids. Given the high DOC-based yield of the RO system (between 81.6 and 88.8% of the initial

DOC pool, Table 2-1) and the fact that the chemical composition of DOM in the concentrate and the rinse solutions are fairly similar, the bulk characteristics of the DOM concentrate are most likely very close to those of the non-treated initial DOM sample suggesting limited fractionation. Molecular-level fractionation modulated by contrasting affinities for the aromatic polyamide membranes exhibited by the range of dissolved compounds found in DOM could be an issue when carrying out studies exploiting organic biomarkers and should be thoroughly tested for each class of biomarker compounds before deciding whether the DOM sorbing onto the membranes should be recovered. Furthermore, chemical alteration of the targeted biomarkers at high pH, and thus of the biogeochemical message that they carry, should also be verified to ensure that information drawn from such studies is accurate. The extent to which each family of biochemicals routinely used in biomarker studies is affected by such fractionation and chemical alteration should be further studied.

Chapter 3.

3 Assessing the carbon dynamics and greenhouse gases production in natural and perturbed boreal aquatic systems: A bulk isotopic approach

Submitted to Global Biogeochemical Cycles as:

Alexandre Ouellet, Jean-Baptiste Plouhinec, Nicolas Soumis, Marc Lucotte, Karine Lalonde and Yves Gélinas

3.1 Abstract

Carbon (C) cycling in freshwater aquatic systems has high natural variability within a narrow range of chemical and biological conditions, which makes the understanding of the processes that control C dynamics and carbon dioxide (CO_2) exchanges with the atmosphere extremely difficult. Human perturbations such as watershed wood harvesting and long term reservoir impoundment lead to profound alterations in C dynamics and result in a more extensive range of chemical and biological conditions when both perturbed and natural systems are examined together. We exploited these anthropogenic alterations to assess the controls on C cycling in five lakes and two reservoirs from the southern Canadian boreal forest during the spring and Summer of 2007. Several bulk analytical techniques were used, including the measurement of dissolved greenhouse gases (CO_2 and methane, CH_4), oxygen (O_2), dissolved organic carbon (DOC), as well as total nitrogen and phosphorus (TN and TP). Dissolved and fine particulate organic matter integrated over the whole water column, as well as dissolved inorganic carbon (DIC) and total particulate organic carbon (POC) above and below the thermocline were analyzed for elemental and stable isotopic compositions (atomic C:N ratios, $\delta^{13}C_{org}$, $\delta^{13}C_{inorg}$ and $\delta^{15}N_{tot}$). While the number of water bodies studied in this work does not allow a systematic comparison of C cycling and greenhouse gases between perturbed and natural aquatic systems, general trends emerged which are presented and discussed. Based on the six systems studied, it appears that human perturbations lead to higher concentrations of DOC, TN and CO_2 in the water column, as well as higher CO_2 fluxes to the atmosphere and lower oxygen saturation levels. These differences are all related to the increased export of terrestrial organic matter and nutrients which, as

supported by the $\delta^{13}C_{DIC}$ and $\delta^{13}C_{POC}$ results, leads to enhanced bacterial activities in the water bodies.

3.2 Introduction

Surface waters of most lakes worldwide are supersaturated in carbon dioxide (CO_2), with partial pressures (pCO_2) that can be as high as three times the equilibrium concentration (Kling et al. 1990; Cole et al. 1994). Several potential sources of carbon (C) are fuelling dissolved CO_2 supersaturations have been identified, such as ground water dissolved inorganic carbon (DIC), terrigenous DIC runoffs, as well as remineralization of dissolved and particulate organic carbon (DOC and POC) through photo-oxidation and bacterial decomposition (McCallister and del Giorgio 2008, Dubois et al. 2009, and references therein). Growing evidence suggests that terrigenous organic matter (OM) inputs followed by photo-oxidation and/or respiration are the major drivers of pCO_2 supersaturation (del Giorgio et al. 1997; Sobek et al. 2003; McCallister and del Giorgio 2008) in most freshwater systems. Terrigenous OM inputs in lakes are mainly controlled by rivers and watershed runoffs (Schindler et al. 1997), and help sustain the aquatic food web through incorporation of DOC into bacterial biomass and/or respiration by heterotrophic bacteria (Pace et al. 2004; Berggren et al. 2007; McCallister and del Giorgio 2008). Indeed, lakes with DOC concentrations higher than 0.42 – 0.50 mmol L^{-1} are likely to behave as net heterotrophic systems (Prairie et al. 2002), leading to the observed pCO_2 supersaturation levels. Increases in the inputs of terrigenous OM to aquatic systems through flooding (*e.g.* reservoirs, beaver dams) or watershed wood harvesting are thus likely to affect C cycling in aquatic systems.

Reservoirs are typically created for water flow regulation or hydro power production. Just like natural lakes, reservoirs are net sources of GHG to the atmosphere (Duchemin et al. 1995; St-Louis et al. 2000; Tremblay et al. 2005). Greenhouse gases emissions from new reservoirs are very high during the first 3 years following impoundment and return to constant values within 10 years (Tremblay et al. 2005). However, because of the very high spatial and temporal variability in GHG fluxes between the water surface and the atmosphere in lakes and reservoirs, it is still unclear whether GHG emissions from mature reservoirs stabilize at levels higher than those measured for nearby natural water bodies following the first 10-15 years after impoundment. Discrepancies exist in the literature about yearly averaged CO_2 and methane (CH_4) emissions from mature Quebec reservoirs compared to neighboring lakes (Duchemin et al. 1995, 1999; Tremblay et al. 2005). These differences can be partly explained by inconsistencies in GHG flux measurements using the most common methods, *i.e.*, thin boundary layer equations and floating chambers and by the naturally large variations in GHG fluxes from season to season (Duchemin et al. 1999; Lambert and Fréchette 2005; Soumis et al. 2008). Furthermore, most comparisons of GHG fluxes between lakes and reservoirs have been carried out during summer when lakes are stratified while most reservoirs are well mixed (Marty et al. 2005). Therefore very little consideration is given to the summer accumulation of GHG in hypolimnetic lake waters, which are released upon water turnover in the fall; in addition, the water column is well-mixed over most of the reservoir area throughout the year, this leads to increased oxygen levels in the deeper parts of the reservoir and to enhanced bacterial OM degradation that contributes to the total atmospheric GHG emissions.

Wood harvesting in the boreal forest leads to higher DOC, total nitrogen and phosphorus (TN and TP, respectively) exports from land to lakes (Carignan et al. 2000b; Lamontagne et al. 2000), and to increased benthic algal and bacterial biomass (Planas et al. 2000). High inputs of terrigenous and colored DOC in water bodies might also attenuate light penetration and decrease the activity and biomass of primary producers (Schindler et al. 1997; Planas et al. 2000; Karlsson et al. 2009). Only small variations in bacterial respiration (BR, CO_2 production) have been observed despite the large variations in net primary production (NPP, CO_2 fixation; del Giorgio et al. 1997). Prairie et al. (2002) have shown that BR is lower than NPP in lakes with low DOC concentrations and exceeds NPP in high DOC lakes. Additional inputs of DOC resulting from wood harvesting attenuates light penetration, which could inhibit NPP and promote BR and GHG emissions to the atmosphere, whereas increases in exports of TN and TP from land to aquatic systems could increase NPP (Schindler et al. 1997; Carignan and Steedman 2000; Prepas et al. 2001; Karsson et al. 2009). While wood harvesting enhances the inputs of nutrients and carbon into aquatic systems, to our knowledge no one has assessed the impact of such increased inputs on the aquatic C cycle and on the concentrations of dissolved CO_2 and methane (CH_4) and their fluxes to the atmosphere.

Carbon cycling in boreal freshwater aquatic systems is characterized by high variability within a fairly narrow range of natural chemical and biological conditions, which makes the understanding of the processes that control C dynamics and CO_2 exchanges with the atmosphere extremely difficult. In this study, we exploited the impact on C cycling of human perturbations such as long-term reservoir impoundment and watershed wood harvesting to assess C dynamics in freshwater systems. Our working

hypothesis is that the trends found when including both natural and perturbed systems reflect those in natural systems, although over a much wider range of chemical and biological conditions, and thus that they will not be masked by the random variability inherent to aquatic environments. The underlying assumption is that the major players controlling C cycling are the same in perturbed and natural systems, although their relative importance likely differs. We thus used a wide array of bulk water chemical proxies measured on samples collected in the summer of 2007 to assess C dynamics in freshwater systems with a natural or perturbed watershed (lakes and reservoirs with a natural or wood harvested watershed). In particular, we tried to assess how natural systems respond to human perturbation, and how this response affects GHG fluxes at the air-water interface. To minimize the extent of random variability, we collected our samples during a season when in-lake physico-chemical conditions are fairly stable (Summer), and we selected water bodies with similar characteristics in the southeastern Canadian boreal region, thus facilitating comparison of the aquatic C cycle between the different systems.

3.3 Materials and methods

3.3.1 Study sites

Two hydroelectric reservoirs and five natural lakes situated in the boreal forest of the Province of Quebec (Canada; 46°10′ to 47°46′ N; 76°12′ to 78°24′ W) were sampled for short periods (3 to 7 days spent at each site, with several daily GHG measurements) in May (for water DIC and total POC samples only) and July of 2007.

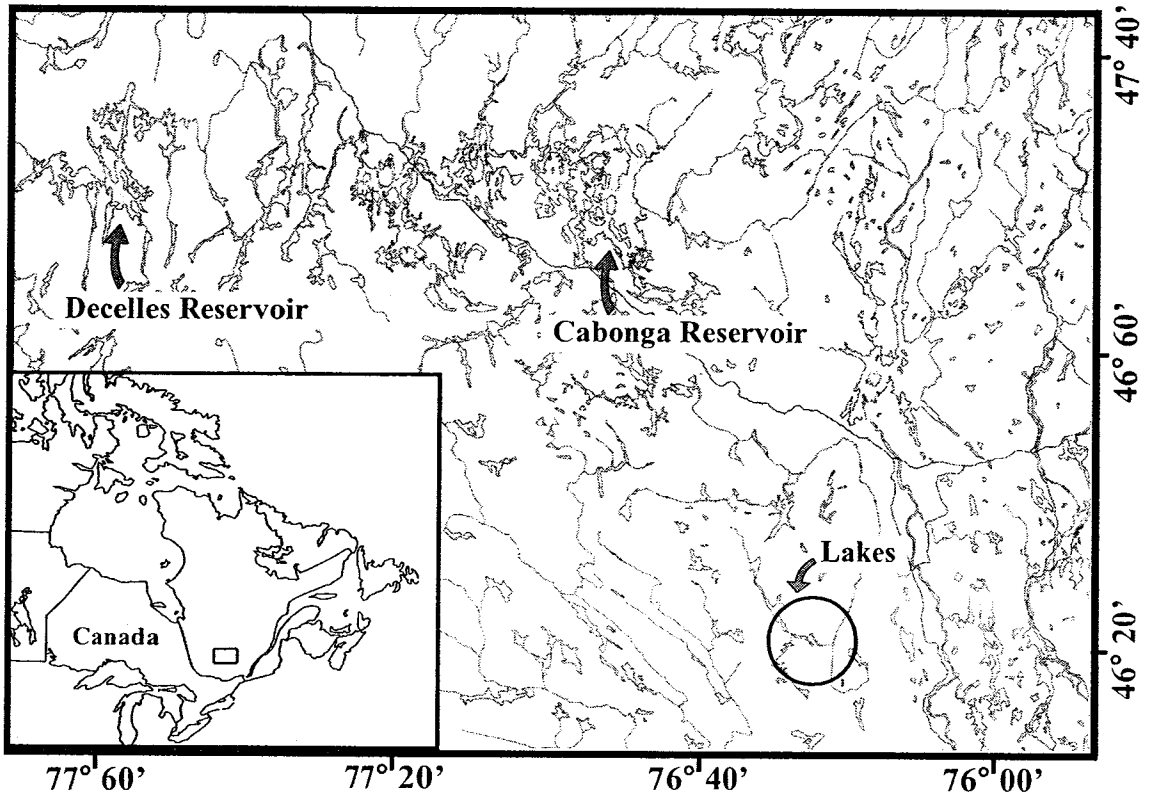

Figure 3-1. Map of eastern Canada and selected sampling sites. Exact coordinates are listed in Table 3-1.

An extended report of seasonal variations in bulk water chemical parameters (*e.g.* DOC, GHG) in these aquatic systems will be published elsewhere. Our sampling strategy, dictated by logistic and financial considerations, only captures a snapshot picture of systems that are highly variable; it is however suitable since our main goal is not a systematic comparison of natural and perturbed systems. The watershed of one reservoir (Decelles) and two lakes (Clair and Bouleau) were wood harvested less than 2 years before sampling, whereas the watersheds of the remaining water bodies were not exploited. While wood harvesting activities represented only about 1 to 5% of the total watershed drainage area, they were located in the direct vicinity of the water bodies, with non-harvested protection bands of about 20-m along brooks and water bodies. We

estimated conservatively from satellite pictures the percentage of the near lake/reservoir shoreline (within 2-km from shore) directly affected by the harvested land at about 10-25% for lakes, and about 5% for the Decelles Reservoir.

The Cabonga and Decelles reservoirs were impounded in 1928 and 1938, respectively. Both are thus representative cases of mature hydroelectric reservoirs. All lakes and reservoirs had watersheds with 42-74% tree coverage (conifers – mostly spruce, and broad-leaf deciduous species such as maple, white birch and yellow birch) and 5 to 32% peatland coverage, with the rest mainly being moist soils with less than 1% of uncovered bedrock; additional details on these water bodies are listed in Table 3-1.

For normalizing spatial and depth variability, DOM, POM, nutrients and dissolved GHG (CO_2 and CH_4) were sampled at four stations within each lake, while nine and eleven stations were sampled in the Cabonga and Decelles reservoirs, respectively. Each sampling station was selected randomly at pelagic or littoral locations most representative of the lake/reservoir, and visited more than once and up to eight different occasions.

Table 3-1. Characteristics of the sampled water bodies

Water body	System	Land use	Lake area (km^2)	Drainage area (km^2)	Mean slope[a] (%)	# of stations	Water depth (m)[b]	T° depth (m)[c]	Photic depth (m)[d]	Coordinates
Brock	Lake	Natural	0.82	6.35	N/A	4	3 to 27	6	14.2	46°16'26.4"N 76°20'35.2"W
Mary	Lake	Natural	0.58	1.80	1.26	1	1.5 to 10	5	N/A	46°15'37.2"N 76°12'50.8"W
Jean	Lake	Natural	1.88	7.31	5.87	4	6 to 32	5.5	8.4	46°21'43.9"N 76°20'42.1"W
Clair	Lake	Wood harvested	1.75	47.0	7.75	4	5 to 17	4.5	4.0	46°11'06.7"N 76°24'53.2"W
Bouleau	Lake / flooded	Wood harvested	0.34	8.23	7.1	4	4 to 20	3.0	3.0	46°14'16.5"N 76°27'13.9"W
Cabonga	Reservoir	Natural	434	2 616	N/A	9	3 to 23	none	3.0 to 7.3	47°20'07.0"N 76°34'51.0"W
Decelles	Reservoir	Wood harvested	237	13 131	N/A	11	2 to 21	none	2.5 to 3.4	47°41'50.9"N 78°10'38.9"W

[a] Watershed mean slope calculated from : Slope = 100*tan(angle), where the maximum angle is 45 degrees and tan represents the tangent function. [b] Ranges of sampling sites water depth, which including the deepest location in lakes. [c] T° stands for thermocline. [d] Depth at which light intensity falls below the 1% level.

3.3.2 Field sampling

Carbon dioxide and CH_4 concentrations and fluxes were obtained using the method and equations of Soumis et al. (2008), based on the work of Cole and Caraco (1998). Briefly, four 30-mL samples of surface water were collected with 60-mL syringes. Upon return to the laboratory, 30-mL of ultrapure nitrogen (N) gas were added to each one to create an inert gas headspace. The syringes were hand-shaken for exactly one minute and seated horizontally for phase equilibration for two minutes. The water was then slowly expelled from the syringes and its temperature recorded for equilibrium calculations. The concentration of the gas samples were measured with a Varian-Star 3400 gas chromatograph fitted with flame ionization and thermal conductivity detectors for CH_4 and CO_2 analysis, respectively. All GC analyses were performed within four hours of sampling. Water temperature and wind speed one meter above water level were recorded on site; wind speed was extrapolated to 10 meters using the method described in Soumis et al. (2008). Quantification was done using a certified external gas standard of CO_2 and CH_4, each at a concentration of 1.01 % (Scotty 48, Mix 218, Supelco); details of the GHG flux calculation are available in Appendix A.

Water for nutrient analyses was sampled in acid rinsed 60-mL HDPE bottles and kept frozen until analysis. Two 4-mL samples for DOC analysis were collected at each site, doped using mercury dichloride ($HgCl_2$) and kept at 4°C until analysis. Water column GHG, DOC and nutrients profiles were also performed at 0.5 to 5 meters interval using a 12-V submersible pump. Preliminary comparison of profiles acquired using a pump and a Kemmerer sampler showed that more reproducible results were obtained for GHG using the pump while obtaining the same level of accuracy (data not shown). Water

temperature, dissolved oxygen and pH profiles were recorded using a YSI 6600 multiprobe system.

Large volumes (200-250 L) of water (integrating the entire water column down to a maximum depth of 10 meters) were collected at each sampling site in 50-L pre-rinsed Nalgene containers. The water was passed through a 70-μm nylon mesh filter upon collection. DOM (< 0.45 μm) and FPOM (0.45 – 70 μm) were separated using a tangential flow filtration (TFF) system fitted with a 0.45-μm polyvinylidene difluoride cartridge filter. The TFF system was coupled to a RealSoft PROS/2S reverse osmosis (RO) system to concentrate DOM as described by Ouellet et al. (2008). Briefly, upon feeding the TFF with bulk water using a peristaltic pump, the retentate (containing FPOM) was returned to the original container while the permeate was fed to the RO system for DOM concentration. Dilute NaOH rinses of the RO membranes was done between each sample to limit carry over between samples. Carbon mass balance calculations showed that the mean DOC recoveries of the system were of 86.9 ± 2.4 %, while the mean total OC recoveries (FPOC + DOC) were of 90.4 ± 3.5 % (Ouellet et al. 2008). The POM and DOM samples were doped with $HgCl_2$ (~ 0.3 mM final concentration) and freeze-dried in preparation for elemental (C, N and Fe) and isotopic analysis ($\delta^{13}C_{org}$ and $\delta^{15}N_{tot}$).

Water for DIC and POC analyses was sampled every 1 to 5 meters over the entire water column to a maximum of 20 meters in each water body in spring and summer of 2007. Water samples for DIC analysis were stored in air-tight 500-mL amber glass bottles (no head space), preserved with $HgCl_2$ and kept at 4 °C until analysis. The

corresponding POC samples were collected on combusted GF/F filters (0.7-μm nominal pore size) and freeze-dried.

3.3.3 Soil leaching experiment

Humus-free soil litter and sliced soil cores (1-cm resolution) collected around the water bodies under study in May and July 2007 were freeze-dried and homogenized in preparation for elemental and isotopic analysis. Additionally, three non-freeze-dried representative boreal forest soil litters (O horizon) as well as the organic, sub-organic and inorganic soil layers (A, B and C horizons) of each core were mixed in a 35-mL Teflon tube with milli-Q water (1:1 v/v) and extracted three times. Volume aliquots of the extracts were filtered using 0.7-μm GF/F filters and freeze-dried for elemental and isotopic analysis while the remaining aliquots were analyzed for inorganic N content using a TRAACS 800 AutoAnalyser system.

3.3.4 DOC, total nitrogen and total phosphate measurements

Dissolved organic carbon analysis was done in duplicate or triplicate using a Shimadzu 5000A Total Carbon Analyzer, with a reproducibility of ± 5%. TN (dissolved organic nitrogen plus nitrate and nitrite) and TP (organic phosphorus plus phosphate) were analyzed using standard $NaOH/K_2S_2O_8$-based methods (818-47 and 812-86T respectively) from Bran Luebbe Analyzing Technologies on a TRAACS 800 AutoAnalyser.

3.3.5 Elemental and isotopic measurements

The C and N concentrations as well as $\delta^{13}C$ and $\delta^{15}N$ compositions were acquired on all integrated DOM and FPOM samples as well as on the soil and soil leachate samples using an EuroVector 3028-HT elemental analyzer coupled to an Isoprime GV

Instruments isotope ratio mass spectrometer (EA-IRMS). Elemental and isotopic calibration was done using IAEA-C6 sucrose standard ($\delta^{13}C$ = -10.45 ± 0.03‰; C = 42.11%, Coplen et al. 2006), IAEA-N1 ammonium sulfate ($\delta^{15}N$ = 0.43 ± 0.07‰; N = 10.60%, Böhlke and Coplen 1995) and β-alanine, a pre-calibrated in-lab standard ($\delta^{13}C$ = -25.98 ± 0.23‰; C = 40.45% and $\delta^{15}N$ = -2.21 ± 0.24‰; N = 15.72%). The samples were decarbonated using HCl fumigation prior to C analysis (Hedges and Stern 1984); OC (with acidification) and TN (no acidification) concentrations and stable isotope compositions are thus reported here. Reproducibility for the elemental and isotopic analyses was < 1% and < 0.3 ‰, respectively.

Dissolved organic carbon concentrations and isotopic ratios were acquired with an Isoprime Multiflow instrument and using two pre-calibrated in-house $CaCO_3$ powders ($\delta^{13}C$ = -3.91 ± 0.08 ‰ and 9.58 ± 0.08 ‰, respectively). Standards were accurately weighed to obtain final C concentrations ranging between 1 and 10 mg L^{-1}. Degassed deionized water was added to the powder and quickly transferred to air-tight vials for quantitative analysis. Between 0.5 and 1.5 mL of standard or sample was transferred through the septum of an air-tight and helium-purged 4-mL vial containing 50 µL of phosphoric acid. The vials were mixed and digested for 60 minutes at 60 °C prior to analysis. Standard water blanks and vial blanks were also analyzed to correct for water and air contamination.

3.3.6 DOM-complexed iron

The iron content of the concentrated DOM samples collected with the reverse osmosis system were analyzed for iron by direct injection using an Agilent 7500 series ICP-MS following acidification with nitric acid and internal standard addition

(scandium). Quantification was done through external calibration with a Certipur ferric nitrate standard. Five replicate measurements were acquired for each sample, with a precision and accuracy better than 3%.

3.3.7 Statistical analyses

Greenhouse gases, DOC and nutrient measurements were first averaged for each sampling station independently of the number of samples analyzed. Average values for entire water bodies were then calculated using the values obtained from each sampling stations, and standard deviations were propagated using the pooled standard deviations (Harris 1999). This method prevented the over-representation of the stations with higher sampling frequencies; our results thus integrate spatial and temporal (*i.e.* daily) variations over the short period spent at each site. Where applicable, the significance of the observed trends was tested using the Welch's t test, which allows the evaluation of parameters having unequal data variance and replicates.

3.4 Results

3.4.1 Greenhouse gases

Averaged CO_2 and CH_4 concentrations in surface waters for the four scenarios studied in this work are presented in Table 3-2. The non-harvested Lake Brock and Lake Jean had significantly lower ($p < 0.0005$) averaged dissolved CO_2 concentrations (21.4 ± 6.0 and 26.7 ± 8.6 μmol L^{-1}, respectively) compared to the non-harvested Reservoir Cabonga (38.8 ± 9.2 μmol L^{-1}). The wood harvested Lake Bouleau, which was recently flooded following the erection of a beaver dam, had very high dissolved CO_2 concentrations (80.4 ± 13.0 μmol L^{-1}).

Table 3-2. Carbon dioxide and methane concentrations in surface waters and fluxes to the atmosphere

Water body	# of stations	n [a]	$[CO_2]$ (μmol L^{-1})		$[CH_4]$ (nmol L^{-1})		Wind speed [b]	CO_2 Fluxes [c] (mmol CO_2 m^{-2} d^{-1})		CH_4 Fluxes [c] (μmol CH_4 m^{-2} d^{-1})	
			Average [d]	Range	Average [d]	Range	Average [d]	Average	Range	Average	Range
Brock	4	11	21.4 (6.0)	14.7 - 31.8	99.4 (19.3)	62.9 - 141	2.1 (3.4)	4.0	0.9 - 8.9	31	0 - 146
Jean	4	22	26.7 (8.6)	19.4 - 50.4	73.2 (27.5)	33.6 - 218	7.0 (6.0)	13.0	2.9 - 55.0	214	0 – 939
Clair	4	16	31.1 (10.1)	10.7 - 43.8	41.3 (12.6)	10.7 - 54.9	5.9 (4.3)	17.0	5.8 - 30.2	123	0 - 519
Bouleau	4	20	80.4 (13.0)	62.5 - 106	72.6 (25.7)	40.8 - 156	6.8 (3.7)	60.4	29.1 – 105.1	417	10 - 1515
Cabonga	9	35	38.8 (9.2)	13.1 - 61.9	57.8 (14.9)	22.2 - 129	11.4 (5.3)	28.7	7.7 - 54.1	434	18 - 2420
Decelles	11	62	41.5 (6.3)	27.7 - 59.8	67.3 (20.8)	27.0 - 145	11.2 (6.2)	38.6	10.3 – 104.5	579	0 – 2875

[a] Total number of measurements evenly distributed within the number of sampling stations. [b] Wind speed at 1 m above water surface. [c] Due to large variations in wind speed, standard deviations of corresponding averages were not calculated. [d] Standard deviations are shown between parentheses (details in materials and methods section). The total sampling and analysis error was 4.1 ± 1.7%.

A comparison of the non-harvested lakes and reservoirs with their wood harvested counterparts (the recently flooded Lake Bouleau excluded) shows that the latter had significantly higher surface water CO_2 concentrations (reservoirs: $p < 0.025$; lakes: $p < 0.1$). Surface water CH_4 concentrations were about three orders of magnitudes lower than those of CO_2 (10.7 to 106.4 μmol L^{-1}) and varied widely (from 10.7 to 218.9 nmol L^{-1}), with no clear relationship with reservoir operation, wood harvesting, water column depth and oxygen level; the only noticeable trend was that sites sampled under low wind conditions had higher surface CH_4 concentrations.

The diffusive CO_2 and CH_4 fluxes to the atmosphere calculated using the BLE equations are presented in Table 3-2. In our study, the two natural lakes monitored for GHG had significantly lower CO_2 fluxes than the non-harvested Reservoir Cabonga ($p < 0.0005$), the flooded Lake Bouleau ($p < 0.0005$), and wood harvested lakes ($p < 0.1$); the Cabonga Reservoir also emitted significantly less CO_2 to the atmosphere ($p < 0.01$) compared to the wood harvested Decelles Reservoir. The methane concentrations and fluxes measured in Lake Brock were obtained in periods of low wind, which explains the high water concentration levels and low fluxes recorded for this lake. Independently of the year of impoundment, flooded systems (Lake Bouleau and both reservoirs) were emitting significantly more methane ($p < 0.0005$) to the atmosphere suggesting higher anaerobic OM degradation in the sediment (Striegl and Michmerhuizen 1998; Steinmann et al. 2008). Although this hypothesis should be verified, methane found in the pelagic zones (Table 3-2) likely originated from diffusion through the thermocline as very little hypolimnetic accumulation was observed (equivalent to less than 0.2 and 7 % of the daily CH_4 and CO_2 atmospheric emissions respectively, data not shown).

The CO_2 fluxes measured in the Cabonga Reservoir (average of 28.7 mmol m^{-2} d^{-1}; range of 7.7 to 54.1 mmol m^{-2} d^{-1}) are similar to values reported in other studies for the same reservoir during periods of no ice cover (31.8 and 31.4 mmol m^{-2} d^{-1}, St-Louis et al. (2000) and Tremblay et al. (2005) respectively). Diffusive CH_4 fluxes measured in the Cabonga Reservoir in this study are about half (434 µmol m^{-2} d^{-1}) those reported by Tremblay et al. (2005), which used floating chambers that capture both bubbling and diffusive GHG emissions. Bubbling fluxes were previously estimated to account for 36% of the total yearly CH_4 emissions in boreal reservoirs whereas they are not significant for CO_2, representing less than 0.1 % of the total yearly CO_2 emissions (Duchemin et al., 2000).

3.4.2 Water chemistry

The concentration of DOC, TN and TP, as well as pH in the surface waters of the natural and perturbed aquatic systems are presented in Table 3-3. Averaged water pH and DOC concentrations co-varied (Table 3-3 and Figure 3-2A; $r^2 = 0.55$) with more acidic, DOC-rich waters observed in the perturbed systems. The non-harvested reservoir and the wood harvested systems had significantly lower pH values ($p < 0.0005$ and < 0.01, respectively).

Table 3-3. Water chemistry variables measured in this project

Water body	# of stations	[DOC] (mmol L^{-1})		pH		N, P	[TN] (µmol L^{-1})	[TP] (µmol L^{-1})
		n [a]	Average [b]	n [a]	Average [b]	n [a]	Average [b]	Average [b]
Brock	4	7	0.217 (0.010)	4	7.83 (0.20)	8	10.1 (0.6)	0.34 (0.02)
Mary	1	1	0.394 (N/A)	N/A	N/A	1	15.7 (N/A)	0.40 (N/A)
Jean	4	16	0.326 (0.048)	8	7.31 (0.31)	12	12.1 (1.2)	0.27 (0.03)
Clair	4	10	0.505 (0.099)	7	6.73 (0.26)	10	16.0 (1.2)	0.24 (0.06)
Bouleau	4	18	0.699 (0.096)	8	6.55 (0.36)	19	21.3 (2.5)	0.39 (0.12)
Cabonga	9	33	0.415 (0.072)	19	6.98 (0.22)	30	13.0 (1.2)	0.24 (0.06)
Decelles	10	37	0.633 (0.079)	13	6.68 (0.37)	7	19.0 (0.6)	0.33 (0.05)

[a] Total number of measurements evenly distributed within the number of sampling stations. [b] Standard deviations are shown between parentheses (details in materials and methods section).

Lower averaged DOC concentrations were found in water bodies with an unperturbed watershed (0.217 to 0.415 mmol L^{-1}) compared to systems with a harvested watershed (0.505 to 0.699 mmol L^{-1}; $p < 0.0005$). The same was observed for TN (9.3-17.5 µmol L^{-1} *vs.* 13.1-30.6 µmol L^{-1}; $p < 0.0005$). Including all systems, there was a strong positive linear relationship between DOC and TN concentrations ($r^2 = 0.86$, Figure 3-2B).

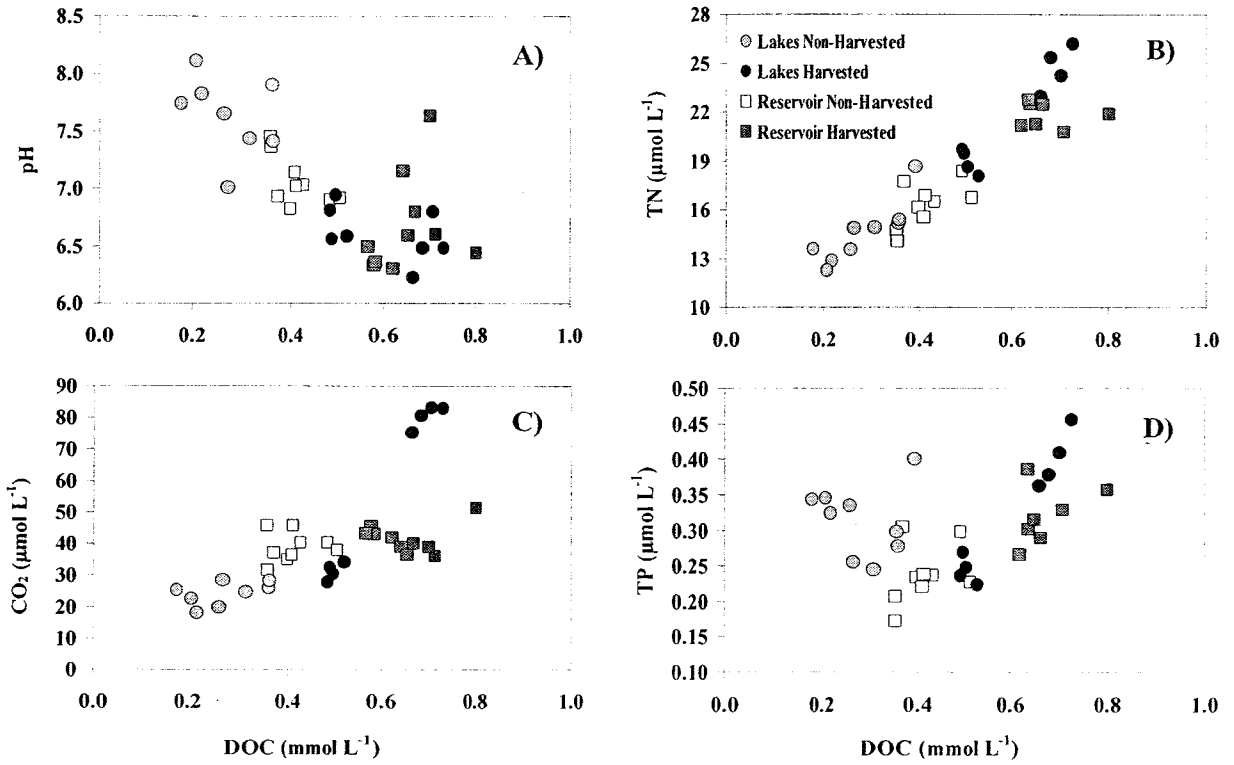

Figure 3-2. Relationship between measured bulk water parameters and dissolved organic carbon (DOC). In A) pH, B) total nitrogen (TN), C) carbon dioxide (CO_2), and D) total phosphorus (TP).

When considering only the perturbed systems, correlations between DOC and TP ($r^2 = 0.64$; Figure 3-2D) and CO_2 and TP ($r^2 = 0.65$, not shown, in agreement with Sobek et al. 2003) stand out with TP concentrations in natural lakes that are significantly higher than in the non-harvested Cabonga Reservoir ($p < 0.0005$).

To gain information on the balance and extent of net heterotrophy (CO_2 producing bioprocesses) and net autotrophy (CO_2 consuming bioprocesses) in our systems, CO_2 concentrations and oxygen percentage saturation levels (% O_2) were grouped by zones corresponding to contrasting physico-chemical characteristics within lakes and reservoirs (epi/hypolimnion, photic, and aphotic; Figure 3-3). In lakes with wood harvested watersheds, the thermocline was always positioned at a depth corresponding to the

bottom of the photic zone (Table 3-1). A strong correlation (r^2 = 0.80) between CO_2 concentrations and % O_2 of hypolimnetic lake water was observed (Figure 3-3A).

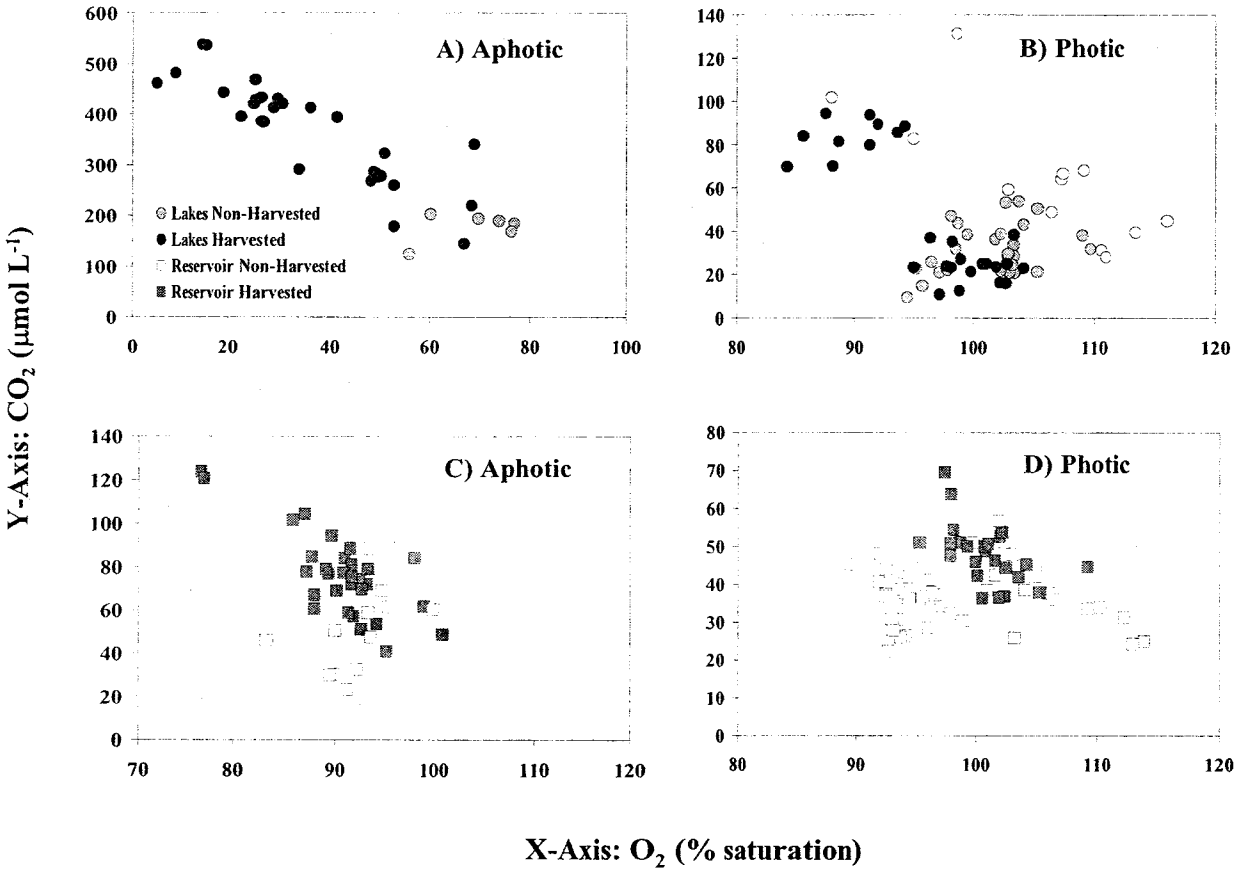

Figure 3-3. Relationship between carbon dioxide (CO_2) and dissolved oxygen (O_2) saturation levels. In A) the aphotic hypolimnetic zone (lakes), B) the photic epilimnetic zone (full circles, lakes) and the photic hypolimnetic zone (empty circles, natural lakes only), C) the aphotic epilimnetic zone (reservoirs), and D) the photic epilimnetic zone (reservoirs).

Generally, higher % O_2 were found in the photic epilimnetic and/or compared to the aphotic hypolimnetic water masses in lakes (Figure 3-3B). Reservoirs are hydrologically distinct from lakes, with dynamic changes in water level (filling in the spring and early summer, and draining during the winter) and water circulation, which both efficiently mix water columns preventing thermocline formation at most sampling sites (Marty et al. 2005). As shown in Figure 3-3C (aphotic epilimnion in reservoirs) and -3D (photic epilimnion in reservoirs), CO_2 concentrations were negatively correlated to

% O_2 in the Decelles Reservoir, with greater correlation in the aphotic compared to the photic zone (r^2 = 0.57 and 0.28, respectively). These results suggest that epilimnetic CO_2 production through heterotrophy (and photo-oxidation in the photic zone) was greater than primary O_2 production through autotrophy whereas no definitive trend emerged for the Cabonga Reservoir.

3.4.3 Terrestrial and aquatic bulk organic matter analyses

To estimate the importance of terrestrial litter and soil as OM sources in the aquatic cycle of C, a DOM leaching experiment was carried out on samples collected in the vicinity of the water systems. The litter samples had $\delta^{13}C$, $\delta^{15}N$ and (C:N) compositions of -27.2 ± 1.1 ‰, -1.0 ± 0.9 ‰, and 35.1 ± 2.0, respectively, while soil OM from deeper horizons was generally more enriched in $\delta^{13}C$, $\delta^{15}N$ and had higher (C:N) ratios (Table 3-4).

Table 3-4. Bulk organic carbon and nitrogen analyses for soils and their dissolved organic matter extracts.

Sample	Soil depth (cm)	Soil				Soil extract			
		OC (%)[a]	$\delta^{13}C$ (‰)[b]	$\delta^{15}N$ (‰)[b]	$(C:N)_a$	OC (%)[a]	$\delta^{13}C$ (‰)[b]	$\delta^{15}N$ (‰)[b]	$(C:N)_a$
Boreal soil litter	surface	41.2	-27.2	-1.0	35.1	38.2	-26.0	0.7	21.6
Mary	1-2	37.9	-27.1	0.8	20.7	22.3	-25.2	4.8	9.5
	7-9	30.3	-25.8	6.3	22.9	22.9	-24.2	11.2	8.4
	12-15	5.4	-24.9	5.5	35.9	22.8	-24.5	9.5	9.4
Jean	1-2	50.5	-26.7	-0.7	30.7	36.4	-25.0	2.4	16.3
	9-12	22.9	-25.4	3.1	66.8	42.6	-23.8	5.4	21.3
	15-20	2.8	-25.1	N/A	N/A	18.1	-23.9	4.9	20.1
Cabonga	1-2	47.4	-26.2	1.6	36.6	46.9	-26.2	4.2	17.6
	7-9	8.5	-26.4	3.0	44.0	34.3	-24.1	4.3	25.7
	12-15	4.0	-25.5	4.4	35.6	25.4	-25.3	7.1	18.4
Decelles	1-2	49.2	-27.9	-3.4	53.4	41.8	-26.5	-0.7	28.5
	12-15	21.4	-26.3	0.6	115.7	40.9	-25.7	2.5	38.6
	15-20	4.4	-26.2	-2.0	251.9	37.7	-25.6	-0.4	77.0

[a,b] Analytical uncertainties of 1%[(a)] and 0.2‰[(b)].

Litter and soil leached significant quantities of water soluble OC and organic N (> 99% of leached TN was organic N; results not shown). The low (C:N) ratios measured for the leached material thus suggest that it is composed of N-rich, most likely hydrophilic labile OM. In most cases, the $\delta^{13}C$ signatures of the soil leachates were enriched by 1 to 2 ‰ compared to those of the initial bulk material (Table 4-4), while the enrichment was even greater for $\delta^{15}N$ (1 to 5 ‰). Soil leachates (C:N) ratios were also much lower than those of bulk OM (difference ranging between 11 and 175). Such elemental and isotopic fractionation suggests that a compositionally different pool of OM was released upon extraction of the soil OM with distilled water.

The bulk results obtained from the water column depth-integrated DOM and FPOM samples are shown in Table 4-5. For DOM, only small variations in $\delta^{13}C$ and $\delta^{15}N$ compositions were observed between water bodies, in agreement with data reported for different Quebec lakes and reservoirs (Hélie 2004; McCallister and del Giorgio 2008; Dubois et al. 2009). These small variations in stable isotope signatures were accompanied by increases in %OC and C:N of DOM, as well as increases in the concentration of DOM-complexed iron, highlighting the increased terrestrial inputs of disturbed system (Table 3-5, Figure 3-4A).

Table 3-5. Bulk organic carbon and nitrogen analysis for dissolved and fine particulate organic matter

Water body	# of stations	DOM						FPOM				
		OC (μmol L^{-1})	OC (%)[a]	$\delta^{13}C$ (‰)[b]	$\delta^{15}N$ (‰)[b]	$(C:N)_a$	Fe (nmol L^{-1})[c]	OC (μmol L^{-1})	OC (%)[a]	$\delta^{13}C$ (‰)[b]	$\delta^{15}N$ (‰)[b]	$(C:N)_a$
Brock	1	148	9.1	-28.0	-0.4	21.3	77.2	12.9	21.6	-28.6	0.2	12.1
Mary	1	184	6.3	-26.3	-2.7	21.6	37.0	25.1	25.6	-27.7	0.9	11.8
Jean	1	221	10.9	-26.8	-1.7	29.8	30.7	37.1	27.2	-28.6	-0.3	14.0
Clair	1	434	16.8	-27.1	-1.1	32.0	443.5	80.8	33.4	-28.6	0.1	18.7
Bouleau	1	506	16.9	-27.5	-1.9	33.2	N/A	77.5	27.8	-30.4	0.2	23.7
Cabonga	7	299 (39)	13.2 (1.4)	-27.0 (0.2)	-1.2 (1.0)	33.4 (3.9)	100.6 (65.9)	44.9 (27.6)	28.2 (5.7)	-28.7 (0.4)	-0.3 (0.6)	19.1 (2.4)
Decelles	6	543 (73)	18.8 (2.8)	-27.1 (0.2)	-1.6 (1.5)	41.6 (8.3)	450.2 (135)	43.5 (21.6)	26.0 (4.7)	-28.7 (0.5)	1.6 (0.3)	24.9 (4.5)

[a,b] Analytical uncertainties of 1%[(a)] and 0.2‰[(b)]. [c] Iron complexed to dissolved organic matter exclusively.

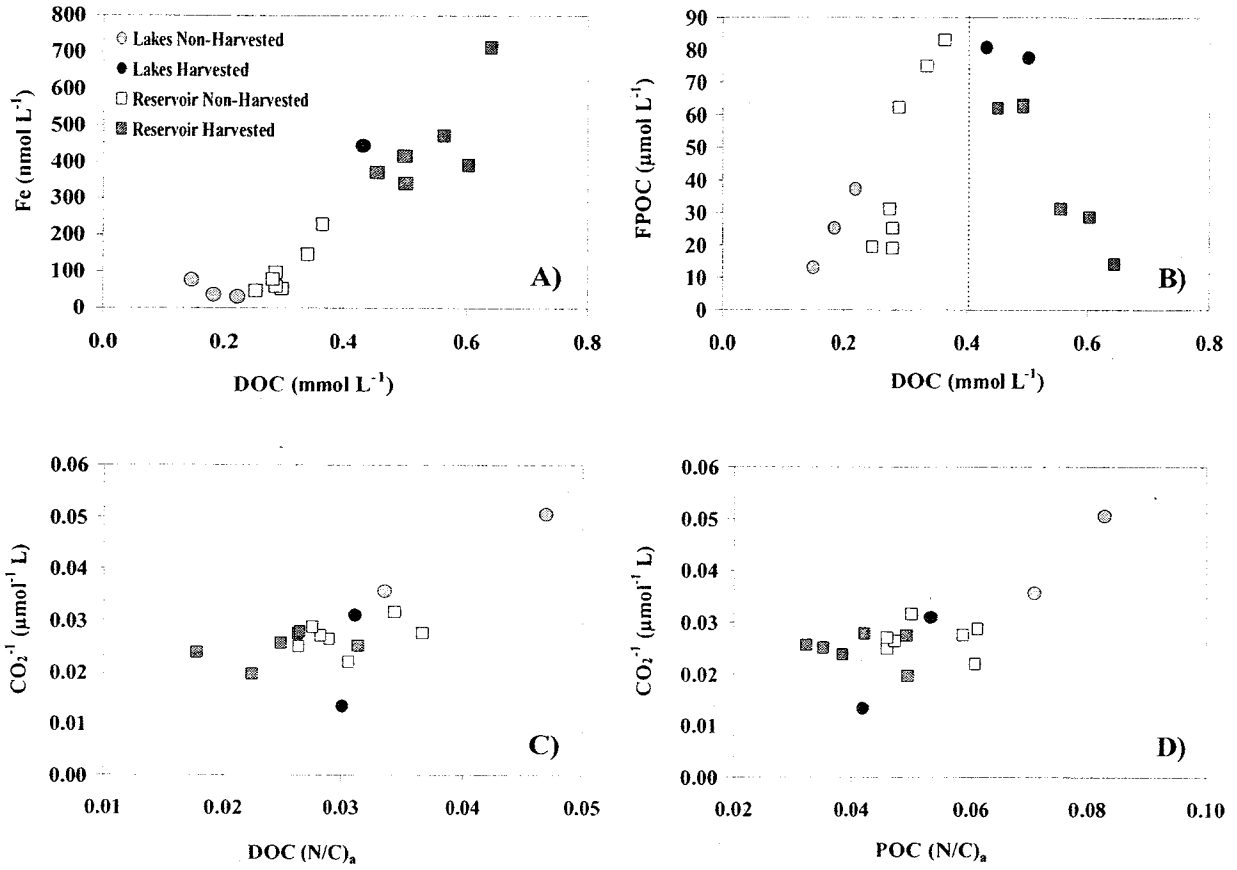

Figure 3-4. Relationships between dissolved or particulate OM collected by tangential flow filtration - reverse osmosis and key parameters from the water column. (A) DOM-associated iron *vs.* DOC concentrations; (B) FPOC *vs.* DOC; and CO_2 *vs.* atomic N:C ratio of (C) DOM and (D) POM.

In boreal systems, FPOM can be supplied to water bodies through two major sources, namely soil litter and autochthonous derived matter (phytoplankton, bacteria and debris). Terrestrial C_3 plants have traditionally been assigned $\delta^{13}C$ and $\delta^{15}N$ compositions of -27‰ and 0.4‰, respectively (Meyers 1997). Similar $\delta^{13}C$ values were found in this work for boreal forest soil litter and top soil layer (-27.2 ± 1.1 and -26.1 ± 0.9 ‰ for the O and A horizons, respectively; Table 3-4). The $\delta^{13}C$ composition of phytoplankton measured by Marty and Planas (2008) during the summer in different boreal lakes and reservoirs of Quebec averaged -32.7 ± 1.7 ‰. In agreement with above values, the $\delta^{13}C_{FPOC}$ signatures measured in this study ranged between -27.7 and -30.4 ‰, likely

reflecting a mix of the terrestrial (litter and soil) and algal end-members. This result is supported by the measured atomic $(C:N)_{FPOM}$ (Table 3-5), which falls between the values obtained for the two end-members analyzed in this study (terrestrial litter: 35.1 ± 2.0, Table 3-4; and cultivated algae: 9.7 ± 0.1, data not shown). Higher $(C:N)_{FPOM}$ values were found for perturbed water bodies (as high as 31.2 in the Decelles reservoir), and suggest greater inputs of terrestrial OM in these systems. FPOC and DOC concentrations were linearly correlated, although with contrasting slopes for non-harvested and harvested systems (positive and negative correlation, respectively, Figure 3-4B), which suggests that reservoir operation and wood harvesting both had an effect on FPOC concentrations.

Perdue and Koprivnjak (2000) reported on the non linear relationships in mixing models where (C:N) ratios were plotted against stable C isotopic compositions. It was mathematically shown that scatter plots reflect relationships between the denominators rather than the numerators. In Figures 3-4C and -4D the (N:C) ratio plotted as a function of $[CO_2]^{-1}$ concentrations show that in surface water, CO_2 concentrations were correlated with the (N:C) ratio of depth integrated DOM and POM (both with $r^2 = 0.50$); weaker correlation were found with the (C:N) ratio (r^2 of 0.30 and 0.31, respectively; not shown).

3.4.4 Dissolved inorganic carbon (DIC)

The $\delta^{13}C$ signatures of DIC ($\delta^{13}C_{DIC}$) are useful for constraining the sources and sinks of C in aquatic systems. Plots of $\delta^{13}C_{DIC}$ *vs.* $[DIC]^{-1}$ are used to gain insight on the mixing behaviour (heterotrophic *vs.* autotrophic activity) of the DIC pool through seasonal variations in $\delta^{13}C_{DIC}$ signatures. The spring and summer $\delta^{13}C_{DIC}$ depth profiles

were compiled and plotted on Figure 3-5. Independently of wood harvesting, lakes often exhibited lower $\delta^{13}C_{DIC}$ values (as low as -41 ‰, Figures 3-5A and -5B) compared to reservoirs (Figures 3-5C and -5D).

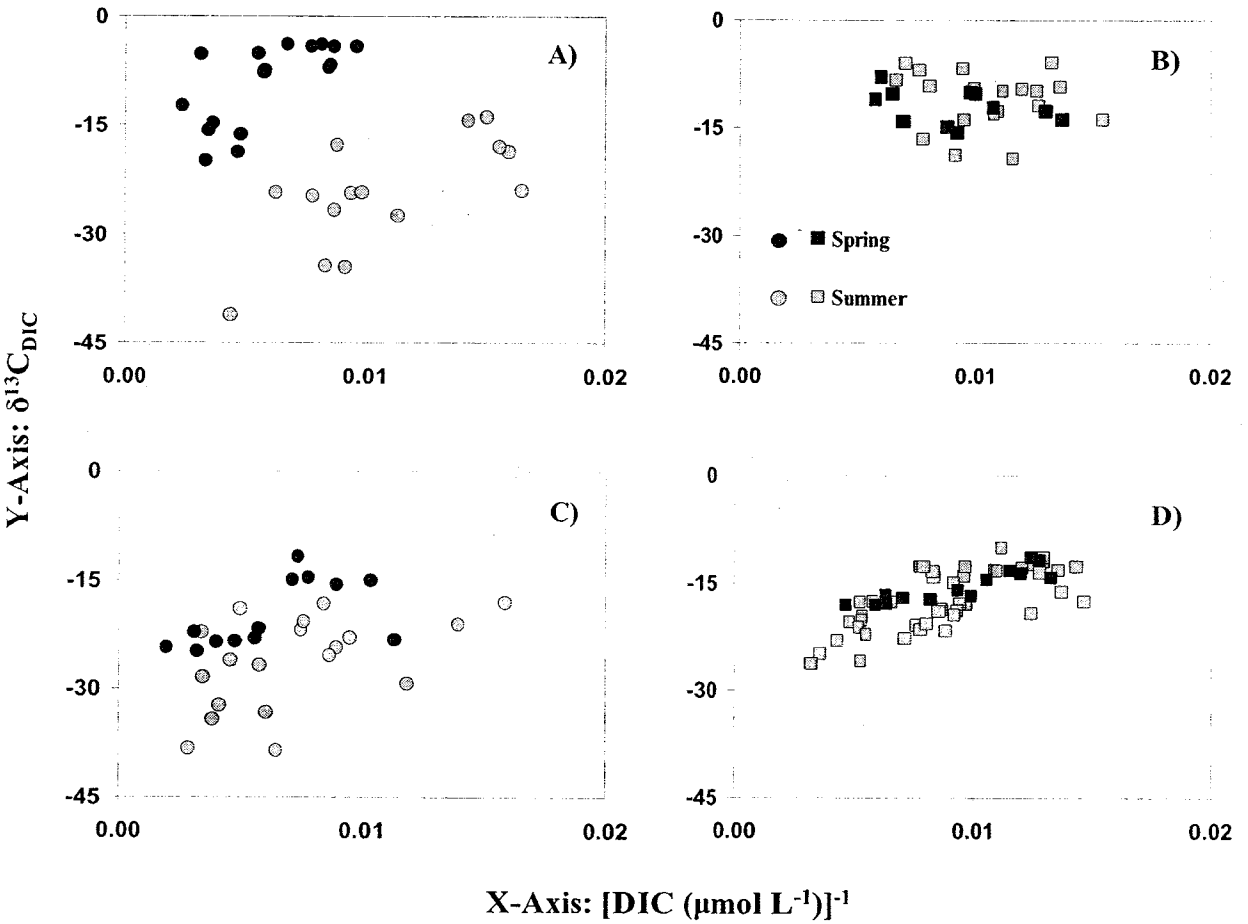

Figure 3-5. Relationship between the δ13C signature of DIC and the inverse of DIC concentrations in the water column. (A) natural lakes (Brock and Jean), (B) non-harvested reservoir (Cabonga), (C) harvested lakes (Clair and Bouleau) and (D) harvested reservoir (Decelles).

Such low C isotopic values indicate that a significant fraction of highly depleted CH_4 originating from methanotrophic activity is oxidized and contributes to the total DIC pool. Because sedimentary methane $\delta^{13}C$ compositions fluctuate by as much as 16 ‰ within periods as short as 24 hours (Jedrysek 1995), its contribution to total $\delta^{13}C_{DIC}$ cannot be calculated with accuracy. Isotopic evidence of methane contribution to the DIC

pool was observed independently of the lake but only for high DIC concentration samples within or just below the thermocline. Substantial seasonal $\delta^{13}C_{DIC}$ differences were measured in natural lakes; in the spring of 2007, Lake Brock and Lake Jean were characterized by higher concentrations and a ^{13}C-enriched DIC pool (-3.9 to -18.7 ‰), while DIC concentrations and $^{13}C_{DIC}$ compositions were lower in the summer (-13.9 to -41.3 ‰). Such seasonal variation was also observed in perturbed lakes although the DIC was generally more $\delta^{13}C$-depleted in these water bodies. This suggests that in addition to methane oxidation, photo- and bacterial oxidation of the reactive and $\delta^{13}C$ depleted DOC pool was probably contributing to the $\delta^{13}C_{DIC}$ depletion (Osburn et al. 2001; McCallister and del Giorgio 2008).

3.4.5 POC isotopic variations

To identify POC sources and to document their relationship to DIC (Lehmann et al. 2004; Cole et al. 2002), $\delta^{13}C_{DIC}$ was plotted against $\delta^{13}C_{POC}$ for samples collected at different depths in each water body (Figure 3-6). Both parameters were correlated in the spring for harvested systems (Figures 3-6C, $r^2 = 0.44$ and -6D, $r^2 = 0.60$) suggesting high primary production (enriched $\delta^{13}C_{DIC}$) following the melting of the ice cover. In summer, only the wood harvested Reservoir Decelles exhibited a moderate correlation between $\delta^{13}C_{DIC}$ and $\delta^{13}C_{POC}$ (Figure 3-6D, $r^2 = 0.43$), which likely reflects high heterotrophic activities (depleted $\delta^{13}C_{DIC}$, see discussion).

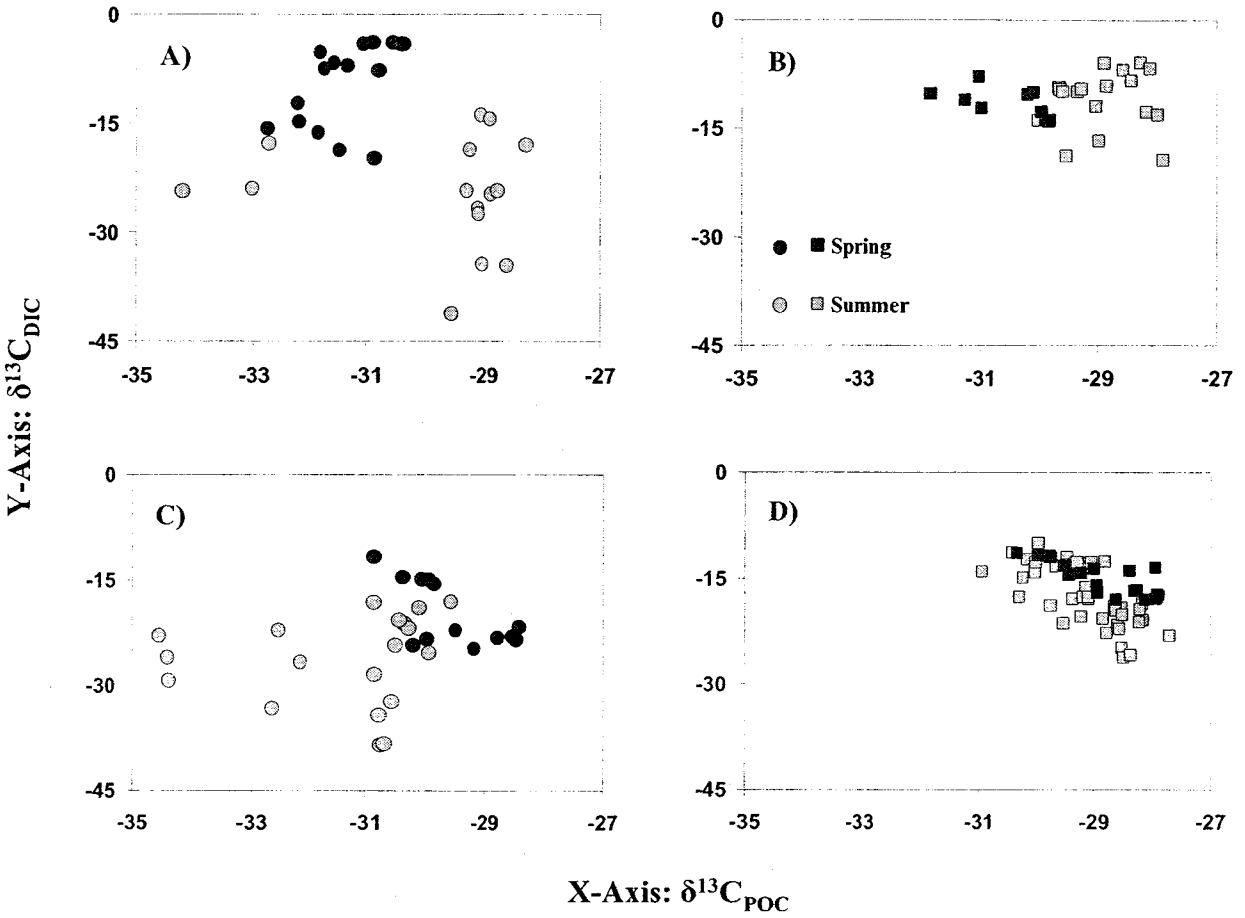

Figure 3-6. Relationship between the δ13C signatures of DIC and POC. Both fractions were sampled at same depths in the water column of (A) natural lakes (Brock and Jean), (B) non-harvested reservoir (Cabonga), (C) harvested and flooded lakes (Clair and Bouleau) and (D) harvested reservoir (Decelles).

Spring $\delta^{13}C_{POC}$ results presented in Figures 3-6A and -6B show that water bodies with an unperturbed watershed are dominated by algae-derived POM ($\delta^{13}C$ signature of algae, $\delta^{13}C_{algae}$, equal to -32.7 ± 1.0 ‰, as per Marty and Planas, (2008) and (C:N) ratios that ranged between 9.2 and 11.8 (results not shown)). Wood harvested lakes and reservoirs (Figures 3-6C and -6D, respectively) were characterized by a higher relative proportion of terrestrial POM in the spring, as shown by their $\delta^{13}C$ signature and (C:N) ratios closer to those of litter (-27.2 ± 1.1 ‰, and 11.3 to 23.5, respectively; Table 3-4). In summer, we observed an enrichment in $\delta^{13}C_{POC}$ for systems with a natural watershed,

which contrasts with the small summer $\delta^{13}C_{POC}$ depletion relative to spring values in wood harvested lakes. $\delta^{13}C_{POC}$ depletions in summer generally coincided with lower $(C:N)_{POM}$ ratios (results not shown), which are explained by a higher relative abundance of phytoplankton, zooplankton and/or bacteria (with atomic C:N ratios varying from 8 to 12, 5 to 6, and 4 to 7, respectively; (del Giorgio and France 1996; Kaiser and Benner 2008; K. Homblette et al. 2009)).

The $\delta^{13}C_{FPOC}$ isotopic composition (0.45 to 70-µm size fraction; Table 3-5) did not vary much between systems (-27.7 to -30.4 ‰); however generally more depleted values were measured for total POC (> 0.70-µm; -28.2 to -34.5 ‰) suggesting that the larger phytoplankton and zooplankton cells removed during the collection of FPOC are substantially depleted in $\delta^{13}C$ relative to terrestrial and bacterial POM. The most depleted $\delta^{13}C_{POC}$ values (-34.4 ± 0.1 ‰, Figure 3-6C, harvested or flooded lakes) were measured for samples collected within the photic zone of Lake Bouleau and, as suggested by $(C:N)_{POM}$ ratios of 9.29 ± 0.56 (n = 3), were mainly of phytoplanktonic origin. Samples with $\delta^{13}C_{POC}$ compositions of -32.5 ± 0.3 ‰ and $(C:N)_{POM}$ ratios of 5.88 ± 1.41 (n = 3) were found below the photic zone and in the bottom waters of the same lake, suggesting zooplankton- and/or bacteria-dominated POM. Contrary to Lake Bouleau, Lake Clair $\delta^{13}C_{POC}$ composition varied less, ranging between -29.6 and -31.3 ‰. In general, samples collected in the photic zone of disturbed lakes had similar $(C:N)_{POM}$ signatures (8.97 ± 0.54, n = 7) that corresponded to phytoplankton-dominated POM. The higher variability in $\delta^{13}C_{POC}$ compared to $\delta^{13}C_{FPOC}$ in lakes agrees with published data (del Giorgio and France 1996; McCallister and del Giorgio 2008; Marty and Planas 2008). In this study, $\delta^{13}C_{POC}$ results obtained for Lake Bouleau suggest that the aphotic POM samples and

POM samples collected right above the sediment were a mix of secondary producer communities that feed on both phytoplanktonic and terrestrial sources (Montgomery et al. 2000). Similar $\delta^{13}C_{POC}$ results were found in natural lakes and could be explained in the same way (Figure 3-6A). Although, such $\delta^{13}C_{POC}$ patterns were not found in reservoirs, a result that likely reflects lower variability in the relative contributions from main POM sources (phyto- and zooplankton, terrestrial OM and bacteria) and more dynamic mixing of the water column.

3.5 Discussion

3.5.1 Using water chemistry and bulk analyses to study carbon cycling

Although the information obtained from water chemistry parameters and bulk OM analysis of particulate and dissolved samples is much less detailed than that obtained through more advanced spectroscopic or molecular-level analyses, it can provide a general picture of the differences in C cycling between natural aquatic systems and those affected by human perturbations.

In our sample set, Lake Bouleau represents the most heavily impacted water body with wood harvesting activities on its watershed and the presence of a recently erected beaver dam that led to local flooding of the surrounding vegetation. Much higher surface water CO_2 and CH_4 concentrations were measured in this system compared to other lakes and reservoirs (Table 3-2). Very low dissolved O_2 concentrations were also recorded in the water column of this lake (saturation level of only ~3% near the sediment-water interface) suggesting important OM degradation or CH_4 oxidation to CO_2 in the generally shallow water column of this dendritic lake (Steinmann et al. 2008). The specific physical characteristics of Lake Bouleau and the much higher GHG concentrations measured in

this system (Figures 3-2 and 3-4) make it more comparable to a recently flooded, rather than a stabilized reservoir and as a result this lake was considered to be in a transient phase with respect to water column and sediment C dynamics. Because its carbon dynamics are not in equilibrium with the environmental conditions, Lake Bouleau cannot always be directly compared to the other systems. However, we decided to retain it in our sample set as it still sometimes falls within the correlations found for other systems.

Several authors have found a positive relationship between allochthonous OM inputs in a water body and the watershed-to-lake area ratio (Carignan and Steedman 2000; Larson et al. 2007). We tested whether the differences in CO_2 concentrations measured in the different systems could be explained by differences in OM inputs caused by different watersheds size. Plotting these two variables for lakes and reservoirs with a natural watershed reveals that they were entirely decoupled (slope of -0.06 and r^2 of 0.08), thus suggesting that the size of the watershed was not the main driver of CO_2 concentrations in the surface waters. When including the systems with a wood-harvested watershed, a weak positive linear correlation was found ($r^2 = 0.32$; not shown), however, the correlation may be due to the fact that the natural lakes had the smallest watershed-to-area ratios. These results suggest that the high dissolved CO_2 concentrations were more closely coupled to the additional inputs of allochthonous OM caused by increased erosion in the wood harvested systems rather than to natural OM inputs from a large watershed (Sobek et al. 2003). While other factors such as primary production and ground water inputs can also influence the dissolved CO_2 concentrations, allochthonous DOC exports to water bodies followed by biological and/or photochemical degradation most likely was the primary driver of CO_2 supersaturation in these lakes.

The inputs of terrestrial dissolved organic acids were also the most probably cause for the increased acidity of wood harvested systems (Figure 3-2A). Because the aquatic systems in this study were all located within the same geological region, variations in dissolved bicarbonate concentrations are not likely to have caused important pH changes (Soumis et al. 2004). Interestingly, DOC concentrations were strongly correlated to both Fe and TN when all systems are considered (Figures 3-2B and -4A, respectively). As iron originates mainly from land, the DOC-Fe covariation suggests that the increases in DOC and TN in wood harvested systems were due to increased inputs of terrestrial OM.

Because a significant fraction of the water column DOM in perturbed water bodies was derived from land, it is surprising to measure much higher DOM (C:N) ratios in aquatic systems with wood harvested watersheds when compared to DOM that leaches from litters and soils. Litter and soil leachates were characterized by (i) a relatively large polar (N-rich and water soluble and therefore assumed to be bio-available) DOM fraction, and (ii) an isotopically and compositionally different signature, both for C and N, compared to bulk OM from soil samples. Litters and soils represent an important source of labile and readily available N (Stepanauskas et al. 2000), most likely in the form of proteins, amino acids and amino sugars (which are characterized by low (C:N) ratios and ^{13}C-enriched OC (Galimov 2006)). The (C:N) ratios and $\delta^{13}C$ signatures for DOM from the lakes and reservoirs studied here were all higher (21.3 to 41.6) and more depleted (-26.3 to -28.0 ‰) than the corresponding leachates from the litter and organic soil layers (9.5 to 28.5 and -25.0 to -26.0 ‰, respectively). Therefore, DOM found in these systems likely consisted of a mix of water-soluble material (or bacteria smaller than 0.45μm) either leached from the surficial soil layers, or derived from in-lake OM

production and/or reutilization (Schiff et al 1997; Stepanauskas et al. 2000; McCallister and del Giorgio 2008).

Surprisingly, high dissolved CO_2 concentrations were measured for systems in which DOM and FPOM was N-depleted (low (N:C) ratios; Figures 3-4C and -4D), suggesting either that CO_2 concentrations were higher when the dominant OM sources in the system were terrestrially-derived (C-rich compounds) or when N-containing compounds of the DOM pool were preferentially degraded, leaving behind C-rich compounds (Table 3-5). We propose that bacterial remineralization of allochthonous N-rich organic compounds into nitrates fuelled the N requirements of aquatic organisms. As reported elsewhere (del Giorgio and Cole 1998), the quality, or lability, of OM positively affects bacterial growth efficiency; we thus interpret the low $(N:C)_{DOM}$ ratio as the result of heterotrophic processes in these water bodies. Indeed, significantly lower $(N:C)_{DOM}$ were found in reservoirs and wood harvested systems compared to natural lakes ($p < 0.005$).

3.5.2 Linking heterotrophy and primary productivity to DIC

Several studies report attempts to identify the sources and variations in $\delta^{13}C_{DIC}$ in lakes (Lehmann et al. 2004; McCallister and del Giorgio 2008; Dubois et al. 2009). In our study, spring $\delta^{13}C_{DIC}$ values were substantially enriched in natural and wood harvested lakes (Figures 3-5A and -5C). Lehmann et al. (2004) observed an enrichment in $\delta^{13}C_{DIC}$ owing to the preferential fixation of $^{12}CO_2$ by primary producers. In contrast, Dubois et al. (2009) concluded that primary productivity, DIC-rich groundwater preferentially degassing enriched $\delta^{13}C_{DIC}$, and littoral methanotrophic activity could explain the enriched $\delta^{13}C_{DIC}$ compositions in CO_2-saturated lake waters. The relationships between

$[DIC]^{-1}$ and $\delta^{13}C_{DIC}$ shown for lakes in Figure 3-5C (spring [$r^2 = 0.34$]) and for reservoirs in Figure 3-5D (spring and summer [$r^2 = 0.81$ and $r^2 = 0.50$], respectively) suggest that the concentration and stable isotope composition of the DIC pool were mostly controlled by the combined influence of DOM degradation (causing low $[DIC]^{-1}$ and a depletetion $\delta^{13}C_{DIC}$) and photosynthesis (causing high $[DIC]^{-1}$ and an enrichment $\delta^{13}C_{DIC}$) in harvested systems. Other sources might also have contributed to the concentrations and signatures measured in these systems which could explain the absence of these correlations for lakes during the summer.

Our GHG emissions measurements (Table 3-2) suggest that bubbling accounted for about half of the CH_4 emissions in boreal reservoirs during the summer; $\delta^{13}C_{DIC}$ enrichment could therefore be explained by the splitting of acetate into CO_2 and CH_4 (resulting in ^{13}C-enriched CO_2 and ^{13}C-depleted CH_4, respectively; Steinmann et al. 2008). However, the DIC samples that were collected in the oxygen-rich hypolimnetic zone of the lakes were δ^{13}C-depleted (Figures 3-5A and -5C) whereas more enriched $\delta^{13}C_{DIC}$ values were obtained when DIC concentrations are low. This result suggests that the processes leading to depleted $\delta^{13}C_{DIC}$ signatures were predominantly, although not exclusively, microbial degradation of DOM (producing $\delta^{13}C_{CO_2}$ from -26.3 to -28.0 ‰, Table 3-5) and CH_4 oxidation. Alternatively, the enriched $\delta^{13}C_{DIC}$ and low DIC samples found in photic zones probably reflected preferential ^{12}C fixation through primary production.

3.5.3 In-lake bioprocesses affected by DOM cycling

Most of the water chemistry parameters measured in this study co-varied with DOC, suggesting that DOC plays a major role in modulating bioprocesses controlling the

global carbon cycle in aquatic systems. For example, the increase in allochthonous DOC inputs associated with wood harvesting caused a decrease in light penetration (Table 3-1 and light absorption spectroscopic data to be published elsewhere) which, in turn, likely inhibited hypolimnetic photosynthesis (in agreement with recent findings by Karlsson et al. 2009) and lead to higher CO_2 accumulation and fluxes (Figures 3-2C, -3A and Table 3-2). In our study, hypolimnetic photosynthesis occurred only in unperturbed lakes owing to the greater light penetration depths resulting from the lower DOC concentrations (Figure 3-3B empty circles, Table 3-1). Dissolved O_2 production (autotrophic activity) sometimes even surpasses bacterial O_2 utilization in these systems, resulting in O_2 supersaturation. Epilimnetic oxygen saturation levels in natural lakes (as opposed to perturbed lakes) were also in most cases >100 %, again suggesting that autotrophy played an important role in lower GHG supersaturation levels. Epilimnetic CO_2 concentrations were for the most part decoupled from O_2 saturation levels; this phenomenon was mostly observed in non harvested systems and suggests that processes other than heterotrophy, most likely photo-oxidation, were significant CO_2 production pathways. Net heterotrophy was observed in aphotic hypolimnetic lake water where a strong correlation between CO_2 and O_2 was measured (r^2 = 0.80; Figure 3-3A); this result suggests that dissolved O_2 in aphotic hypolimnetic waters was mainly consumed via bacterial OC degradation and methanotrophic CH_4 oxidation.

The hypothesis of a decrease in autotrophic activity with higher DOM concentrations is supported by the positive correlation (r^2 = 0.59) found between FPOC and DOC in systems with DOC concentrations lower than ~0.4 mmol L^{-1}, which becomes negative (r^2 = 0.85) in wood harvested systems with DOC levels higher than ~0.4 mmol

L^{-1} (Figure 3-4B). These results suggest that the lower FPOC concentrations were modulated by the higher DOC inputs derived from wood harvesting (as for the Decelles Reservoir). Although FPOM abundance is not the best proxy for estimating primary production (chlorophyll a data unfortunately is not available), its low abundance, depleted isotopic composition (~ 29.1 ‰) and high $(C:N)_a$ ratios (~ 21.3), combined with the depleted $\delta^{13}C_{DIC}$ (-11.4 to -24.9 ‰) and high $[CO_2]$ found in Decelles Reservoir suggest low primary production, higher bacterial/terrestrial OM sources and predominance of heterotrophic processes over autotrophy (Figures 3-3D and -6D, Table 3-2 and -5).

The same is true for all wood harvested systems in which the increase in DOC concentrations following wood harvesting disturbed the heterotrophic-autotrophic balance such that higher CO_2 concentrations and atmospheric fluxes were measured in these systems compared to water bodies with lower DOC concentrations. Similar conclusions were reached by Prairie et al. (2002), who reported that the epilimnetic C fluxes are positively correlated with DOC concentrations. They concluded that lakes with low epilimnetic DOC concentrations (< 0.420 mmol L^{-1}) are net autotrophic systems while lakes with higher DOC concentrations are net heterotrophic systems.

Higher FPOC concentrations were measured in samples with lower DOC concentrations (as in natural lakes and Cabonga Reservoir), which were associated with more enriched $\delta^{13}C_{DIC}$ compositions, likely because of greater primary productivity. The lakes summer $\delta^{13}C_{POC}$ data suggest important bacterial activity with stratification ($\delta^{13}C_{DIC}$ values ranging between -14.4 and -41.3 ‰, Figures 3-6A and -6C). Reservoir Cabonga summer DOC concentrations likely were not high enough to limit primary productivity,

as suggested by the absence of a significant correlation in Figures 3-3C, -3D (CO_2 *vs* O_2) and -6B ($\delta^{13}C_{DIC}$ *vs* $\delta^{13}C_{POC}$). Together, the $\delta^{13}C_{DIC}$ and POC data suggest that natural lakes were more oligotrophic than reservoirs which, owing to large differences in their hydrologic regime, were characterized by different proportions of primary producers and heterotrophic bacteria (also observed by Houel et al. (2006)).

3.6 Summary and implications

Although the small number of water bodies studied in this work does not allow a rigorous comparison of C cycling and GHG exchanges at the air-water interface for the unperturtubed and perturbed scenarios considered here, general trends emerge that provide a framework for further studies.

3.6.1 Effects of mature reservoir operation on C cycling

Natural systems were characterized by intense primary production and bacterial respiration, as suggested by the high dissolved O_2 saturation levels and CO_2 concentrations (Figures 3-3B and -3D), as well as by the generally low DIC concentrations of relatively enriched $\delta^{13}C_{DIC}$ compared to perturbed systems (Figures 3-5A and -5B). The Cabonga Reservoir (mature reservoir with a natural watershed) was on average emitting significantly more CO_2 to the atmosphere ($p < 0.0005$) and displayed significantly higher dissolved CO_2 concentrations in the boundary layer ($p < 0.0005$) compared to natural lakes. While it is true that reservoirs are greater GHG emitters during the summer, lakes accumulate GHG in the hypolimnion during the stratified period, which leads to delayed emissions upon mixing of the water column in the fall (lake turnover). A preliminary estimate of the total mass of CO_2 accumulated in the hypolimnion of the studied lakes just before the fall water turnover event however

represented a very small fraction of daily atmospheric CO_2 fluxes (less than 7%, calculated for each lake during the summer of 2007; results not shown). The difference in CO_2 fluxes between lakes and reservoirs measured in this study therefore cannot be explained by summer hypolimnetic CO_2 accumulation alone. Groundwork using lipid biomarkers suggest that the higher epilimnetic CO_2 concentrations and atmospheric fluxes in reservoirs could simply be due to the fact that the water column and sediment surface remains oxic throughout the summer, thus enhancing OM degradation and GHG production through heterotrophy (results to be published elsewhere).

3.6.2 Effects of wood harvesting on the aquatic cycle of carbon

Oxygen saturation levels as well as CO_2 concentrations and fluxes to the atmosphere provide insights into the effect of wood harvesting on the C cycle in aquatic systems. In lakes, during the stratified period, GHG production and oxygen depletion in the hypolimnion were for the most part decoupled from the processes affecting C cycling in the epilimnion (Kim et al. 2006). As shown in this study, greater hypolimnetic CO_2 accumulation and oxygen depletion is observed in wood harvested lakes, most likely due to enhanced OM degradation but also to the absence of primary productivity in the hypolimnion. All perturbed systems in our study were greater GHG emitters than their non-harvested counterparts during the stratified period. Emissions were most likely regulated through the enhancement of bacterial degradation to the detriment of primary productivity, which varied greatly with light penetration depth. The correlation between allochtonous inputs of DOC, TN and dissolved CO_2 concentrations suggest that the additional inputs of terrestrial OM and nutrients upon wood harvesting plays an important role in shifting the balance between autotrophy and heterotrophy in favour of the latter.

The conclusions of several other studies (*e.g.* Peters and del Giorgio 1994; Sobek et al. 2003; McCallister and del Giorgio 2008) also support the idea that lake heterotrophy is fuelled by allochtonous inputs; this study agrees with others and shows that wood harvesting around lakes and reservoirs modify the aquatic cycle of C through the increase in DOC concentrations which, through bacterial and photo-oxidation, leads to visible increases in GHG emissions (16.5 to 45.3 %, $p < 0.1$ and 7.0%, $p < 0.01$ for non-flooded lakes and reservoirs respectively). It is noteworthy that these effects were observed even though only a small proportion of the watershed was affected by wood harvesting activities.

3.6.3 General Implications

Only a limited number of studies have focused on the modifications in the aquatic cycle of C upon changes in land exploitation. Although we observed differences in the processes leading to higher GHG emissions with reservoir operation and wood harvesting, more work should be done to better understand their controls and rates. Amongst other things, the gradual transfer of hypolimnetic GHG to the epilimnion as the thermocline deepens during the summer should be assessed, together with its contribution to the yearly GHG emissions following lake turnover in the fall. To efficiently compare yearly GHG fluxes in lakes and mature reservoirs located in a natural watershed, year round monitoring efforts should be initiated in water bodies with similar geo/physico/ecological characteristics to assess seasonal and year-to-year variability, and to include non-linear events (such as ice breakup in the spring and water turnover in the fall) that are severely underrepresented in the literature. The causes and significance of the differences in the C cycle and CO_2 emissions between natural lakes and non-

harvested reservoirs still are not fully understood. Further studies should target the role of the contrasting redox conditions prevailing in the water column and surface sediments of reservoirs (oxic) and lakes (hypolimnion of stratified lakes becoming increasingly O_2-depleted during the summer), and how they affect OM degradation rates in sediments.

Wood harvesting more profoundly affects C cycling than mature reservoir operation because it leads to the export of fresh, and thus more reactive, terrestrial OM to aquatic systems. Its effects however, should decrease rapidly with forest re-growth. Recent forest cutting favors heterotrophy over autotrophy, which results in the gradual depletion of O_2 and potential loss of animal and fish populations. The recovery period needed for aquatic systems to return to their pre-harvesting conditions should thus be evaluated carefully through long-term biogeochemical monitoring. Our findings also show that wood harvesting history should be documented when selecting water bodies for large scale GHG emission studies, particularly in cases where the emissions from mature reservoirs and natural lakes are compared. Much higher variability and important biases may be introduced if significant portions of the watersheds are exploited for wood harvesting. Finally, our results further suggest that the current Canadian regulations prescribing non-harvested buffer strips of only 20 m between water bodies/streams and harvested areas is not sufficient as they could not prevent large quantities of DOM and nutrients to leach into the water bodies and alter the biogeochemical processes controlling C cycling in these systems.

The complexity and interdependence of the different processes that modulate C cycling in lakes and reservoirs, combined with their inherently high spatial and temporal variability, makes it exceedingly difficult to identify the major players controlling C

pathways and fluxes in these systems. The differences in C cycling between natural water bodies may be subtle, yet they reflect the biogeochemical and climatic alterations that determine the relative importance of the different processes affecting C sources and fate. By extending the range of aquatic biogeochemical conditions beyond those normally found in non-perturbed systems, human perturbations amplify these differences and help documenting how aquatic systems react and adjust to the added stress. The same mechanisms control C dynamics in natural and perturbed systems, although at a varying relative importance, which determine the resulting biogeochemical conditions existing in the water bodies. Lakes and reservoirs are thus in a perpetual state of steady-state pseudo-equilibrium, continuously adjusting to change on a multitude of spatial and time scales. One of the major challenges in these types of studies is thus to identify links between a specific source of stress and the biogeochemical response of the aquatic system.

Chapter 4

4 Assessing carbon and nitrogen dynamics in natural and perturbed boreal aquatic systems: An amino acid approach

Submitted to the Limnology and Oceanography as:

Alexandre Ouellet, Luc Tremblay, Marc Lucotte and Yves Gélinas.

4.1 Abstract

Aquatic systems of the boreal forest are supersaturated in dissolved greenhouse gases (GHG) and are considered natural GHG emitters. The goal of this study was to better understand the cycling of carbon (C) and nitrogen (N) in these systems, their direct link with GHG production, as well as the effect of human perturbations (reservoir operation and wood harvesting) on these processes. Greenhouse gases concentrations, bulk elemental and isotopic (%C, %N, $\delta^{13}C_{org}$ and $\delta^{15}N_{tot}$) compositions, and D- and L-amino acid (D-AA and L-AA) yields were analyzed in the dissolved and particulate fractions from the water column as well as in the sediments from a series of boreal lakes and reservoirs. Dissolved organic matter (DOM) and fine particulate organic matter (FPOM) C:N atomic ratios, stable isotopic signatures, and relative abundances of AA confirm the major role played by bacteria in these systems and suggest that human perturbations lead to increased exports of terrestrial DOM, which result in higher surface water CO_2 and CH_4 concentrations compared to natural systems. Concentrations of bacterial D-AA in DOM were positively correlated with surface water concentrations of GHG, whereas a negative correlation was found between D-AA and GHG in the sedimentary organic matter (SEOM). Principal component analysis showed that the AA composition of the DOM pool was, to some extent, modulated by leaching of terrestrial material from the surrounding soils, whereas that of the FPOM pool was influenced by variations in the relative abundances of phytoplanktonic- and bacterially-derived material. Low D-Asx:D-Ala ratios were measured in the FPOM of perturbed systems and might reflect a shift in the type of bacteria contributing to FPOM. While the effect of reservoirs leaves a microbial and molecular imprint on the aquatic cycle of carbon for

more than half a century after impoundment, wood harvesting results in transient changes that might be important in the first few years, but that are likely to decrease with forest re-growth. Amino acids are proving to be an extremely valuable tool for broadly characterizing the major pathways and players that control the fate of C and N in aquatic systems, and their link to GHG concentrations and fluxes.

4.2 Introduction

Worldwide lakes and reservoirs are typically supersaturated with greenhouse gases (GHG, namely CO_2 and CH_4 in this work; Kling et al. 1990; Cole et al. 1994; Duchemin et al. 2000). Although processes such as GHG-saturated ground water discharges could explain the high dissolved GHG concentrations in surface waters, increasing evidence suggests that the bacterial and photochemical degradation of terrigenous organic matter (OM), mostly dissolved (DOM), could be the primary cause for the observed supersaturation (Sobek et al. 2003; McCallister and del Giorgio 2008; Chapter 3). Carbon cycling in freshwater aquatic systems is however characterized by high random variability, which makes understanding of the subtle processes that control C dynamics and GHG exchanges with the atmosphere extremely difficult. By stressing the systems in ways that lead to changes in biogeochemical conditions that go beyond the range of natural variability, human perturbations such as reservoir operation and wood harvesting can help to identify the major controls on the aquatic cycle of C. Our working hypothesis is that the trends found when comparing natural and perturbed systems reflect those in natural systems, although over a much wider range, and thus that they are not masked by the random variability inherent to aquatic environments. We also assume that the major players controlling C cycling are the same in perturbed and natural systems, although their relative importance likely differs.

Watershed wood harvesting and reservoir impoundment/operation lead to increased exports of dissolved organic carbon (DOC), nitrogen and phosphorus from terrestrial systems to the water bodies and severely alter the aquatic C cycle, resulting in an enhancement of algal and bacterial biomass, as well as to higher dissolved GHG

concentrations (Carignan et al. 2000b; Planas et al. 2000; Chapter 3). The amplitude of these changes depend on several factors including the characteristics of the watershed affected by flooding or wood harvesting activities, the pre-harvesting of wood before flooding, the harvesting method and mitigation measures such as non-harvested protection bands around water bodies (Chapter 3). The return to normal biogeochemical conditions likely takes place only with forest re-growth for wood harvested systems, while reservoirs remain greater emitters (compared to lakes) for at least 10-15 years (Tremblay et al. 2005), and maybe for much longer (Duchemin et al. 2005; Chapter 3). Recent efforts to quantify GHG emissions generated from reservoir operation however have not been accompanied by an assessment of the dominant hydrological, physical and biological processes responsible for the production and consumption of GHG in the water column. To the best of our knowledge, no study has successfully identified changes in OM processing and sources, including bacterial, in relation with dissolved GHG concentrations in response to anthropogenic forcing associated to land use.

The anthropogenic exploitation of a watershed alters aquatic OM sources, quantity and processing, which can be effectively evaluated through a combination of bulk and molecular biomarker analyses (*e.g.* Simoneit 2005; Volkman et al. 2007). Amino acids (AA) are relatively labile and are characterized by contrasting degradation rates. AA yields and relative abundances have thus been frequently exploited to evaluate OM freshness (Cowie and Hedges 1994; Dauwe et al. 1999; Tremblay and Benner 2009). In addition, Cowie and Hedges (1992) have measured AA in different vascular plants, tree leaves, phytoplankton, macrophytes, zooplankton and bacteria, and found that AA represented >50% of total N in the samples ($\%T_{AA}N$), with little variability among source

organisms. In contrast, AA represented a larger portion of total organic carbon ($\%T_{AA}C$) in plankton or bacteria (> 25%) compared to vascular plants (< 10%). These yields can thus provide clues on the origin of OM; samples exhibiting high $\%T_{AA}N$ but low $\%T_{AA}C$ can be associated with relatively fresh vascular plant contributions (Bourgoin and Tremblay in press).

The D-isomers of AA (D-AA) are also exploited as OM source indicators because of their much higher relative abundance in bacteria compared to other living organisms. D-AA are found mostly in bacterial macromolecules such as peptidoglycan, teichoic acid, lipopolysaccharides, polypeptides, lipopeptides and siderophores (McCarthy et al. 1998; Kaiser and Benner 2008). Their abundance differs among bacteria species; for instance, Kaiser and Benner (2008) measured no D-aspartic acid and D-serine in aquatic phototrophic bacteria and highly variable yields among heterotrophic bacteria. In addition, Gram positive (G+) and negative (G-) bacteria are composed of less than 10% and between 30 and 70% by mass, respectively, of the structural macromolecule peptidoglygan, which generates different yields in D-AA upon hydrolysis (Schleifer and Kandler 1972; Kaiser and Benner 2008). D-amino-acid yields have been used for estimating the bacterial contributions to different OM fractions in freshwater and marine environments (*e.g.*, Tremblay and Benner 2009; Lomstein et al. 2009; Bourgoin and Tremblay in press). To our knowledge, total hydrolyzable amino acids (THAA) and D-AA have never been employed for the study of the aquatic C cycle of forested freshwater ecosystems, and for assessing the effect of human activities on C dynamics in these systems.

The main objective of this work was to assess C dynamics in freshwater systems with a natural or perturbed watershed using AA measurements on a series of samples collected in lakes and reservoirs during the summer of 2007. In particular, we tried to assess how natural systems respond to human perturbation, and how this response affects GHG fluxes at the air-water interface. To minimize the extent of random variability, we collected our samples during the summer season when in-lake physico-chemical conditions are fairly stable, and we selected water bodies with similar characteristics in the southeastern Canadian boreal region, thus facilitating comparison of the aquatic C cycle between the different systems.

Nutrients, GHG as well as stable isotopes of dissolved organic carbon (DOC), dissolved inorganic carbon (DIC), and particulate organic carbon (POC) were measured in a parallel study in the same water bodies (Chapter 3). The results obtained highlighted the delicate balance between CO_2 production through bacterial/photochemical OM degradation and CO_2 fixation by primary producers, and how biogeochemical changes in the water bodies caused by human perturbations influence dissolved GHG concentrations and fluxes to the atmosphere. In the present study, THAA and D-AA measurements were coupled to elemental and isotopic analyses of dissolved, fine particulate, flocculate and sedimentary OM (DOM, FPOM, FLOM and SEOM respectively) to link GHG supersaturation in surface waters to bacterial biogeochemical processes controlling carbon dynamics in freshwater systems.

4.3 Materials and Methods

4.3.1 Study sites

Two hydroelectric reservoirs and five lakes situated in the boreal forest of the Province of Quebec (Canada; 46°10′ to 47°46′ N; 76°12′ to 78°24′ W) were sampled in summer of 2007 (Figure 4-1, Table 4-1). The Cabonga and Decelles reservoirs were impounded in 1928 and 1938, respectively, and are thus representative of mature hydroelectric reservoirs. Portions of the watershed of one reservoir (Decelles) and two lakes (Clair and Bouleau) were recently wood harvested (between 2004 and 2007), whereas the watersheds of the remaining water bodies were not exploited. While wood-harvesting activities represented only about 1 to 5% of the total watershed drainage area, they were located in the direct vicinity of the water bodies, with non-harvested protection bands of about 20 m along brooks and water bodies. We conservatively estimate the percentage of the lake/reservoir shoreline directly affected by at least a 2-km wide strip of harvested land at about 10-25% for lakes, and about 5% for the Decelles Reservoir. All lakes and reservoirs had watersheds with more than 70% tree coverage (conifers – mostly spruce, and the broad-leaf deciduous species maple, white birch and yellow birch); additional details on the studied water bodies are listed in Table 4-1.

Table 4-1. Environmental settings and station description

Water body	System	Land use	Area (km^2)	Watershed area (km^2)	Station	Station description	Depth (m)[a]	T_m [b]	Coordinates
Mary	Lake	Natural	0.58	1.80	LMAR	Deepest zone	9 to 10	5	46°15'37.2"N 76°12'50.8"W
Jean	Lake	Natural	1.88	7.31	LJEA	Deepest zone	28 to 32	5.5	46°21'43.9"N 76°20'42.1"W
Clair	Lake	Wood harvested	1.75	47.0	LCLA	Deepest zone	15 to 17	4.5	46°11'6.70"N 76°24'53.2"W
Bouleau	Flooded lake	Wood harvested	0.34	8.23	LBOU	Deepest zone	17 to 20	3	46°14'16.5"N 76°27'13.9"W
Cabonga	Reservoir	Natural	434 [c]	2 616	RCAB-6	River output	6 to 10	none	47°25'31.1"N 76°37'42.7"W
					RCAB-10	Off main channel	9 to 17	none	47°17'24.4"N 76°36'24.1"W
Decelles	Reservoir	Wood harvested	237 [c]	13 131	RDEC-1	River output	18 to 21	none	47°45'39.6"N 78°18'51.3"W
					RDEC-2	Off main channel	2 to 3	none	47°41'53.6"N 78°15'33.7"W

[a] Station depth was measured several times during sampling, the max depth range is indicated. [b] Thermocline depth. [c] Areas provided by Hydro-Quebec.

For normalizing spatial and depth variability, water DOM, POM, nutrients and dissolved GHG (CO_2 and CH_4) were sampled at four stations within each lake, nine stations in the Cabonga Reservoir, and eleven stations in the Decelles Reservoir. In this manuscript, only the results corresponding to the deepest station of the lakes and two stations of the reservoirs are presented; a systematic integration of all stations and associated uncertainties for the same sampling sites are available in Chapter 3.

4.3.2 Field sampling

Concentrations of carbon dioxide (CO_2) and methane (CH_4) were measured using the method reported in Soumis et al. (2008). Exactly 30-mL of water from the top 20-cm surface water layer was sampled in a 60-mL syringe in which 30-mL of ultrapure N_2 was added (n = 4 per sampling event). The syringes were shaken for one minute followed by a two minute equilibration period with the syringes resting horizontally. The water was removed and the gaseous samples was injected within 4 hours of sampling in a Varian-Star 3400 gas chromatograph (GC) coupled to flame ionization and thermal conductivity detectors for CH_4 and CO_2 measurement, respectively. The GC was calibrated using a certified gas standard containing 1.01 % of CO_2 and CH_4 (Scotty 48, mix 218). Two surface water aliquots were collected in high density polyethylene bottles and frozen for total nitrogen (TN) analysis. Lake sampling for GHG was carried out above the thermocline that forms in the summer and is considered representative of the whole lake as GHG accumulation in the hypolimnion represented less than 7% of the total daily emissions in the studied lakes (Chapter 3).

For OM analysis, a large quantity (200-250-L) of water from each sampling site, integrated over the entire water column or the first 10-m, was sampled in 50-L Nalgene

containers using a submersible pump and pre-filtered with a 70-μm nylon mesh filter. From 25 to 50-L of water were collected at each 0.5 to 1-m depth interval, depending on the water column depth. FPOM and DOM fractions were isolated by a tangential flow filtration device using a 0.45-μm polyvinylidene difluoride (PVDF) filter coupled to a RealSoft PROS/2S reverse osmosis (TFF-RO) system following the method described in Ouellet et al. (2008). Briefly, a peristaltic pump introduced the pre-filtered (< 70-μm) water sample into the TFF unit, which redirected the FPOM fraction (0.45 – 70-μm) into the original container while the permeate (DOM) was collected in a second 50-L Nalgene container. The DOM permeate was concentrated 15-20 times using the RO system, which was carefully flushed and rinsed between sample runs (Ouellet et al. 2008). Total DOM recoveries approached 90% using this method. The FPOM and DOM samples were bacterially quenched with mercury (II) chloride and kept in the dark at 4°C until analysis.

Flocculate material, which formed a highly dynamic and unstable layer just above the sediment-water interface, was gently collected by a SCUBA diver using 60-mL polyethylene (PE) syringes, while sediments were sampled using a Mackereth corer (Mackereth 1958) or by a SCUBA diver using 7.5-cm diameter Plexiglas tubing. The sediment was sliced at 1-cm intervals from 0 to 5 cm. Both FLOM and SEOM fractions were transferred to 50-mL polypropylene centrifuge tubes and freeze dried. Equal masses of the three first centimeters of each sediment core were freeze dried and were combined prior to analysis. Because of diving limitations, flocculates and sediments from LCLA and RCAB-6 were not sampled in the exact same location as the water samples, and might be subject to spatial variability.

4.3.3 Elemental and isotopic measurements

Samples for TN measurements were reacted with NaOH-$K_2S_2O_8$ and analyzed using a standard colorimetric method (#818-47) from Bran Luebbe Analyzing Technologies on a TRAACS 800 AutoAnalyser. Carbon and nitrogen elemental and isotopic compositions (%C, %N, $\delta^{13}C_{org}$ and $\delta^{15}N_{tot}$, respectively) for DOM, FPOM, FLOM and SEOM samples were obtained using an EuroVector 3028-HT elemental analyzer coupled to an Isoprime GV Instrument stable isotope ratio mass spectrometer (EA-IRMS). Elemental and isotopic standardizations as well as the instrumental linear response changes with intensities were done using the VPDB-calibrated standards IAEA-C6 Sucrose ($\delta^{13}C$ = -10.45 ± 0.03‰; %C = 42.11) and IAEA N1 Ammonium sulfate ($\delta^{15}N$ = 0.43 ± 0.07‰; %N = 10.60%) as well as β-alanine, a pre-calibrated in-house standard ($\delta^{13}C$ = -25.98 ± 0.23‰; %C = 40.45 and $\delta^{15}N$ = -2.21 ± 0.24‰; %N = 15.72). Organic C and total N percentages in the samples were obtained through multipoint calibration of the IRMS response using sucrose and alanine for %C, as well as alanine and ammonium sulfate for %N. Before $\delta^{13}C_{org}$ analysis, samples were decarbonated using vapor-phase HCl (Hedges and Stern 1984); %N and $\delta^{15}N_{tot}$ were analyzed separately on non-acidified aliquots to avoid N loss during acidification.

4.3.4 Iron associated to DOM

Following DOM isolation by RO, the analysis of iron complexed to DOM (Fe_{DOM}) was carried using an Agilent 7500 series ICP-MS following acidification with nitric acid and addition of an internal standard (scandium). Quantification was achieved through external calibration with a Certipur ferric nitrate standard. Five replicate measurements were acquired for each sample.

4.3.5 Sedimentation rates

Sediment accumulation rates were determined through the analysis of ^{210}Pb and its radioisotope daughter ^{210}Po using an alpha spectrometer, as described in Houel et al. (2006). Briefly, 0.5-g sediment aliquots were spiked with a recovery standard (^{209}Po), reacted in Teflon beakers with a 5:3 mixture of HCl (12 N) and HNO_3 (15 N) and evaporated to dryness on a hot plate. This step was repeated twice. A 2:2:1 mixture of HCl (6 N), HNO_3 (15 N) and HF (24 N) was then added to the sample and evaporated to dryness on a hot plate. The residual material was dissolved using 0.5 N HCl (< 100 mL) to which 0.2 g of ascorbic acid was added. Upon mixing, a silver disk was introduced into the solution, onto which the polonium deposited. Prior to the sedimentation rate calculation, the supported lead activity that was determined from the deeper sediment signal was subtracted from the upper core samples; then, sedimentation rates were calculated using the negative value of λ (0.0448) for ^{210}Pb divided by the slope of a $\ln^{210}Pb$ *vs.* depth plot, as described by Ghaleb (2009). We attempted to determine the sedimentation rate in Reservoir Decelles but sediment bio- and hydroturbation likely skewed ^{210}Pb depth profiles, making it impossible to obtain accurate measurements.

4.3.6 Amino acids measurements

The D/L-AA methodology used in this work is described in Kaiser and Benner (2005). Briefly, hydrolysis of the DOM, FPOM, FLOM and SEOM fractions (5 to 200 mg of sample, or 2 to 3 mg of OC) was done using 6 N HCl in a sealed ampoule containing 0.12 µM ascorbic acid placed at 110°C for 20h. Removal of HCl was done by drying under a N_2 stream followed by two water addition and drying steps. On-line high performance liquid chromatography (HPLC) precolumn derivatization was done using o-phthaldialdehyde with either N-isobutyryl-L-cysteine or N-isobutyryl-D-cysteine in a pH

9.5 borate buffer. The addition of the L- conformational reagent results in D-L and L-L diastereomers, from D-AA and L-AA respectively, which are separated using an achiral stationary phase. The absence of co-elution and proper quantification of the AA were verified in a second run using the D-reagent producing D-D and L-D diastereomers.

The HPLC analysis was carried out using an Agilent 1200 system and a C-18 LiChrospher 100 RP-18 column (4 × 250 mm, 5 μm beads) protected by a 4 × 4 mm LiChrospher guard column. The separation was done under isothermal condition (20°C) and at a flow rate of 0.8 mL min^{-1}. A segmented linear mobile phase gradient was used, beginning with 100 % 40 mM aqueous KH_2PO_4 (pH 6.2) and reaching 39, 54 and 60 % MeOH/ACN (13:1 v/v) mix after 50, 72 and 80 min, respectively. Detection was done by fluorescence with excitation and detection wavelengths set to 330 nm and 450 nm, respectively. External standard solutions of 23 AA were used for the calibration. These AA were: L- and D-aspartic acid (Asp), L- and D-glutamic acid (Glu), L- and D-serine (Ser), L-histidine (His), L-threonine (Thr), L-and D-alanine (Ala), L-arginine (Arg), L-tyrosine (Tyr), L-methionine (Met), L- and D-valine (Val), L-phenylalanine (Phe), L-isoleucine (Ile), L-and D-leucine (Leu), L-lysine (Lys), glycine (Gly), β-alanine (β-Ala), γ-aminobutyric acid (γ-Aba).

Chemical racemization during hydrolysis was corrected by using the mean racemization rates for free and protein amino acids reported by Kaiser and Benner (2005). Negative or zero D-AA peaks after correction were considered as hydrolysis artefacts and were rejected. D-AA showing more than 15 % peak area difference with the L- and D-reagent runs were also discarded. Such variability indicated coelution problems. Hydrolysis converted asparagine (Asn) and glutamine (Gln) to aspartic acid (Asp) and

glutamic acid (Glu), respectively. As a result, the terms Asx and Glx were used for these AA. The relative standard deviation was evaluated at 5–12 % (n = 3) for individual AA with slightly higher values measured for less abundant AA such as D-AA (Kaiser and Benner, 2005). No flocculate material was sampled for Lake Mary, and the Lake Bouleau THAA sediment data were discarded due to untraceable manipulation errors which resulted in large numerical inconsistencies.

4.3.7 Statistical Analysis

Where applicable, the significance of the observed trends was tested using the Welch's t-test, which allows evaluating parameters having unequal data variance and replicates. Between system comparisons of DOC, dissolved nitrogen (DN), FPOC and fine particulate nitrogen (FPN) concentrations were based on the combined average values for the different sampling sites. Standard deviations were propagated using the pooled standard deviations (Harris, 1999). This analysis prevented the over-representation of systems with a higher number of sampling locations.

A principal components analysis (PCA) was carried out with mole percentages of the AA as the main variables using Matlab 7.0 software (The Mathworks). The PCA is applied to large data sets and extracts new vectors called principal components (PC), which explain varying proportions of the variability of the data set. There are as many PC outputs as there are variable inputs. In this study, we ran separate PCA on DOM or FPOM samples for which 23 L- and D-AA were used as input variables. PC generates both scores and loadings. Scores are defined as positions within the PC space and loadings are defined as the contribution of individual variables to the PC. Thus higher loading values in the first two PC vectors (above 0.30 and 0.25 for DOM and FPOM

respectively) represent variables that are prone to change with land utilization and were thus employed in the second PCA analysis, as explained in the discussion below.

4.4 Results

4.4.1 Greenhouse gases and bulk organic matter analyses

Surface concentrations of dissolved carbon dioxide and methane, as well as DOC, dissolved nitrogen (DN), FPOC and fine particulate nitrogen (FPN) concentrations at all stations that were analyzed for AA are summarized in Table 4-2. Dissolved CO_2 and CH_4 concentrations at the stations selected for AA analysis were within the standard deviation of the average values reported for the entire water bodies. Natural lakes exhibited lower dissolved CO_2 concentrations compared to perturbed systems. Water bodies with harvested watersheds were generally associated with high water dissolved CO_2 concentrations; even though these latter systems had higher watershed surface area (SA) to water SA ratios. The fact that no SA ratio relationship to dissolved CO_2 concentration was observed for water bodies with a forested watershed (Chapter 3) suggests that CO_2 concentrations were controlled by factors other than lake or watershed areas. The effect of small water temperature variations between the different systems was negligible as the same conclusions and level of significance ($p < 0.05$ or 0.1) are reached when expressing GHG concentrations in partial pressures or percentages of saturation. Independently of reservoir operation, harvested systems had significantly higher DOC ($p < 0.0005$), DN ($p < 0.0025$) and FPOC ($p < 0.0025$) concentrations compared to natural ones (Table 4-2).

Table 4-2. Water chemistry at the studied sites

Water body	Station	n[a]	$[CO_2]$ (µmol L^{-1})[b] Ave[c,d]	$[CO_2]$ (µmol L^{-1})[b] Range	$[CH_4]$ (nmol L^{-1})[b] Ave[c,d]	$[CH_4]$ (nmol L^{-1})[b] Range	[DOC][e] µmol C L^{-1}	[DN][e] µmol N L^{-1}	[FPOC][e] µmol C L^{-1}	[FPN][e] µmol N L^{-1}
Mary	LMAR	N/A	N/A	N/A	N/A	N/A	184	8.5	25.1	2.1
Jean	LJEA	6	28.1 (11.5)	20.9 - 50.4	51.9 (9.8)	33.6 - 61.5	221	7.4	37.1	2.6
Clair	LCLA	5	32.3 (8.7)	25.6 - 43.8	38.8 (9.5)	28.3 - 48.5	434	13.6	80.8	4.3
Bouleau	LBOU	5	75.1 (10.7)	65.6 - 87.9	68.4 (21.9)	45.7 - 104.4	506	15.3	77.5	3.3
Cabonga	RCAB-6	6	34.9 (6.7)	27.9 - 42.5	54.6 (10.2)	44.4 - 66.1	294	8.1	62.2	3.8
	RCAB-10	3	45.7 (14.2)	26.4 - 51.1	71.9 (20.9)	54.8 - 96.6	278	8.5	31.0	1.9
Decelles	RDEC-1	7	42.0 (4.3)	35.8 - 45.2	63.9 (18.4)	28.2 - 90.4	498	8.9	63.1	2.4
	RDEC-2	7	39.0 (9.3)	28.3 - 53.8	87.5 (30.2)	55.1 - 145.6	497	12.3	62.5	2.0

[a] Four replicates were measured for each sampling event (n). [b] Surface concentrations. [c] Averages for a single station were calculated using individual replicates; when stations were visited more than once, standard deviations (within parenthesis) were calculated using common error propagation equations. [d] The averaged total sampling and analysis error was of 4.1 ± 1.7%. [e] Depth integrated samples.

The elemental and stable isotope signatures of the water column integrated DOM and FPOM samples from all stations, as well as the corresponding FLOM and SEOM values are shown in Table 4-3. Water column particles were relatively enriched in OC (> 25.6%) compared to underlying flocculates and sediments (1.7 – 23.1%), indicative of important OM removal with sedimentation. $\delta^{13}C_{org}$ and $\delta^{15}N_{tot}$ values within each fraction exhibited little variability. The most important differences measured were between fractions. $\delta^{15}N_{tot}$ values were higher in FLOM and SEOM than in the water column DOM and FPOM samples indicating more extensively processed OM fractions (Anova single factor: $p < 0.0001$; Meyers 1997).

Higher concentrations of iron specifically associated with DOM (Fe_{DOM}), which originates almost exclusively from land, were found in perturbed systems compared to natural ones. Compared to natural lakes, reservoirs had about 1.5 time more Fe_{DOM}, while wood harvested systems contained more than 4 times Fe_{DOM} (Table 4-3). Higher DOM atomic C:N ratios were measured in perturbed systems (32.0 to 56.1) compared to natural lakes (21.6 to 29.8). Higher FPOM $(C:N)_a$ ratios were also found in wood harvested systems (18.7 to 31.2) compared to non-harvested lakes and reservoirs (11.8 to 16.5; Table 4-3) indicating greater terrestrial FPOM inputs. FLOM and SEOM $(C:N)_a$ ratios varied between 11.4 and 25.5 with a general trend towards higher values in the sediments from perturbed systems. Flooded systems (Lake Bouleau and both reservoirs) contained N-poor FPOM, (high $(C:N)_a$ ratio), FLOM with a lower $(C:N)_a$ ratios, which increased again in SEOM. The opposite trend with depth was measured for the other systems (non-flooded lakes). In non-flooded systems, it appears that a preferential degradation of N

(high $(C:N)_a$ ratios in FLOM) was followed by an enrichment in N in sediments exhibiting the lowest $(C:N)_a$ ratios among all the fractions.

Lakes were characterized by large variations in sedimentation rates, which were not linked to wood harvesting (Table 4-3). The measured sedimentation rates were lower in lakes than what was measured in the Cabonga Reservoir (Houel et al., 2006). The integrated age of the 0-3 cm sediment layer used in this study ranged between 5.5 and 88 years. Noteworthy, the biogeochemical signal attributable to short-time perturbations such as recent wood harvesting might not be perceptible in the SEOM fraction since it integrates information from several pre-harvesting years in addition to the few years following wood harvesting.

Table 4-3. Bulk elemental and isotopic analysis of the collected fractions

Water body	Station	DOM					FPOM			
		OC (%)	$\delta^{13}C_{org}$ (‰)[a]	$\delta^{15}N_{tot}$ (‰)[a]	$(C/N)_a$	Fe (nmol L^{-1})[b]	OC (%)	$\delta^{13}C_{org}$ (‰)[a]	$\delta^{15}N_{tot}$ (‰)[a]	$(C/N)_a$
Mary	LMAR	6.3	-26.3	-2.7	21.6	37.0	25.6	-27.7	0.9	11.8
Jean	LJEA	10.9	-26.8	-1.7	29.8	30.7	27.2	-28.6	-0.3	14.0
Clair	LCLA	16.8	-27.1	-1.1	32.0	444	33.4	-28.6	0.1	18.7
Bouleau	LBOU	16.9	-27.5	-1.9	33.2	N/A	27.8	-30.4	0.2	23.7
Cabonga	RCAB-6	14.1	-27.1	-2.3	36.4	51.8	32.4	-29.4	-0.6	16.3
	RCAB-10	13.0	-26.9	-0.7	32.6	78.0	25.6	-29.0	-0.6	16.5
Decelles	RDEC-1	16.1	-27.2	-3.0	56.1	342	27.9	-28.3	1.6	26.0
	RDEC-2	23.4	-27.0	-1.7	40.5	415	31.9	-28.2	0.9	31.2

Water body	Station	FLOM				SEOM [c]				
		OC (%)	$\delta^{13}C_{org}$ (‰)[a]	$\delta^{15}N_{tot}$ (‰)[a]	$(C/N)_a$	Rate (mm $year^{-1}$)[d]	OC (%)	$\delta^{13}C_{org}$ (‰)[a]	$\delta^{15}N_{tot}$ (‰)[a]	$(C/N)_a$
Mary	LMAR	N/A	N/A	N/A	N/A	3.89	23.1	-28.1	1.5	11.4
Jean	LJEA	11.0	-25.6	3.5	22.3	0.44	10.0	-25.4	0.6	13.1
Clair	LCLA	1.7	-29.6	3.7	25.5	0.72	2.7	-29.2	2.1	13.3
Bouleau	LBOU	15.0	-29.6	2.0	13.0	0.34	14.5	-29.1	1.3	15.2
Cabonga	RCAB-6	1.8	-27.4	1.2	18.9	5.57 [e]	5.6	-27.6	1.8	14.7
	RCAB-10	6.9	-28.0	3.8	12.4	N/A	7.8	-28.2	3.1	16.6
Decelles	RDEC-1	5.0	-27.4	5.1	18.1	N/A	2.8	-28.0	2.1	19.4
	RDEC-2	6.3	-27.9	2.8	15.7	N/A	5.7	-27.5	1.4	19.1

[a] Analytical uncertainty of ± 0.2‰. [b] Iron complexed to dissolved organic matter exclusively. [c] The first 3 cm of the core were homogenized and used for the analyses. [d] Sedimentation rates were calculated as explained in the methods section. [e] Houel et al. 2006.

4.4.2 L- and D-Amino acid analyses

The relative abundances of AA in the DOM, FPOM, FLOM and SEOM fractions from the different water bodies are listed in Table 4-4. THAA accounted only for < 2% of total DOC ($\%T_{AA}C$) and for 5 to 19 % of FPOC. The $\%T_{AA}C$ measured for FPOM were higher in natural lakes, with percentages greater than 14 %, than in reservoirs and systems with a wood harvested watershed (5.1 to 10.7 %). No clear trend emerged in the FLOM and SEOM fractions but $\%T_{AA}C$ generally increased with depth, from FPOM to FLOM to SEOM, in perturbed water bodies.

The percentage of total N included in AA ($\%T_{AA}N$) was lower in the dissolved phase (10.2 to 17.9 %) than in the other fractions (17.2 to 63.0 %). The $\%T_{AA}N$ of DOM in natural and wood harvested lakes (10.6 ± 0.5 %) was significantly lower than in reservoirs (14.7 ± 2.2 %, $p < 0.0005$). The opposite trend was obtained for FPOM with much higher $\%T_{AA}N$ in lakes (52.1 ± 5.6 %) than in reservoirs (28.6 ± 9.1 %, $p < 0.0005$). Amino-acid constitutes the major N pool in the FLOM and SEOM fractions, accounting for 45.1 ± 6.6 % and 53.9 ± 7.9 % of total N, respectively, with no significant difference between the different systems.

The relative abundances of the different AA change significantly upon OM degradation and can thus be used as indicators for the diagenetic state of OM. Degradation indices (DI) exploiting these changes (Dauwe et al. 1999) were calculated for our data set (Table 4-4). High DI values, suggestive of relatively fresh OM, were obtained for FPOM in reservoirs (0.223 to 0.458) and in the natural Lake Mary (0.671). In contrast, reservoir DOM DI values were generally lower than those recorded in lakes, suggesting that reservoir DOM was more degraded than in lakes. Degradation index

values are however affected by sorption/desorption processes that influence partitioning of the different AA between the dissolved and solid phases (Aufdenkampe et al. 2001); comparisons of DI across the dissolved and particulate phases are thus not straightforward (see discussion below). The DI values calculated for SEOM varied between -0.537 and 0.311, with slightly higher values for lakes with low sediment accumulation rates (Lake Jean and Lake Clair; Table 4-4), suggesting that water bodies with greater sedimentation rates accumulated OM that was generally more altered.

Table 4-4. Carbon and nitrogen normalized total hydrolysable amino acids (THAA) yields and degradation indices

Station	THAA		
	$\%T_{AA}C$ [a]	$\%T_{AA}N$ [a]	DI [b]
DOM			
LMAR	1.8	11.3	0.107
LJEA	1.2	10.3	-0.138
LCLA	1.1	10.2	-0.061
LBOU	1.1	10.5	-0.196
RCAB-6	1.3	13.6	-0.712
RCAB-10	1.9	17.9	-0.437
RDEC-1	0.9	13.8	-0.187
RDEC-2	1.2	13.3	-0.640
FPOM			
LMAR	19.1	59.2	0.671
LJEA	14.1	51.4	-0.501
LCLA	10.0	52.2	-0.194
LBOU	6.9	45.5	-0.111
RCAB-6	5.6	17.2	0.458
RCAB-10	10.7	38.7	0.362
RDEC-1	5.4	26.4	0.223
RDEC-2	5.1	32.0	0.389
FLOM			
LMAR	–	–	–
LJEA	5.1	32.4	-0.105
LCLA	6.6	49.4	-0.456
LBOU	12.1	45.7	-0.424
RCAB-6	8.6	47.0	-0.481
RCAB-10	11.0	44.8	-0.371
RDEC-1	8.5	43.0	-0.963
RDEC-2	12.2	53.6	-0.192
SEOM			
LMAR	16.9	50.3	-0.537
LJEA	16.8	58.6	-0.148
LCLA	17.6	63.0	0.311
LBOU	–	–	–
RCAB-6	13.1	51.6	-0.459
RCAB-10	8.7	39.1	-0.880
RDEC-1	16.0	55.0	-0.501
RDEC-2	11.1	59.8	-0.139

[a] Percentage of total organic carbon (OC) and nitrogen (TN) included in amino acid structures. [b] Degradation index calculated as in Dauwe et al. (1999).

Amino-acids distributions, expressed in mole percentages (mol%) of THAA (sum of D and L isomers) and grouped according to the chemical nature of their side chain, are presented in Figure 4-1. Glycine (Gly) was the most abundant AA in most samples. In addition to the diagenetic trends illustrated by the DI, hydrophilicity dictates THAA relative abundances in the different OM fractions. In contrast to the solid phases, the relative contribution of histidine (His) to THAA was high in DOM probably owing to the hydrophilic nature of its side-chain. The opposite trend was observed for lysine (Lys) and arginine (Arg) having hydrophobic side-chains. Mole percentages of His in DOM were lower in reservoirs compared to lakes, with levels almost two times higher in the latter. The occurrence of other AA seemed to be influenced by wood harvesting. For instance, Gly, leucine (Leu) and methionine (Met) accounted for a greater mol% of THAA in DOM from wood harvested water bodies, while the relative contribution of alanine (Ala) was smaller in these systems.

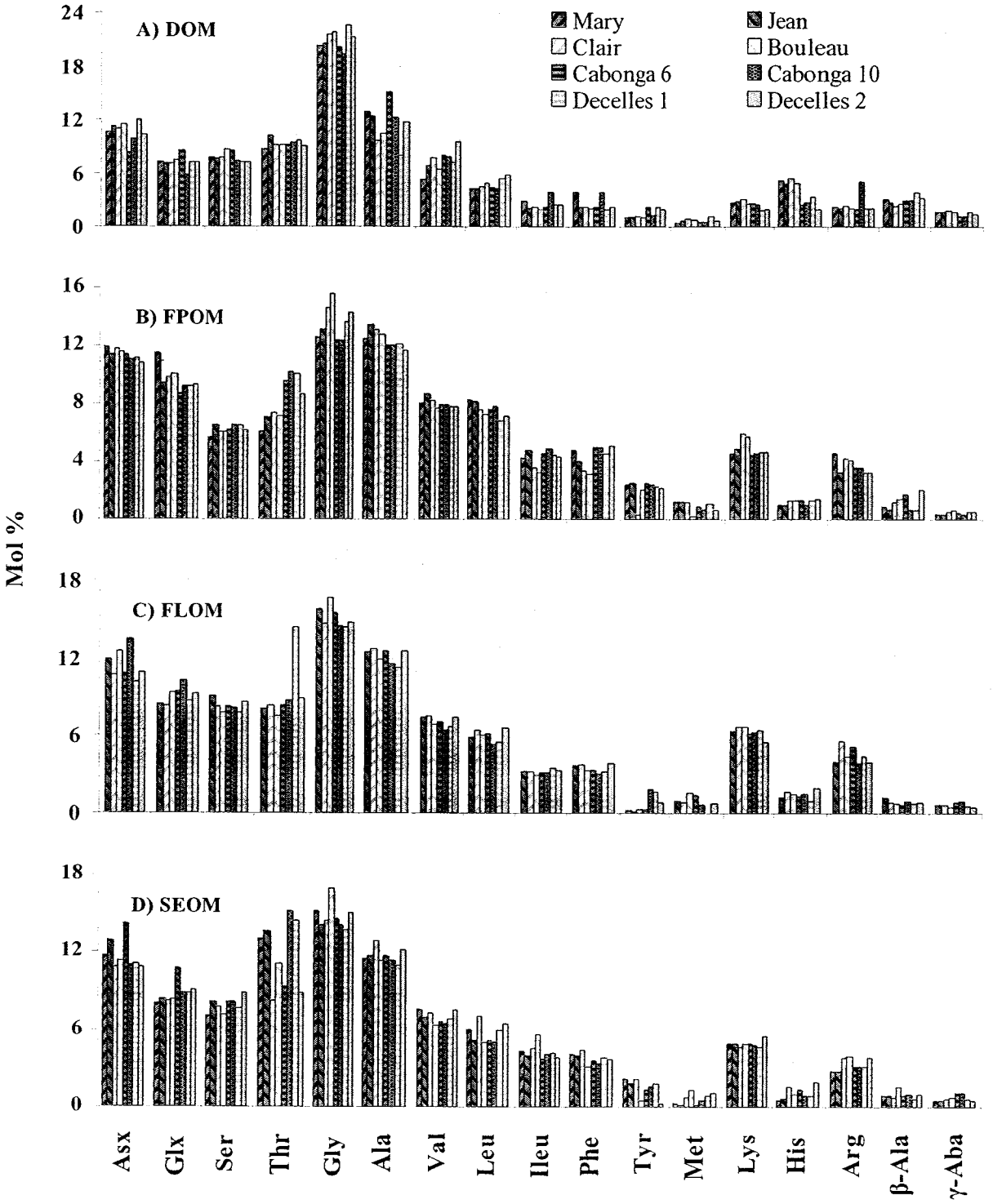

Figure 4-1. Sum of the mole percentages total hydrolysable amino acids. D + L amino acids isomers found in the (A) DOM, (B) FPOM, (C) FLOM, and (D) SEOM fractions of the different water bodies, and classified according to the chemical characteristics of their side chain: Acidic (Asx, Glx), hydroxilic (Ser, Thr), neutral (Gly, Ala, Val, Leu, Ileu), Aromatic (Phe, Tyr), Sulfuric (Met), Basic (Lys, His, Arg) and non protein (β-Ala, γ-Aba).

The non-protein amino acids β-Ala and γ-Aba, which are formed through the partial decarboxylation of aspartic and glutamic acids, respectively, are exploited as diagenetic proxies since their relative abundance increases with more advanced OM degradation (Cowie and Hedges 1994). The sum of the relative abundances measured for the two non-protein AA (%[β-Ala + γ-Aba], Figure 4-1) in POM, FLOM and SEOM samples averaged 1.6 ± 0.6 %, 1.5 ± 0.3 %, and 1.6 ± 0.4 %, respectively, and were within the range normally found for fresh OM (0 - 3 %; Cowie and Hedges 1994). β-Ala and γ-Aba were more abundant in DOM, averaging 4.5 ± 0.5 %. γ-Aba was enriched in the DOM and FPOM fractions of wood harvested lakes and reservoirs compared to natural lakes and non-harvested reservoirs (Figure 4-1), in agreement with other results that reveal larger inputs of reworked soil-derived OM upon wood harvesting (Chapter 3).

Expressing THAA concentrations per volume of water rather than per mass of freeze-dried material allows comparing the abundance of peptide/protein material in systems with widely different carbon dynamics. Such normalization highlights higher volume-normalized THAA concentrations in the dissolved phase of disturbed systems (flooded/wood-harvested lakes and reservoirs) paralleled by higher volume-normalized THAA levels in the particulate phase of lakes (independent of wood harvesting; Table 4-5). We attribute the higher volume-normalized THAA in the DOM of perturbed systems to larger inputs of soil DOM (Table 4-2; Stepanauskas et al. 2000), which comprises only a small but significant proportion of nitrogen-containing molecules (derived mostly from bacteria and their remains). In contrast, the higher volume-normalized D-AA and THAA of FPOM in lakes compared to reservoirs is attributed to greater relative proportion of plankton and bacterial cells against the N-depleted terrestrial FPOM inputs (Table 4-5).

Table 4-5. Volume-normalized total hydrolysable amino acids and D-amino acids concentrations

Station	THAA ($\mu mol\ L^{-1}$)	D-AA ($nmol\ L^{-1}$)
DOM		
LMAR	0.806	53.7
LJEA	0.647	33.3
LCLA	1.150	46.2
LBOU	1.357	75.5
RCAB-6	0.974	76.7
RCAB-10	1.251	77.8
RDEC-1	1.076	75.6
RDEC-2	1.460	99.0
FPOM		
LMAR	1.051	45.9
LJEA	1.171	53.2
LCLA	1.868	118.2
LBOU	1.235	67.8
RCAB-6	0.772	42.2
RCAB-10	0.732	34.7
RDEC-1	0.763	36.5
RDEC-2	0.721	39.0

The relative abundances of D-AA measured in the different samples are shown in Table 4-6. As observed for THAA yields, DOM had the lowest C- and N-normalized yields of D-AA. However, the highest % D-AA (sum of D-AA *vs.* THAA) were found in DOM and FPOM, with lower values measured in FLOM and SEOM. D-Asx was generally the most abundant D-AA (120 to 883 nmol mol C^{-1} and 3.06 to 11.9 μmol mol N^{-1}; Table 4-6), especially in FPOM and SEOM, followed by D-Ala and D-Glx (78.5 to 449 nmol mol C^{-1} and 1.75 to 6.01 μmol mol N^{-1}). D-Ser yields were similar in all the particulate fractions (19.8 to 57.7 nmol mol C^{-1} and 0.36 to 0.78 μmol mol N^{-1}), with slightly lower relative abundances in DOM. D-Ala yields were significantly lower in the DOM of wood harvested systems (33.6 ± 3.8 nmol mol C^{-1}) relative to the non-harvested ones (70.9 ± 10.5 nmol mol C^{-1}; $p < 0.0005$).

Table 4-6. Relative abundances of D-amino acids in all fractions

Station	% D-AA [a]	D-Asx	D-Glx	D-Ser	D-Ala	D-Asx	D-Glx	D-Ser	D-Ala	D-Asx: D-Ala [c]
		nmol mol OC^{-1} [b]				μmol mol TN^{-1} [b]				
DOM										
LMAR	6.67	66.2	56.3	27.5	77.1	1.43	1.21	0.59	1.66	0.86
LJEA	5.15	40.6	25.9	11.3	55.0	1.21	0.77	0.34	1.64	0.74
LCLA	4.02	31.1	20.3	15.5	29.9	1.00	0.65	0.49	0.96	1.04
LBOU	5.56	42.8	27.4	21.1	38.8	1.42	0.91	0.70	1.29	1.10
RCAB-6	7.88	69.6	22.7	26.8	77.1	2.53	0.83	0.98	2.81	0.90
RCAB-10	6.22	75.6	31.8	24.0	74.6	2.47	1.04	0.78	2.44	1.01
RDEC-1	7.03	50.7	24.1	6.5	30.7	2.84	1.35	0.37	1.72	1.65
RDEC-2	6.78	58.8	26.8	10.2	35.0	2.39	1.09	0.42	1.42	1.68
FPOM										
LMAR	4.37	883	449	38.9	234	10.4	5.31	0.46	2.77	3.77
LJEA	4.55	655	365	39.5	190	9.19	5.12	0.55	2.67	3.44
LCLA	6.33	634	320	30.3	321	11.9	5.99	0.57	6.01	1.98
LBOU	5.49	376	205	22.1	186	8.92	4.86	0.53	4.42	2.02
RCAB-6	5.46	278	143	22.2	159	4.54	2.34	0.36	2.60	1.74
RCAB-10	4.74	465	254	25.8	256	7.65	4.18	0.42	4.21	1.82
RDEC-1	4.79	242	122	19.8	140	6.28	3.18	0.51	3.63	1.73
RDEC-2	5.40	253	134	22.8	139	7.88	4.18	0.71	4.34	1.82
FLOM										
LMAR	–	–	–	–	–	–	–	–	–	–
LJEA	3.42	142	78.5	24.9	133	3.17	1.75	0.56	2.96	1.07
LCLA	2.77	120	87.8	22.7	156	3.06	2.24	0.58	3.99	0.77
LBOU	3.18	345	186	49.7	249	4.50	2.42	0.65	3.25	1.38
RCAB-6	3.43	183	161	41.3	227	3.45	3.03	0.78	4.28	0.81
RCAB-10	3.47	335	222	49.4	218	4.88	3.23	0.72	3.18	1.54
RDEC-1	2.73	188	145	27.1	145	3.42	2.63	0.49	2.63	1.30
RDEC-2	2.36	251	184	29.3	156	3.93	2.88	0.46	2.44	1.61
SEOM										
LMAR	3.22	541	231	36.0	319	6.12	2.62	0.41	3.61	1.69
LJEA	3.53	580	281	55.2	343	7.61	3.69	0.72	4.50	1.69
LCLA	2.97	404	257	57.7	395	5.36	3.41	0.77	5.25	1.02
LBOU	–	–	–	–	–	–	–	–	–	–
RCAB-6	3.19	375	277	51.2	248	5.44	4.01	0.74	3.50	1.55
RCAB-10	2.75	185	140	26.4	158	3.07	2.32	0.44	2.63	1.17
RDEC-1	2.35	320	228	36.3	231	4.15	2.95	0.47	2.99	1.39
RDEC-2	2.43	245	156	28.1	150	4.67	2.97	0.54	2.86	1.63

[a] Sum of the D-AA mole percentages in THAA pool. [b] Molar concentrations of the D-AA normalized to moles of OC and TN; Asx, Aspartic acid and Asparagine; Glx, Glutamic acid and Glutamine; Ser, Serine; Ala, Alanine. [c] D-Asx to D-Ala molar ratio.

Calculated D-Asx to D-Ala ratios appeared influenced by human perturbations (Table 4-6). In DOM, these perturbations led to an increase in D-Asx:D-Ala ratios compared to natural systems, with wood harvesting having the greatest impact on the ratio. The opposite trend was found for FPOM with higher D-Asx:D-Ala ratios measured in the natural lakes.

Total dissolved D-AA concentrations (nmol L^{-1}) were positively correlated to dissolved CO_2 and CH_4 concentrations with coefficients of 0.55 and 0.70, respectively (Figures 4-2A and -2B) but with low significance ($p < 0.1$) due in part to the small number of samples available for this study. Lake Bouleau was not included in the regression analysis because of the very high measured CO_2 concentrations measured in this lake, which resulted from the local flooding of land caused by a dam recently erected by beavers (Chapter 3). A negative correlation was found between dissolved CO_2 and CH_4 concentrations and %D-AA (with $r^2 = 0.85, p < 0.005$ and $r^2 = 0.65, p < 0.001$; Figures 4-2C and -2D).

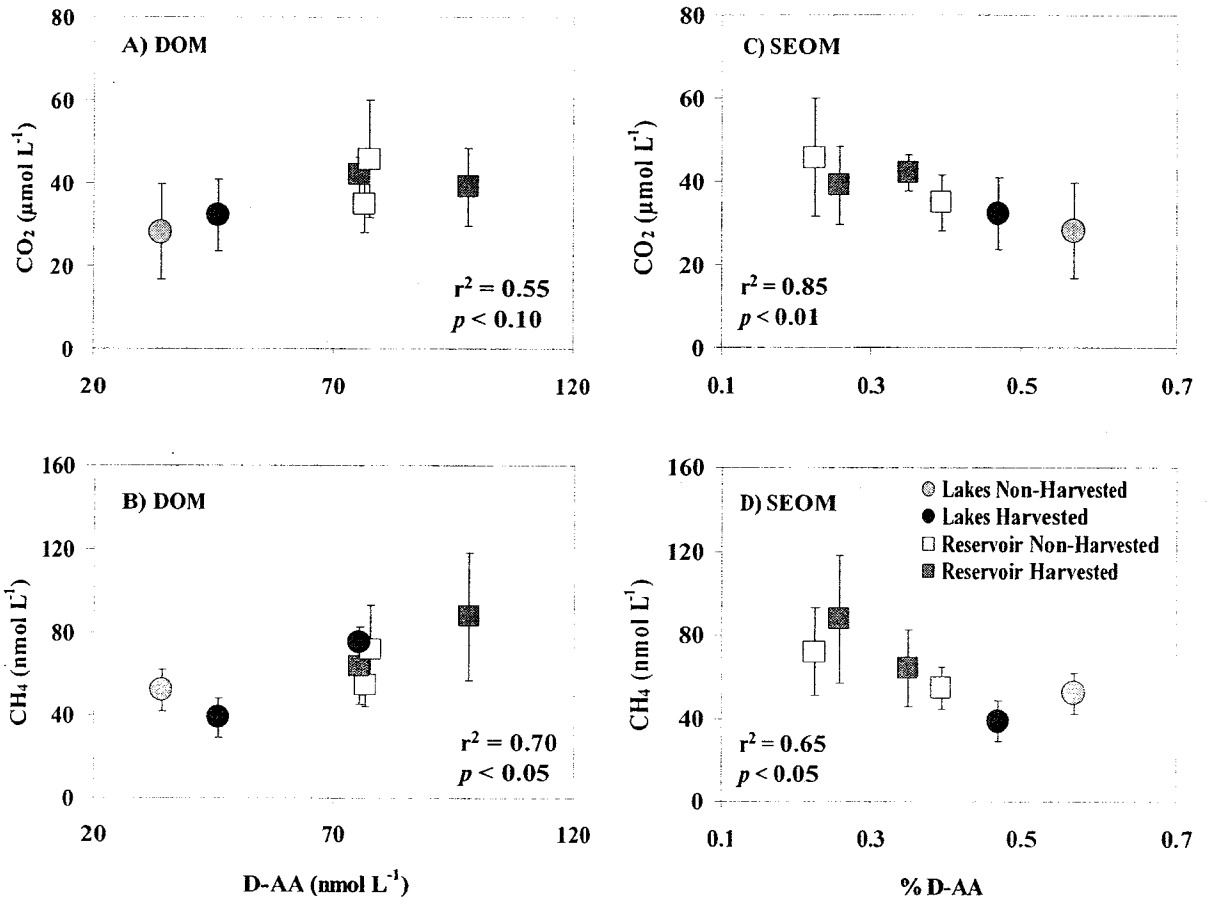

Figure 4-2. Relationship between surface water GHG and D-amino acids. D-AA concentrations in DOM (panel A, B) and % D-AA in SEOM (panel C, D) against dissolved CO_2 and CH_4 concentrations.

4.5 Discussion

4.5.1 Sources of lacustrine OM

Bulk measurements performed on DOM, FPOM, FLOM and SEOM were used to evaluate the natural sources of OM in these systems, as well as those associated with anthropogenic perturbations. The quantitatively important sources of OM in lakes and reservoirs are either allochthonous (terrestrially-derived OM) or autochthonous (OM produced within the water column or in the sediment). Groundwater DOM input could also contribute, although to a much lesser extent, and thus was not considered further in this work.

Higher DOC and FPOC concentrations were measured in perturbed system compared to natural lakes, with wood harvesting having a greater impact than reservoir operation (Table 4-2). Wood harvesting was also associated with higher DN concentrations, particularly in lakes. Such increases and proxies of OM sources suggest that human perturbation leads to the export of terrestrial OM from land into water bodies. For DOM, this hypothesis is supported by higher concentrations of iron specifically associated to DOM (Fe_{DOM}) measured in perturbed systems. As iron present in aquatic systems originates almost exclusively from land, the strong association of DOM and iron ($r^2 = 0.86$, $p < 0.001$) suggests that a considerable fraction of total DOM is derived from soils in these systems. Although less striking, the higher $(C:N)_a$ ratios obtained for DOM from perturbed systems (Table 4-3) also suggest that a greater fraction of water column DOM in these systems originated from the leaching of N-poor superficial soils (Stepanauskas et al. 2000). Using the C and N stable isotope signatures to discriminate between sources of DOM is difficult since DOM $\delta^{13}C_{org}$ values are fairly invariant at around -27‰, while DOM $\delta^{15}N_{tot}$ values are modulated by the signature of the N_{inorg} pool. Based on these values, the major DOM source in aquatic systems is frequently attributed to higher plants (Meyers 2003; Lehmann et al. 2004; McCallister et al. 2004). However, other sources must be considered; in a recent study, DOM leached from superficial soils and litter was isotopically distinct from water column DOM, with carbon and nitrogen stable isotope signatures of -25.0 to -26.5 ‰ and -0.7 to 4.8 ‰, respectively (Chapter 3). Water column $\delta^{13}C$ DOM signatures measured in our systems were also invariant, although with slightly more depleted signatures (Table 4-3), suggesting a

mixture of surficial soil leachate with small contributions from the more depleted autochtonous DOM exudates (phytoplankton: -32.7 ‰ ± 1.7 ‰; Marty and Planas 2008).

The absolute values and the significant differences in FPOM $(C:N)_a$ ratios and D-AA yields between the harvested and non-harvested water bodies provide clues on the source of particulate OM found in these systems. The lower $(C:N)_a$ ratios but higher $\%T_{AA}C$ (>14%) of the FPOM from natural lakes agree with the hypothesis of a greater terrestrial contribution to the FPOM fraction of perturbed systems. The range of $\delta^{13}C$ signatures measured for FPOM in this study reflects a mix of sources likely dominated by phytoplankton (-32.7 ± 1.7 ‰; Marty and Planas 2008), forest litter ($\delta^{13}C$ = -27.2 ± 1.1 ‰, Chapter 3), and bacterial cells and their remains (variable signatures).

The FPOM $\delta^{15}N_{tot}$ signature were in most cases comparable to those of the boreal forest soil litter (-1.0 ± 0.9 ‰; Chapter 3). Because $\delta^{15}N_{tot}$ signatures are affected by a larger number of sources and processing pathways (Lehmann et al. 2004), constraining TN sources using $\delta^{15}N_{tot}$ is more difficult. The more depleted $\delta^{15}N_{tot}$ signatures of DOM compared to soil litter leachates (0.7 ‰; Chapter 3) possibly result from the selective utilization of N by primary producers and bacteria, from isotopic fractionation through sorption/desorption exchanges with the particulate fraction and/or through DOM percolation in soils (Aufdenkampe et al. 2001).

A significant bacterial contribution to the solid phases of the water column and the sediment is likely what causes the important decrease in $(C:N)_a$ ratios measured with sedimentation. This relative enrichment in N was measured in the FLOM samples of flooded systems and in the SEOM samples of non-flooded lakes. A decrease in $(C:N)_a$ ratios suggests an increasing contribution from bacterial cells and their remains (enriched

in N). N-immobilization has been reported in N-depleted detritus where most of the nitrogen fixed by attached microorganisms was inorganic (Melillo et al. 1984; Tremblay and Benner 2006). Moreover, the $\delta^{13}C$ isotopic compositions of flocculate material and sediments were slightly enriched compared to the FPOM counterparts, reflecting microbial reworking of OM in the former. The $\delta^{15}N$ signature became generally more depleted after sedimentation suggesting either denitrification, incorporation into bacterial biomass or degradation and loss of organic nitrogen.

4.5.2 Changes in OM diagenetic state

Assessing the freshness of OM in the different fractions sampled in these systems also provides clues on the dynamics of C and N in aquatic environments. Although directly comparing dissolved and particulate samples is risky (Aufdenkampe et al. 2001), the much lower $\%T_{AA}C$ and $\%T_{AA}N$, as well as generally lower DI values (especially in reservoirs), measured in DOM likely reflects the highly reworked nature of DOM compared to FPOM in freshwater systems (Cowie and Hedges 1994; Tremblay and Benner 2009). The relative abundances of β-Ala and γ-Aba were higher in DOM and provide additional support to this conclusion (Amon and Benner 1996).

The generally lower FPOM $\%T_{AA}C$ and $\%T_{AA}N$ in reservoirs again is attributed to higher inputs of vascular plants and biologically altered debris upon reservoir operation. This finding indicates that FPOM is less diagenetically altered in lakes than in reservoirs. In addition, the waters of natural lakes receive lower quantities of light-absorbing terrestrial DOM allowing greater production of fresh particulate material through photosynthetic activity as terrestrial DOM as been shown to decrease light penetration depth (Schindler et al. 1997; Karlsson et al. 2009; Chapter 3).

The high $\%T_{AA}N$ values measured for FLOM and SEOM suggest relatively fresh organic N near the sediment-water interface in all systems. The presence of fresh N-containing compounds in these fractions can be attributed to autochthonous OM production through bacterial reworking and production. Phytoplanktonic OM produced in surface waters is also believed to contribute to the FLOM and SEOM fractions, although the relative importance of the two sources is difficult to estimate. Significant bacterial contribution during OM diagenesis would also explain why the $\%T_{AA}C$ generally increased with depth (and thus with time) from FPOM to FLOM to SEOM in perturbed water bodies, especially since the starting material in these systems is characterized by low $\%T_{AA}C$ and a strong vascular plant signature (Tremblay and Benner 2006). This bacterial contribution near the sediment-water interface is consistent with the decrease in $(C:N)_a$ ratios observed in FPOM or SEOM.

The percentage of carbon or nitrogen accounted for by AA ($\%T_{AA}C$ and $\%T_{AA}N$, respectively) and the DI are commonly used as indicators of OM freshness, although over different time scales. THAA yields are considered indicators of the first stage of diagenesis whereas DI better reflect more advanced degradation and are less sensitive to the subtle changes occurring over short time scales following the death of living organisms (Davis et al. 2009; Bourgoin and Tremblay in press). These proxies exhibited opposite trends in DOM and FPOM samples, with higher reservoir DOM $\%T_{AA}N$ values corresponding to lower DI values and lower reservoir FPOM $\%T_{AA}N$ (and $\%T_{AA}C$ in this case) values corresponding to higher DI values (Table 4-4). The opposite trends were found in lakes. These contrasting trends likely reflect changes occurring over different time scales and thus affecting different pools of OM. As reservoirs are not flow-through

systems, the continual addition of fresh OM sources in these systems makes the interpretation of these proxies difficult. When fresh OM is incorporated into a pool of altered OM, AA yields can increase while the DI values calculated from the total AA pool remain low. This hypothesis is supported by data obtained in the water column of the St. Lawrence Estuary where deep water POM exhibited low $\%T_{AA}N$ associated with high DI values, while underlying sediments had higher $\%T_{AA}N$ associated with lower DI values (Bourgoin and Tremblay, in press). Such results can be explained by the recycling of POM by sedimentary bacteria that add fresh AA to a relatively altered OM pool as they grow. The contrasting trends between $\%T_{AA}N$ and DI cannot be explained by variations in inorganic N (nitrates) content in the DOM concentrates as inorganic N in the original samples (measured nitrate concentrations; Chapter 3), never exceeded 8% of the total amount of organic N recovered in the DOM concentrate. Furthermore, nitrate concentrations were very similar in all water bodies and thus could not have given rise to the observed trend in $\%T_{AA}N$.

4.5.3 Changes in bacterial abundance

The relative contributions of D-AA vs. THAA (% D-AA) often co-vary with several independent indicators of diagenetic state (Tremblay and Benner 2009) supporting the idea that molecules rich in D-AA exhibit lower degradation rates than those composed exclusively of the L-isomer (*e.g.*, proteins) (Jørgensen et al. 2003; Nagata et al. 2003). High % D-AA in DOM are also promoted by preferential release of some D-AA during bacterial growth (Bjørnsen 1988; Kawasaki and Benner 2006). These processes explain the high % D-AA measured in DOM compared to the other fractions. The generally lower % D-AA found in lake DOM compared to reservoir DOM could

reflect contrasting inputs of terrigenous D-AA stemming from the differences in hydrology between the two types of water bodies. The percentage of D-AA in FPOM increases slightly with reservoir operation and wood harvesting, consistent with a more advanced degradation state of FPOM in perturbed systems.

Carbon- and nitrogen-normalized yields of D-Ala and D-Glx have been used as indicators of bacterial contribution to bulk C and N (Tremblay and Benner 2006; 2009; Kaiser and Benner 2008). Unlike % D-AA, they appear to be relatively insensitive to diagenesis and thus are representative of bacterial C and N content in a sample. In particular, D-Ala has been shown to be representative of bulk bacterial OM in vascular plant detritus (Tremblay and Benner 2006). In agreement with the bulk data presented above, the negative correlation ($r^2 = 0.74$; $p < 0.005$; not shown) found in this work between C-normalized D-Ala abundances and DOC concentrations suggests that non-bacterial sources, most likely terrigenous plants and soil litter, predominantly fuel the high DOC concentrations in perturbed systems. In contrast, the relationships between D-Asx, D-Glx and D-Ser with DOC were much weaker ($r^2 < 0.32$, not shown), suggesting that the variations in the relative abundance of each D-AA were driven by different factors. In general, higher carbon- and nitrogen-normalized D-Asx yields were observed in the DOM of reservoirs compared to lakes, while D-Ala prevailed in all non-harvested systems. These shifts in concentrations possibly reflect additional inputs from soil DOM during reservoir operation. This is in agreement with Stepanauskas et al. (2000) who have shown that D-Asx is a major constituent of the terrestrially-leached D-AA pool (as much as 38 % of total D-AA yields). Noteworthy, the D-Asx to D-Ala ratios calculated for this data set seem to reflect the contribution of soil-derived terrigenous OM to the DOM pool

of aquatic systems (Table 4-6). Human perturbation leads to an increase in D-Asx:D-Ala ratios compared to natural systems, with wood harvesting having the greatest impact on the ratio. Although a lot more work must be carried out to evaluate its validity and robustness, this ratio could be used as a proxy, in combination with other markers, to estimate the contribution of terrestrial OM to the DOM pool in boreal aquatic systems.

We found the opposite trend for FPOM with higher D-Asx:D-Ala ratios measured in the natural lakes. The magnitude of the differences argues against pH-driven preferential adsorption of D-Asx to particles (Hedges et al. 1994; Aufdenkampe et al. 2001) as a major driver of the measured ratios. The most probable explanation for the steep changes in the D-Asx:D-Ala ratios most likely is a change in the bacterial assemblages contributing to FPOM. The D-Asx:D-Ala ratios are highly variable in bacteria; for instance, D-Asx is not found in phototrophic bacteria (cyanobacteria) and G+ bacteria are generally enriched in D-Ala due to their much thicker peptidoglycan structure (Schleifer and Kandler 1972, Kaiser and Benner, 2008). Greater proportion of cyanobacteria or G+ bacteria could thus have caused the lower D-Asx:D-Ala ratios measured in the perturbed systems. In agreement, Prepas et al. (2001) have shown that higher and lower amounts of cyanobacteria and phytoplankton were measured after wood harvesting. Consistantly, G+ bacteria are expected to thrive in the water columns of reservoirs (well oxygenated and warm, with temperature from 17.9 to 23.0°C and O_2 saturation levels > 87.5 %) and harvested lakes (presence of a thermocline and oxygen depletion near the sediment with temperature < 5.6°C and O_2 saturation levels < 25.8 %) while G- bacteria should predominate in cold water columns with high O_2 saturation levels in natural lakes (< 8.8°C and > 93 % O_2; Leduc and Ferroni 1979; Halda-Alija and

Johnson 1999). FPOM bacterial communities within reservoirs appear independent of wood harvesting as the measured FPOM D-Asx:D-Ala ratios do not change significantly between natural and harvested systems. While more work should be carried out to confirm that variations in D-Asx:D-Ala ratios accurately reflects differences in bacterial communities, the preliminary results obtained here appear promising.

Several lines of evidence suggest that bacteria play a key role in the production of GHG in these systems. In this study, D-AA concentrations are associated with the abundance of bacterially-derived material and a parallel is drawn between the abundance of D-AA in DOM or SEOM and the dissolved GHG concentrations (Figure 4-2). Although bacterial activities were not determined in this work, the stronger negative correlation found between surface GHG concentrations and % D-AA in SEOM (r^2 = 0.85, $p < 0.01$, and $r^2 = 0.65$, $p < 0.05$, for CO_2 and CH_4, respectively; Figures 4-2C and -2D) support the hypothesis of a link between heterotrophic activity in the water column and the AA composition of OM depositing in the sediment. In systems with higher concentrations of dissolved GHG, the L-AA containing macromolecules in the SEOM fraction, which are more labile than the D-AA rich ones (Stepanauskas et al. 2000), would be preferentially degraded while the more recalcitrant D-AA containing macromolecules would accumulate in the DOM fraction since peptidoglycan in G- is more recalcitrant than in G+ bacteria (Jørgensen et al. 2003). This hypothesis is supported by the volume normalized D-AA concentrations results (Table 4-5), which suggest that perturbed systems, particularly reservoirs, contain higher proportions of G+ bacteria. The trends highlighted in Figure 4-2 also suggest that the bacterial contribution to total DOM is enhanced as a result of reservoir operation, wood harvesting or flooding,

and that this increase is linked to the high CO_2 and CH_4 concentrations in surface waters (Figures 4-2A and 2B).

4.5.4 Principal component analysis

To identify more complex relationships between parameters and subtle differences between natural and perturbed water bodies, we applied a principal component analysis (PCA) to the relative abundances of AA (in mol % *vs.* THAA, and considering D- and L-AA as separate input variables) in DOM and FPOM. Loading values, corresponding to the contribution of individual variables contained in a PC, were first attributed to each AA through a first PCA run. To reduce the number of variables in the system, only AA with loadings values above 0.30 and 0.25 for DOM and FPOM, respectively, were then used in a second analysis. The two first principal components (PC) of the latter analysis are represented graphically in Figure 4-3 and comprise 11 (D-Asx, L-Asx, Gly, D-Val, D-Leu, L-Leu, L-Tyr, L-Lys, L-His, β-Ala and γ-Aba) and 12 (L-Glx, D-Ser, L-Thr, Gly, D-Ala, L-Ala, L-Ileu, L-Phe, L-Lys, L-His, L-Arg, and γ-Aba) AA for DOM and FPOM, respectively. Interestingly, the four different scenarios (natural lake, wood-harvested lake, reservoir, wood-harvested reservoir) are well separated in the space represented by the first two components and occupy a distinct quadrant when only considering variations in the relative abundances of AA in these samples (Figure 4-3). The variations in AA distribution in the DOM and FPOM fractions are thus coupled to the changes occurring in the aquatic cycle of carbon upon reservoir operation and wood harvesting. As shown above, these perturbations affect the relative importance of DOM exports from land to the water bodies, primary production and bacterial activity in the water column and the sediment. Noteworthy, most AA found in

G+ bacterial peptidoglycan (Gly, D- and L- conformations of Ala, Asp, Glu and Ser as well as L-Lys and L-Thr) had high loading values and thus were thus a major determinant in the PCA analyses.

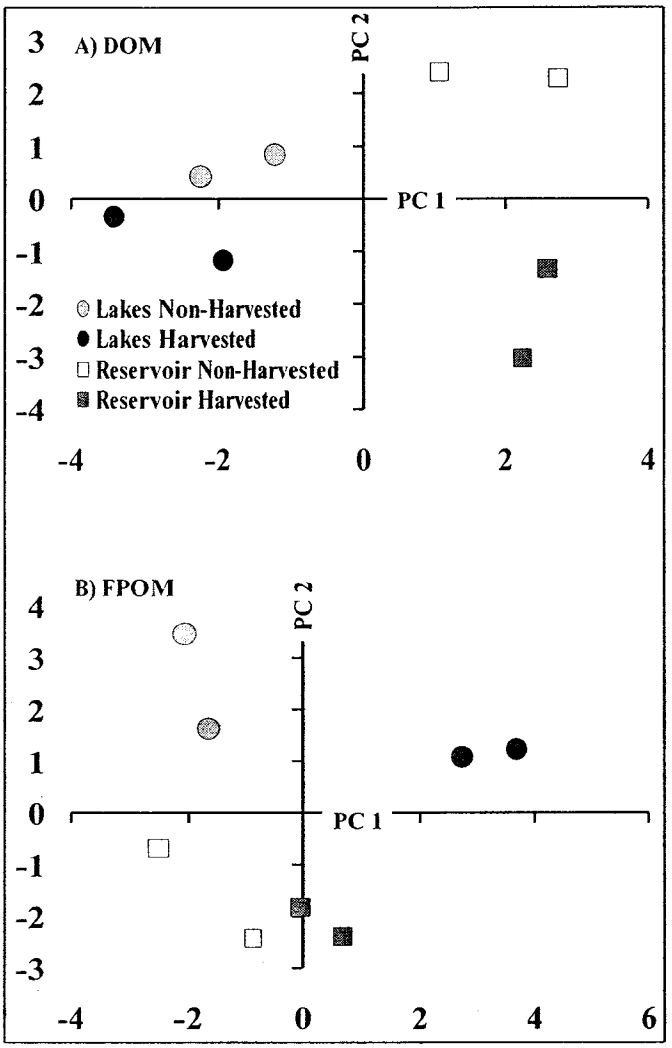

Figure 4-3. Graphical representation of the first two principal components (PC) for relative abundance (mol %) of amino acids. In (A) DOM (D-Asx, L-Asx, Gly, D-Val, D-Leu, L-Leu, L-Tyr, L-Lys, L-His, β-Ala, and γ-Aba) and (B) FPOM (L-Glx, L-Thr, D-Ser, Gly, D-Ala, L-Ala, L-Ileu, L-Phe, L-Lys, L-His, L-Arg and γ-Aba). See text for explanations.

The first PC (PC1) of the second DOM PCA analysis (Figure 4-3A), which accounts for 54.1 % of the total variability and results in scores that are positive for reservoirs and negative for lakes, suggests that reservoir operation exerts a strong influence on the dissolved THAA composition. The second PC (PC2; 31.6 % of the total variability) separates harvested from non-harvested systems. These PC2 scores suggest that the effect of wood-harvesting on DOM composition was more perceptible in the reservoirs than in lakes studied in this work. The scores generated for the PC1 of the DOM dataset were strongly correlated to the % D-AA in dissolved THAA of the lakes (r^2 of 0.99, $p < 0.005$, and 0.66, $p < 0.35$, for lakes and reservoirs samples, respectively; results not shown), which suggests that the AA composition of lake DOM was mostly modulated by bacterial activity and contributions. In contrast, the reservoir DOM AA composition appeared to be controlled not only by bacteria but also by other DOM inputs, such as soil leachates and autochthonous exudates.

A different PCA-based separation pattern was obtained for the FPOM dataset (Figure 4-3B). Principal component 1 accounts for 42.1 % of the total variability and separates harvested from non-harvested water bodies while PC2, accounting for 40 % of the variability, differentiates lakes and reservoirs. As for DOM, FPOM PC1 scores were correlated to D-AA mole percentages in particulate THAA (r^2 of 0.61, $p < 0.05$ including all systems; results not shown), which also argues for a FPOM AA composition that is strongly affected by bacterial inputs. These statistical patterns suggest that bacterial communities and/or contributions to OM are sensitive to changes in the magnitude and composition of OM inputs as well as to changes in the hydrologic regime of aquatic systems.

Variations in AA relative and absolute abundances offers insight into the dynamics of carbon and nitrogen in aquatic systems, in particular with respect to the role of bacteria in the processing of organic compounds, and to predicting how these systems react to anthropogenic perturbations. They thus offer complementary diagnostic information to bulk analyses (Chapter 3), as well as to other organic biomarkers such as lipids and lignin (results to be published elsewhere). Our AA analyses have shown that the effect of reservoir operation on aquatic systems is not only visible at the macroscopic level but can leave a microbial and molecular imprint on the aquatic cycle of carbon and nitrogen for more than half a century after impoundment. The effect of wood harvesting on the other hand, while important in the first few years, is likely to decrease with forest re-growth. Reservoir operation and wood harvesting result in the export of a substantial quantity of terrestrial DOM into water systems and lead to changes in bacterial dynamics and populations as monitored through the analysis of the D-AA pool. The increase in DOM export is the major cause for the higher surface water concentrations of CO_2 and CH_4. In agreement with our previous study (Chapter 3), AA dynamics support the hypothesis of modifications in the balance between heterotrophic and autotrophic processes as being the main cause for the observed differences in dissolved GHG upon reservoir operation or wood harvesting. Amino-acids are proving to be an extremely valuable tool for broadly characterizing the major pathways and players that control the fate of C and N in aquatic systems, and their link to GHG concentrations and fluxes.

Chapter 5.

5 The modulation of the carbon cycling in natural and perturbed boreal aquatic ecosystems: A lipid biomarkers approach

To be submitted to Limnology and Oceanography as:

Alexandre Ouellet, Marc Lucotte and Yves Gélinas

5.1 Abstract

Most worldwide lakes are supersaturated in dissolved carbon dioxide (CO_2) concentrations. Allochthonous organic matter (OM) inputs in aquatic systems are believed to drive the carbon (C) cycle biochemical reactions that lead to greenhouse gas (GHG) production. To better understand the controls on the mechanisms leading to surface water GHG supersaturation, we analyzed fatty acids (FA) and alkanes, including their compound-specific $\delta^{13}C$ signatures, in the dissolved, fine particulate and sedimentary organic matter fractions (DOM, FPOM and SEOM, respectively) from natural lakes, old reservoirs, as well as lakes and reservoirs with a wood harvested watershed. The FA composition in the FPOM fraction suggests that bacteria dominated autochthonous OM production. Phospholipid FA concentrations and $\delta^{13}C$ signatures suggest that a large fraction of the fresh OM biomass originated from prokaryotic bacteria. The composition of the alkane fraction in SEOM suggests higher bacterial biomass in reservoirs compared to lakes, which would lead to lower abundances of terrestrial OM and higher surface water CO_2 concentrations. Our results show that CO_2 production in boreal freshwater systems is largely derived from bacteria mediated terrigenous OM degradation.

5.2 Introduction

Greenhouse gases (GHG), most importantly carbon dioxide (CO_2) and methane (CH_4), are believed to be the main drivers of global warming (IPCC 2007). Lakes and reservoirs, as opposed to marine ecosystems, are generally supersaturated with GHG (Cole et al. 1994; St-Louis et al. 2000). Freshwater lakes and reservoirs are very dynamic ecosystems in which the main forces driving carbon dynamics are profoundly influenced by aquatic organic matter (OM) source, *i.e.* the primary production within the aquatic system (autochthonous source) and terrestrial material exported from surrounding soils and litter (allochthonous source).

Greenhouse gases concentrations in most natural aquatic ecosystems are controlled by similar processes, namely photo- and bacterial oxidation of OM, as well as groundwater and terrestrial inorganic carbon inputs. Although still debated, bacterial OM degradation (heterotrophy) is generally believed to be the major force driving CO_2 supersaturation in boreal lakes and reservoirs (del Giorgio et al. 1997; Carignan et al. 2000a; Prairie et al. 2002; Dubois et al. 2009). Indeed, data from recent studies strongly suggest that allochthonous OM and nutrient inputs followed by OM degradation are the main source of GHG water supersaturation (Sobek et al. 2003; McCallister and del Giorgio 2008). Part of this controversy persists however because natural lakes are characterized by highly variable relative contributions from autotrophic and heterotrophic processes, both in time and space.

Anthropogenic perturbations of watersheds surrounding aquatic systems lead to the additional transfer of high quantities of OM and nutrients to the water bodies (Carignan et al. 2000b; Lamontagne et al. 2000). These additional inputs cause broad

shifts in aquatic biogeochemical conditions that go beyond the natural variability of the systems and that can then be used to better constrain the processes (and their controls) leading to GHG production in freshwater systems. In this study, we exploited the perturbations following long-term reservoir impoundment and operation, and wood harvesting to study carbon dynamics in water bodies of the boreal forest.

A few studies have been carried out to compare GHG supersaturation levels and emissions in old boreal reservoirs (15 years after impoundment) with those of natural lakes. However, there is currently no agreement as to whether both types of system are similar carbon emitters (Duchemin et al. 1995; Tremblay et al. 2005; Chapter 3). Although a considerable number of studies focus on the optimization and comparison of methods to accurately measure GHG concentrations and atmospheric fluxes (Cole and Caraco 1998; Duchemin et al. 1999; Soumis et al. 2008), only a few studies have addressed the long-term effect of increased terrestrial OM loadings on the production of GHG in freshwater systems (Houel et al. 2006; Soumis et al. 2007; Chapter 4). It has been shown, for instance, that watershed wood harvesting increase the transfer of nutrients such as dissolved organic carbon (DOC), total nitrogen and phosphorus (TN and TP) from soils and litter to the water bodies, which stimulates aquatic algal and bacterial populations (Carignan et al. 2000b; Planas et al. 2000, Prepas et al. 2001). Moreover, these studies have also shown that the effects of wood harvesting on aquatic bioprocesses slowly dissipate with forest re-growth. The consequences of terrestrial nutrient inputs on the normal aquatic GHG cycle and production have only recently been measured (Chapter 3, Chapter 4). Forest cutting significantly increases the aquatic production and emission of CO_2 into the atmosphere. Yet, only little information exists on how the

processing of the additional allochthonous OM inputs following anthropogenic perturbations translates into additional dissolved CO_2 levels.

The OM derived from primary production and terrestrial inputs sinks through the water column and into the sediment where it is substantially reworked and degraded to CO_2 in oxic systems, and to CH_4 under anoxic conditions. Terrestrial export of OM to aquatic systems, mostly as dissolved, and *in situ* particulate and sedimentary organic matter (DOM,POM and SEOM, respectively) production are closely linked as watersheds are a source of essential nutrients (*e.g.* nitrogen and phosphorus) that ultimately influence in-lake production (Planas et al. 2000). The study of DOM, POM and SEOM is therefore essential for understanding the processes leading to GHG production, saturation levels and emissions to the atmosphere from freshwater ecosystems (Kling et al. 1990, Cole et al. 1994). Organic matter from the different sources undergoes degradation at contrasting rates based on the reactivity of the different compounds; as a result the more refractory organic molecules are preferentially preserved in the sediments. These resistant molecules reflect the conditions and processes that existed at the time of their synthesis and thus constitute a rich record of the life of an ecosystem. Lipids for instance are resistant biochemicals that are routinely used as biomarkers for identifying sedimentary OM sources and pathways in freshwater, estuarine and marine ecosystems (Cranwell et al. 1987; Zimmerman and Canuel 2001; Arzayus and Canuel 2004). As an example, phospholipid fatty acids (PLFA), which are embedded in the cell membrane of living organisms, have been used extensively as biomarkers for fresh OM as they are quickly mineralized when released upon cell death. PLFA are therefore exquisite proxies for 'living', or very recently living, biomass while the glycolipid derived fatty acids (GCFA)

more closely trace non living remains of biota as they are more resistant to degradation (Rindelberg et al. 1997; Bouillon et al. 2004; Li et al. 2007). Furthermore, because intense bacterial OM reworking in the sediment quickly results in the degradation of most PLFA depositing from the water column, sedimentary PLFA are often considered as a tracer for bacteria in marine sediments. Although less diversified than fatty acids (FA), alkanes are also widely used in the identification of OM sources in the sediments. Their well-known resistance to microbial degradation makes them ideal tools for evaluating OM sources over geological time scales (Eglinton and Hamilton 1967; Hautevelle et al. 2007; Hu et al. 2009).

Traditionally applied to sediments, biomarker analyses have been more recently used on POM and the high molecular weight fraction of DOM (McCallister et al. 2006; Loh et al. 2008). This approach allows for the simultaneous evaluation of recent and historic changes in OM production, loading to, and diagenetic state of the sediment. In this study, FA and alkane biomarkers were analyzed in the DOM, fine POM (FPOM, < 70μm) as well as SEOM, and were used to trace OM production, inputs and degradation processes leading to GHG production and consumption in natural and perturbed systems.

5.3 Methods

5.3.1 Study sites and sampling

Two hydroelectric reservoirs (Cabonga and Decelles) as well as four lakes were sampled during the summer of 2007 in the Abitibi region of the Canadian boreal forest. Three water bodies (Decelles Reservoir, Lake Clair, and Lake Bouleau) were wood harvested to differing degrees within two years of sampling (1 to 5% of their total watershed; Chapter 4, Table 4-1). Both reservoirs have very different morphologies

(Chapter 3, Figure 3-1): Decelles Reservoir is a rather small (237 km^2) but very long and dendritic water body while Cabonga Reservoir is wider and larger (434 km^2), with numerous islands of varying sizes. All the lakes sampled in this work were small, with areas ranging from 0.34 to 1.88 km^2.

In order to evaluate the carbon cycling in the different systems, we sampled DOM, POM and SEOM at the deepest location of the lakes and at two chosen sites in the reservoirs (within a morphologically representative zone and near the river output (details are available in Chapter 4, Table 4-1)). Details on the methodology adopted for the surface GHG sampling can be found in Chapter 3. Briefly, exactly 30 mL of the surface water layer was sampled in four 60-mL syringes in which an additional ultra pure 30 mL of nitrogen was added. The syringes were shaken for 60 seconds and were then allowed to rest horizontally for 2 minutes. The water was removed, its temperature was recorded and the gaseous samples were analyzed with a 3400 Varian gas chromatograph (GC) coupled to a flame ionization detector (FID) and a thermal conductivity detector for CH_4 and CO_2 analyses, respectively. Sample quantification was done through the analysis of a certified gas standard (Scotty 48, mix 218) and the concentrations were corrected following Soumis et al. (2008).

In order to collect sufficient amounts of integrated DOM and fine POM (FPOM), 200 to 250 L of pre-filtered water (70-μm nylon mesh), 12V submersible pumps were used. All samples were integrated over the entire water column by 0.5 to 1-m increments to a maximum of 10 meters and were collected in pre-rinsed 50-L Nalgene containers. Following water collection, both DOM and FPOM fractions were separated using a tangential flow filtration reverse osmosis (TFF-RO) system (as described in Chapter 2)

and were doped with $HgCl_2$ (~0.3 mM final concentration). Three liters of the concentrated DOM and all the FPOM samples were freeze-dried and kept in glass containers for further analysis. The sediments were sampled at or near a sediment-accumulating zone using a Mackereth corer system (Mackereth 1958) or scuba divers equipped with 3-cm wide and 1-m long plexiglass cylinders. The sediments were sliced at each centimeter from 0 to 5 cm, frozen and freeze-dried in PE 50-mL centrifuge tubes. Equal quantities of the first three cm of the sediment cores were pooled prior to the analyses. Sedimentation rates for all lakes were determined using the ^{210}Pb method described in Chapter 4. Sedimentation rates for Reservoir Decelles were impossible to obtain most likely because of large bio- and hydroturbation.

5.3.2 Biomarker analysis

5.3.2.1 Lipid extraction

Prior to the lipid extraction, 0.1 mg of fully deuteurated internal standards, namely n-docosane, pentadecanoic acid and n-octadecyl alcohol, were added to the DOM, FPOM and SEOM samples. Lipids were extracted 3 times using a 2:1:0.8 mixture of chloroform, methanol and water. The lipid fractions were combined and evaporated using a rotary evaporator or under a gentle stream of pure nitrogen. Lipids were redissolved in hexane and separated by polarity (using deactivated silica) into hydrocarbons (F1; 10 mL of 25% toluene in hexane), glycolipids (F2; 10 mL of 20% ethyl acetate in hexane) and phospholipids (F3; 12 mL of methanol) fractions that were collected in 24-mL vials. The hydrocarbon fraction was gently evaporated to decrease sample volume, quantitatively transferred into 2-mL vials, further reduced to 200 µL and directly analyzed by GC-FID. Both the glycolipids and phospholipid fractions (F2 and

F3) were saponified using 5 mL of 0.5 M KOH in methanol in capped 24-mL vials for 2 hours in a sand bath maintained at a temperature of 100°C. Following the reaction, 1.5 mL of 5% NaCl was added and the alcohols were extracted 3 times with 3 mL of CH_2Cl_2 (F2 and F3 neutral lipids). The remaining basic aqueous solutions F2 and F3 (methanol - water) were acidified to pH 2 with 6N HCl and the FA that they contained were extracted 3 times with 3 mL of CH_2Cl_2. The FA (F2 and F3 acidic lipids) were dried using combusted (450°C, 4h) Na_2SO_4.

5.3.2.2 Gas chromatography analysis

Fatty acids from both glycolipids and phospholipids (F2A and F3A) were gently N_2-evaporated to dryness and esterified using 1 mL 10% BF_3 in methanol for 2 hours at 100°C. Following the esterification, 2 mL of 5% NaCl was added and the fatty acids methyl esters (FAME) were extracted 3 times with 2 mL of hexane. The fatty acids FAME were subsequently dried using Na_2SO_4. Alkanes (F1) and FAME (F2A and F3A) were quantified and molecularly characterized using gas chromatography systems coupled to flame ionization and mass spectrometer detectors. (GC-FID/MS). The quantification of FA was made against external standards (Supelco D2887 alkane and Supelco37 FAME mixes, respectively) using a 6890 Agilent GC-FID equipped with a 0.25-mm wide, 30-m long DB-5 column that contained a 0.25-μm thick stationary phase. Gas chromatography oven temperatures were programmed from 70°C (hold 1 min) to 230°C (16°C/min) and then to 310°C (10°C/min, hold 19 min) at a helium flow of 2 mL/min for alkanes. The ramp program for the FAME fractions was from 45°C (hold 1 min) to 140°C (15°C/min), 214 (4°C/min), 216 (0.5°C/min), 219 (4°C/min), 223 (0.5°C/min) and to 310°C (10°C/min, hold 15 min) at a helium flow of 1.5 mL/min. The

alkanes and fatty acid identification was done relative to the retention times of external standards and using a Varian 3800 GC equipped with the same chromatography column as the one used for quantification. The Varian 3800 GC was coupled to a Saturn ion trap mass spectrometer model 2000.

5.3.3 Elemental and isotopic measurements

5.3.3.1 Bulk organic matter analysis

Carbon and nitrogen elemental and isotopic compositions (%C, %N and $\delta^{13}C_{org}$ respectively) for DOM, FPOM and SEOM samples were obtained using an EuroVector 3028-HT elemental analyzer coupled to an Isoprime GV Instrument stable isotope ratio mass spectrometer (EA-IRMS). Isotopic standardization as well as instrumental linear response changes with intensities were measured using the VPDB-calibrated standards IAEA-C6 Sucrose ($\delta^{13}C$ = -10.45 ± 0.03 ‰, %C = 42.11; Coplen et al., 2006) as well as β-alanine (a pre-calibrated in house standard ($\delta^{13}C$ = -25.98 ± 0.23 ‰; %C = 40.45 and %N = 15.72)). Carbon and nitrogen percentages of the samples were obtained against wide range calibration curves which were obtained from sucrose and alanine for %C as well as from alanine and ammonium sulfate for %N. Before EA-IRMS $\delta^{13}C_{org}$ analysis, samples were decarbonated using vapor-phase HCl (Hedges and Stern 1984). Percent N were analyzed separately on non-acidified aliquots to avoid nitrogen loss during acidification. Method reproducibility was determined with one triplicate analysis in each sample set.

5.3.3.2 Biomarker $\delta^{13}C$ signature analysis

In-house $\delta^{13}C$ calibration of a series of alkane standards (C_{14}, C_{16}, C_{18}, C_{21}, C_{23} and C_{26}; >95 % purity) was carried out using the EA-IRMS. Isotopic calibration was

done using the IAEA-C6 sucrose standard and β-alanine described above. The isotopic compositions of the alkane in-house standards are, from C_{14} to C_{26}: -34.37 ± 0.07 ‰, -34.07 ± 0.05 ‰, -33.43 ± 0.06 ‰, -30.09 ± 0.04 ‰, -28.34 ± 0.03 ‰ and -29.78 ± 0.03 ‰, respectively (n = 6). These in-house standard isotopic signatures were verified against a certified C_{36} standard (-30.00 ± 0.04 ‰; Indiana University) using an Agilent GC coupled to an Isoprime (Elementar Americas Inc.) stable isotope ratio mass spectrometer (GC-IRMS). All carbon isotopic signatures were standardized to the international VPDB limestone standard (Chapter 1).

Alkanes (F1 of FPOM and SEOM) and phospholipids FAME (F3 of DOM, FPOM and SEOM) were analyzed on the GC-IRMS. The precision of the isotopic analyses was better than ± 0.6 ‰. The methanol-BF_3 solutions from the kits that were used for the fatty acid derivatizations were also analyzed to subsequently correct the measured $\delta^{13}C$ isotopic ratio for all measurements according to this equation:

$$\delta^{13}C_{FAME} = [\delta^{13}C_{FA}{}^{*}(f_{FA}) + \delta^{13}C_{M}{}^{*}(f_{M})]$$

where $\delta^{13}C_{FAME}$ is the is the measured FAME isotopic signatures, $\delta^{13}C_{FA}$ is the original and unknown isotopic signature of a given FA before the derivatization reaction, f_{FA} is the fraction of carbon from this same FA before reaction, $\delta^{13}C_{M}$ is the isotopic signature of methanol used in the esterification reaction, and f_{M} the fraction of total carbon in the derivatized molecule which represents the added methoxy group to the FA.

5.3.3.3 Fatty acid and alkane nomenclature

The FA presented in this chapter as well as in Appendix B are listed by carbon length (prior to derivatization) followed by the number of carbon double bounds starting from the aliphatic chain (ω), and by whether it is a cis- (c) or trans- (t) conformation (*e.g.*

C16:1ω7c). In this study, the sum of the branched (br) lipids is used (*e.g.* brC15:0 or brC15 for FA and alkanes, respectively). When they were sufficiently abundant, the $\delta^{13}C$ of the iso and anteiso branched FA, which are defined as methyl branched FA at the ω2 and ω3 aliphatic positions (*e.g.* a-C15:0), are also presented.

5.4 Results

5.4.1 Bulk organic matter and greenhouse gases

The bulk carbon (C) percentages, the stable C isotope signatures and the atomic C to nitrogen (N) ratio $(C:N)_a$ for the DOM, FPOM and SEOM fractions, as well as the dissolved and fine particulate organic carbon (DOC and FPOC respectively) and the surface water GHG concentrations are summarized for each sampling site in Table 5-1. The assessment of bulk OM sources though elemental and isotopic analysis was not within the scope of this study as these results were presented and discussed elsewhere (see results and discussion sections, Chapter 4). However, these results are needed to support the biomarker discussion presented below.

Significantly higher water dissolved CO_2 concentrations were obtained in Reservoir Cabonga and the wood harvested systems compared to natural ones ($p < 0.0005$ and $p < 0.1$, respectively). In addition, significantly higher DOC concentrations were measured in wood harvested systems ($p < 0.0005$) while generally higher FPOC concentrations were obtained in all perturbed systems. Higher $(C:N)_a$ ratios were also measured in the DOM and FPOM fractions of perturbed systems. As discussed in Chapter 4, these results show that additional terrestrial OM is introduced in aquatic systems upon wood harvesting or reservoir operation.

Table 5-1. Bulk chemical results and surface water GHG concentrations of the sampled lakes (L.) and reservoirs (R.)

Water body	Station	DOM				FPOM				SEOM			GHG Averages[c,d]		
		OC (%)	$\delta^{13}C$ (‰)[a]	$(C:N)_a$	[DOC][b] µmol C L^{-1}	OC (%)	$\delta^{13}C$ (‰)[a]	$(C/N)_a$	[FPOC][b] µmol C L^{-1}	OC (%)	$\delta^{13}C$ (‰)[a]	$(C/N)_a$	*n* [e]	$[CO_2]$ (µmol L^{-1})[f]	$[CH_4]$ (nmol L^{-1})[f]
L. Mary	LMAR	6.3	-26.3	21.6	183.6	25.6	-27.7	11.8	25.1	23.1	-28.1	11.4	N/A	N/A	N/A
L. Jean	LJEA	10.9	-26.8	29.8	220.8	27.2	-28.6	14.0	37.1	10.0	-25.4	13.1	6	28.1 (11.5)	51.9 (9.8)
L. Clair	LCLA	16.8	-27.1	32.0	434.0	33.4	-28.6	18.7	80.8	2.7	-29.2	13.3	5	32.3 (8.7)	38.8 (9.5)
L. Bouleau	LBOU	16.9	-27.5	33.2	506.0	27.8	-30.4	23.7	77.5	14.5	-29.1	15.2	5	75.1 (10.7)	68.4 (21.9)
R. Cabonga	RCAB-6	14.1	-27.1	36.4	293.7	32.4	-29.4	16.3	62.2	5.6	-27.6	14.7	6	34.9 (6.7)	54.6 (10.2)
	RCAB-10	13.0	-26.9	32.6	278.4	25.6	-29.0	16.5	31.0	7.8	-28.2	16.6	3	45.7 (14.2)	71.9 (20.9)
R. Decelles	RDEC-1	16.1	-27.2	56.1	498.2	27.9	-28.3	26.0	63.1	2.8	-28.0	19.4	7	42.0 (4.3)	63.9 (18.4)
	RDEC-2	23.4	-27.0	40.5	497.2	31.9	-28.2	31.2	62.5	5.7	-27.5	19.1	7	39.0 (9.3)	87.5 (30.2)

[a] Analytical uncertainty of ± 0.2‰. [b] Depth integrated samples. [c] Averages for a single station were calculated using individual replicates; when stations were visited more than once, standard deviations (between parentheses) were calculated using common error propagation equations. [d] The averaged total sampling and analysis error was of 4.1 ± 1.7%. [e] Four replicates were measured for each sampling event (*n*). [f] Surface concentrations.

5.4.2 Total lipids

Complete alkane and FA biomarker identifications, relative mole percentages (mol%) and compound-specific isotopic signatures analyzed in the DOM, FPOM and SEOM fractions are presented in Appendix B (Tables B-1 to B-8). Alkanes in DOM were also analyzed but are not reported due to their very low abundance and highly variable recoveries from DOM. Fatty acid proxies presented in section 5.4.2.1 were generated using the sum of glyco- and phospholipids fatty acids (GLFA and PLFA; fractions F2A and F3A, respectively), while the compound-specific isotopic signatures presented in section 5.4.2.3 are derived from the PLFA fraction only.

5.4.2.1 Fatty acids

Generally, lower abundances of organic carbon (OC) normalized FA (μmol FA mol OC^{-1}) were observed in the DOM than in the FPOM and SEOM fractions (10 to 39.6, 8.2 to 374 and 117 to 392 μmol FA mol OC^{-1}, respectively). Significantly higher (Welch t-test; $p < 0.001$) and lower ($p < 0.005$) carbon normalized concentrations of FA were recorded in the DOM and FPOM fractions of the natural lakes compared to perturbed systems (Tables B-1 and B-2). The natural Lake Mary had a lower relative contribution of PLFA (fraction F3A) to total FA (fractions F2A + F3A) in DOM and FPOM (48.0 and 67.2 %) whereas all other samples had a higher relative PLFA content (greater than 80 %).

In DOM, the sum of monounsaturated and polyunsaturated FA (MUFA + PUFA) was highly correlated ($r^2 = 0.93$, $p < 0.001$; not shown) to the sum of even-numbered carbon atom short chain FA (ESCFA, which are considered biomarkers for autochthonous aquatic OM; sum of C_{12}, C_{14} and C_{16}; Canuel and Martens, 1993;

McCallister et al. 2006). This result suggests that a significant portion of the fresh DOM originates from autochthonous production. Very weak correlations were obtained in similar scatter plots using the sum of the bacterial biomarker over the ESCFA and the sum MUFA and PUFA. Higher concentrations of the DOC normalized ESCFA (2.5 to 8 times more; Table B-4) were found in the natural lakes compared to perturbed systems, while an identical range of concentrations was found for bacterial biomarkers in both types of systems. DOM from natural lakes thus contained a higher relative contribution of exudates or very recent cell remains from autotrophic primary producers compared to the perturbed systems.

The fatty acid biomarkers of the FPOM (< 70-μm) fraction are useful for obtaining additional information on the carbon cycling in the systems under study. The OC normalized bacterial FA (sum of all branched and odd straight chain FA from C_{13} to C_{18}) was highly correlated with the aquatic FA (ESCFA; Figure 5-1A) in this fraction. Lower bacterial relative abundances were found in FPOM sampled in lakes compared to the two sampled reservoirs, whereas wood harvesting positively influenced bacterial production only in lakes. This result suggests that a major fraction of the aquatic biomass in FPOM was of bacterial origin. A significant correlation was also observed between bacterial FA and even long-chain fatty acids (ELCFA, sum of C_{22}, C_{24}, C_{26} and C_{28}), which are considered terrestrial markers (Canuel and Martens, 1993; Meyers 1997; McCallister et al. 2006; Figure 5-1B). We believe that a significant fraction of the particulate OM pool was of terrestrial origin and constituted a food source for bacteria. As shown in Figures 5-1C and -1D, the sum of all monounsaturated and polyunsaturated FA (MUFA + PUFA) was highly correlated to the sum of aquatic and bacterial

biomarkers, which suggests little contribution from allochthonous matter to the total MUFA-PUFA biomarker pool. The lower bacterial abundance found for the wood harvested Reservoir Decelles-1 sampling site showed a higher relative contribution of primary producers to the FPOM fraction at this site (Figures 5-1A and -1D). Indeed, the highest mole percentages (mol%) measured for a specific algal biomarker, C16:1ω7c, was found in the FPOM of the Decelles-1 site (Table B-2), which supports this conclusion (Arzayus and Canuel 2004).

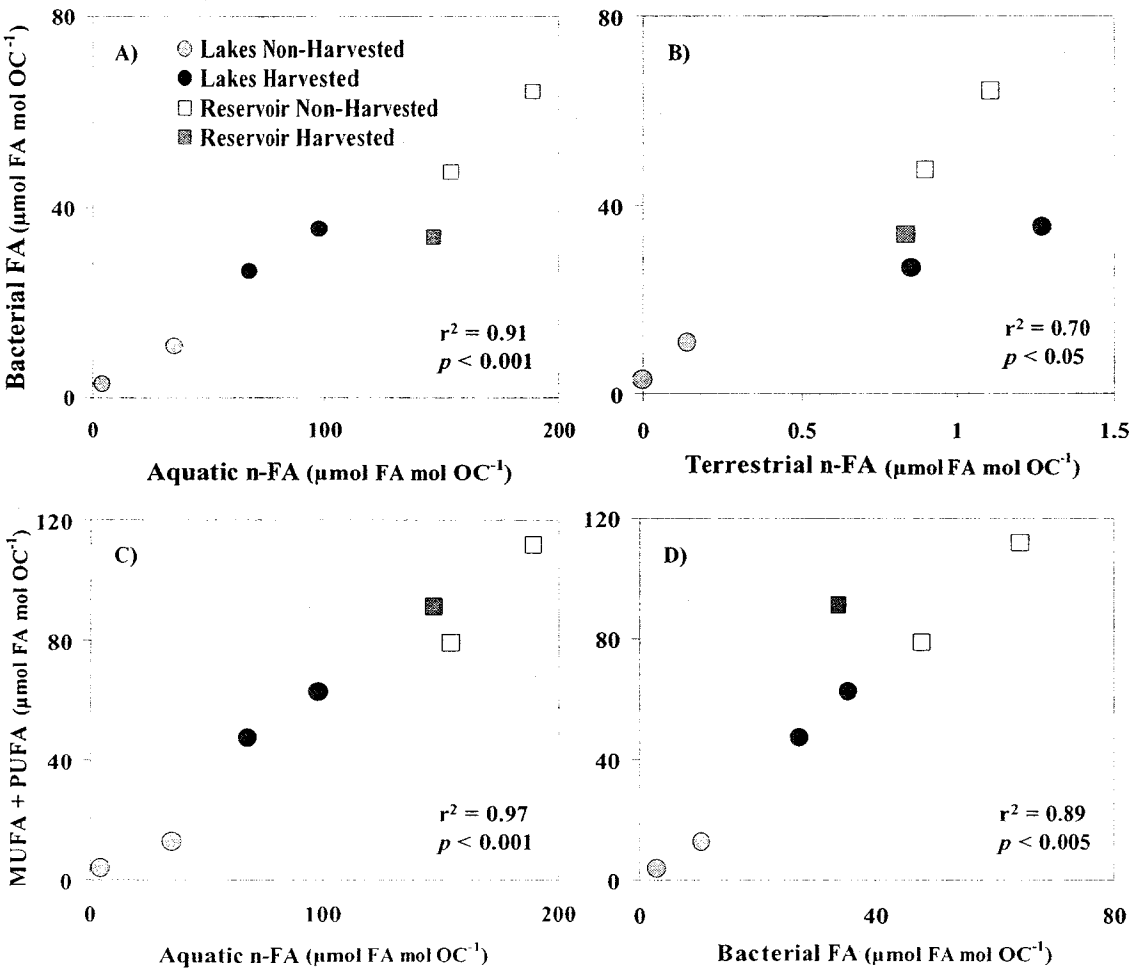

Figure 5-1: Fatty acids (FA) correlations in FPOM. Between the sum of bacterial FA (odd branched and normal C_{13}-C_{17} as well as even branched C_{14}-C_{18}) and the sum of (A) aquatic (nC_{12}, nC_{14}, nC_{16}) FA, (B) terrestrial (nC_{22}, nC_{24}, nC_{26}, nC_{28}) FA; as well as mono and polyunsaturated FA (MUFA+PUFA) over (C) aquatic and (D) bacterial FA. The *p* value corresponds to the significance of the regression.

In the sediment, ECSFA were predominant with relative abundances between 19.4 to 43.5 mol % followed by the bacterial biomarkers (20.1 to 35.4 mol %) and terrestrial ELCFA (2.1 to 7.3 mol %). No clear relationship was observed using the same calculated FA proxies as above. Because of the contrasting sedimentation rates for the different systems studied here (Chapter 4, Table 4-3), the SEOM from the 0 to 3 cm sediment layers used in this work corresponds to different age averages varying between 5 and 88 years). The FA biomarkers are known to be more sensitive to degradation than alkanes and therefore the absence of FA trends in this fraction can be explained by differences in the sedimentary diagenetic state.

5.4.2.2 Alkanes

The sum of alkanes normalized to total OC varied considerably more in FPOM (3.97 to 15.03 μmol Alk mol OC^{-1}) than in SEOM (10.94 to 23.21 μmol Alk mol OC^{-1}). A significantly higher alkane contribution was obtained in the FPOM of natural lakes compared to the perturbed systems (Welch's t-test: $p < 0.01$). The alkane relative abundances correlated positively (not shown) with the sum of the terrestrial land plant biomarkers (C_{27}, C_{29} and C_{31}, $r^2 = 0.88$ and $p < 0.005$) and with the sum of autochthonous biomarkers (C_{15}, C_{17} and C_{19}, $r^2 = 0.68$ and $p < 0.05$; Meyers 1997). These relationships suggest that a predominant fraction of the FPOM was dominated by non-degraded terrestrial matter. Even though fairly large contributions from terrestrial biomarkers were measured in natural lakes, higher contributions from aquatic alkanes (> 30 mol% of C_{17}) were obtained; as a result, the terrestrial to aquatic ratio (TAR) calculated for FPOM (Table 5-1) was lower for non-harvested systems. Such results suggest that autochthonous matter governs the FPOM in natural systems whereas allochthonous OM

inputs caused by wood harvesting and reservoir operation decreased the relative importance of autochthonous OM production. In contrast, the TAR values measured for the SEOM fraction in reservoirs were generally smaller and were paralleled by a larger percentage of bacteria-specific branched alkanes (% bacterial, Table 5-1) compared to lake sediments. High amounts of nC_{16}, known to mainly derive from bacterial biomass, were also measured in both the FPOM and SEOM fractions (Tables B-6 and B-7; Al-Mutlaq et al. 2008).

Table 5-2: Alkane indexes in FPOM and SEOM

Scenario	TAR	CAR	% Bacterial	CPI	UCM/Alk
FPOM					
L. Mary	0.23	0.28	11.47	4.62	4.36
L. Jean	0.37	0.41	14.22	2.42	6.03
L. Clair	1.27	0.96	22.51	0.93	7.20
L. Bouleau	1.52	0.87	15.10	4.21	4.46
R. Cabonga 6	0.71	0.67	16.81	1.14	3.74
R. Cabonga 10	0.91	0.91	16.71	0.99	5.86
R. Decelles 1	2.31	1.19	12.66	0.76	6.37
SEOM					
L. Mary	9.47	2.40	9.04	3.68	0.41
L. Jean	9.02	1.58	4.84	2.00	0.77
L. Clair	8.00	2.00	16.21	3.68	0.48
L. Bouleau	10.61	2.93	15.82	4.92	0.38
R. Cabonga 6	5.55	2.11	26.42	3.84	0.56
R. Cabonga 10	4.53	1.70	32.63	3.25	0.40
R. Decelles 1	3.20	1.55	32.20	2.86	0.38
R. Decelles 2	8.31	2.30	22.81	3.89	0.31

TAR: Terrigenous *vs.* aquatic ratio described as $\Sigma(C_{27}+C_{29}+C_{31})/\Sigma(C_{15}+C_{17}+C_{19})$, Meyers (1997).

CAR: Continental *vs.* aquatic ratio described as $\Sigma(n\text{-}C_{+25})/\Sigma(n\text{-}C_{-24})$, Hautevelle et al. (2007).

% Bacterial: percentage of branched alkanes, this study

CPI: Odd-over-even carbon preference index described as the ratio of odd *vs.* even alkanes from C_{16} to C_{35}, Al-Mutlaq et al. (2008).

UCM/Alk: Ratio of the total intensity of unresolved complex mixture over the sum of the intensities for all resolved alkanes within the same range, Hautevelle et al. (2007).

The continental to aquatic ratio (CAR; Table 5-1) includes all alkanes originating from plants, bacterial and planktonic matter (ratio of the sum of all alkanes longer than

C_{24} to that of alkanes shorter or equal to C_{24}; Hautevelle et al. 2007). Using this index, CAR values similar to the TAR index were found for the FPOM whereas they differed considerably for the sediment, which showed comparable inputs of both terrestrial and aquatic alkanes. The FPOM carbon preferential indexes (CPI: odd over even from C_{16} to C_{35}) were higher in natural lakes (maxima at C_{17}) and in the recently flooded Lake Bouleau (maxima at C_{29}; Table B6) and are interpreted as reflecting high inputs of autochthonous and allochthonous plants. The lower CPI indexes measured in these systems were found in samples with high nC_{16} bacterial alkane concentrations. Finally, the ratio of unresolved complex mixture (UCM), which is due to the presence of a large number of alkane isomers that cannot be resolved chromatographically, to the sum of the resolved alkanes is an indicator of the extent of degradation/alteration of the OM, or of algal/bacterial inputs (Hautevelle et al. 2007). All FPOM samples have higher UCM to alkane ratios compared to the SEOM fractions, however with no clear trend between natural and perturbed systems.

Scatter plots of the bacterial (sum of all branched) over straight chain aquatic ($\leq C_{12-24}$) and terrestrial ($> C_{24-40}$) derived alkanes are shown in Figure 5-2. Unlike for the FA, higher bacterial alkanes were measured in the FPOM of natural lakes.

Surprisingly, no clear or direct relationship was observed between the bacterial, autochthonous and allochthonous carbon normalized biomarkers in SEOM (μmol Alk mol OC^{-1}; not shown) . This lack of relationship is attributed to the integration of the first 3-cm layer of sediment, which corresponds to different ages. To neglect the different sample age, the percentages of bacterial, aquatic and terrigenous alkanes relative to the total alkanes were used (see discussion). Scatter plots of normalized bacterial against

aquatic and terrestrial alkanes are presented in Figures 5-2C and -2D. Noteworthy, the reservoirs had higher relative bacterial contributions to the total alkanes compared to lakes. A clear and significant negative correlation (slope = - 0.97) was obtained between the bacterial and terrestrial biomarkers; this and previous results show that the bacterial biomass is intimately coupled to terrestrial OM and suggest that terrestrial OM plays a major role in bacterial proliferation.

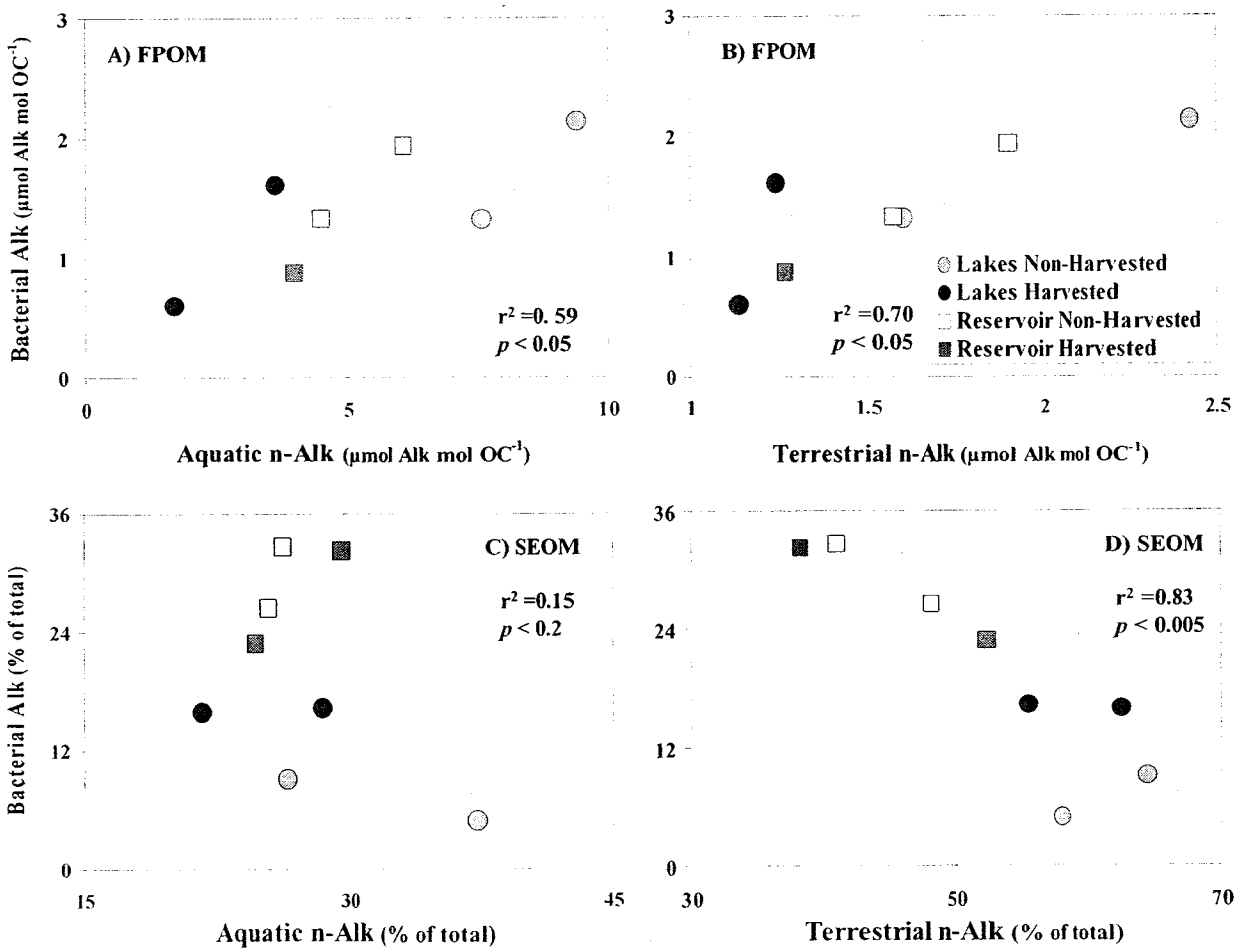

Figure 5-2: Alkane correlations in FPOM and SEOM. Between the sum of bacterial alkanes (Alk; odd and all branched from C_{13} to C_{18}) and the sum of (A) aquatic ($X \leq nC_{24}$) n-Alk as well as (B) terrestrial ($X > nC_{24}$) n-Alk in FPOM. Between the relative contribution (in %) of (A) of bacterial Alk and (A) aquatic n-Alk as well as (B) of terrestrial Alk in SEOM. The *p* value corresponds to the significance of the regression.

Figures 5-3A and -3B present plots of surface water CO_2 concentrations against the relative proportion of bacterial and terrestrial alkane biomarkers. These show that higher surface water CO_2 concentrations were coupled to higher and lower percentages of bacterial and terrestrial biomarkers, respectively. Because GHG concentrations were not measured in Lake Mary during the 2007 summer sampling campaign and also because Lake Bouleau exhibited exceptional CO_2 concentrations (due to recent flooding), both samples were not included in these figures.

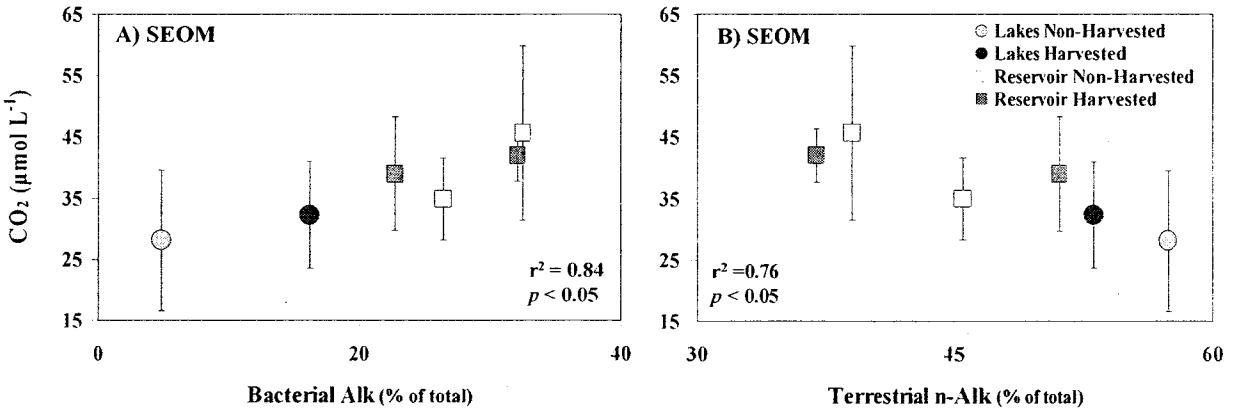

Figure 5-3: Surface water carbon dioxide concentrations correlations with alkane biomarkers. Between water CO_2 concentrations and the relative contribution (in %) of (A) of bacterial alkanes (Alk; odd and all branched from C_{13} to C_{18}) and (B) of terrestrial alkanes (> C_{24}) SEOM. The *p* value corresponds to the significance of the regression.

5.4.2.3 Compound-specific stable isotope signatures

The $\delta^{13}C$ stable isotope signatures that were measured in this study are listed in Tables B-4, B-5 and B-8. This study is, to our knowledge, the first to exploit compound-specific stable $\delta^{13}C$ isotopes of different lipid compounds to assess carbon cycling in the DOM, FPOM and SEOM fractions of water bodies. The total lipid fraction extracted from the samples was always depleted compared to total organic carbon (TOC) (Table 5-1 Appendix B). In general, FA were increasingly depleted in ^{13}C isotopes from DOM, to FPOM and SEOM (range of -17.1 to -76.6 ‰). The stable isotope signatures of the FA

C18:1ω7c, known as a bacterial biomarker, were positively correlated with those of C14:0, C16:0 and C18:0 (r^2 = 0.80, 0.85 and 0.61, respectively; Bouillon et al. 2004), which suggests that, although ubiquitous to autochthonous production, C14:0, C16:0 and C18:0 are effectively incorporated into the bacterial biomass or directly derived from bacterial matter. Despite some disagreement on the source of the C16:1ω7c biomarker in the literature (Arzayus and Canuel 2004; Li et al. 2007), its $\delta^{13}C$ signature was also closely linked to C18:1ω7c (r^2 = 0.87), suggesting that both biomakers originate from a common bacterial source. Very broad variations in the $\delta^{13}C$ signature of the C16:1ω7c biomarkers (up to 50‰) between the different fractions (DOM: -19.7 to -27.0‰; FPOM:-32.8 to -43.4‰; SEOM: -48.4 to -66.7‰) suggest either a dramatic change in the biomass or food sources.

In general, odd and even alkanes in SEOM display a narrower range of stable isotope signatures throughout the data set (-27.4 to -41.2‰; Table B8). Even numbered alkane chains are generally enriched compared to their odd alkane neighbors. The $\delta^{13}C$ isotope signatures of nC17:0 and nC21:0, which display more depleted values compared to their homologues in the sediment, are the only molecules for which a stable isotope signature could be measured in FPOM owing to their high abundances. No significant compound-specific $\delta^{13}C$ depletion or enrichment was associated with reservoir operation and wood harvesting.

5.5 Discussion

5.5.1 Lipids as indicators of organic matter sources

In this work, fatty acids have proven useful in the determination of different sources for autochthonous and allochthonous OM in DOM, FPOM and SEOM. For

instance, the higher carbon normalized FA concentrations measured in the DOM of natural lakes, supported by the higher relative contributions from ESCFA as well as lower DOC and FPOC concentrations (Table 5-1), suggest that the DOM fraction was mainly composed of the living or dead biomass and/or exudates of primary producer and bacteria. However, the DOM from perturbed systems comprised a higher proportion of degraded terrigenous sources (interpretation supported by Fe measurements, Chapter 3 Figure 3-4A). In addition, the higher FPOM $(C:N)_a$ ratios and FPOC concentrations generally measured in the perturbed systems likely were a result of higher terrestrial matter and nutrient exports from land to the water bodies (Table 5-1; also supported by Chapter 3, Figures 3-2A and -2B). This result agrees with the higher allochthonous FA contributions found in the FPOM fraction of perturbed systems (Figure 5-1).

The contradictory high alkane and low FA bacterial biomarkers abundances obtained in the FPOM of natural lakes (Figures 5-1 and -2) shows that conclusions supported by only one type of lipid biomarker could be biased due to contrasting degradation rates of the individual compounds, and argues for the design of multi-proxy studies to assess carbon cycling in complex systems such as these ones. Contrary to the message obtained from the interpretation of the FA biomarker data, FPOM in natural lakes displayed higher carbon normalized aquatic and terrestrial plant derived alkanes for similar levels of bacterial biomarkers. Such disagreement is similar to the conclusions reached using two amino acid biomarker proxies ($\%T_{AA}N$ and DI, Chapter 4 Table 4-4). Our results, along with the low $(C:N)_a$ ratios measured for this fraction, suggest that the FPOM samples were composed of a mixture of fresh and more degraded OM. Since alkanes are more recalcitrant than FA (Meyers 1993), we tentatively propose that the high

bacterial and terrestrial alkane signatures in the FPOM of natural lakes reflect bacterially processed terrestrial inputs as would be found in soils. In contrast, the FPOM fraction from perturbed systems was mostly composed of fresher, less altered terrestrial OM, which lead to an enhanced production of autochthonous bacteria.

5.5.2 Lipids as indicators of organic matter cycling

Estimations of the living and dead biomass in all samples were done through the analysis of phospholipids and glycolipids FA (Guckert et al. 1985; Ringleberg et al. 1997; Bouillon et al. 2004a, 2004b). In all three analyzed OM fractions, phospholipids dominated the total FA content. Dissolved organic matter was dominated by PLFA (> 94% of total FA, except in Lake Mary). This result suggests that the FA found in this fraction either originated from living nanoplanktonic biomass (< 0.45 μm, porosity of the filters used to separate DOM from FPOM), remains of very recently deceased plankton and bacteria cells, or from planktonic and bacterial exudates. In the FPOM and SEOM fractions, > 80% of the total FA were composed of PLFA, also suggesting fresh OM inputs. The very low abundance of terrestrial FA (C_{22}, C_{24}, C_{26}, C_{28}) and high relative contributions from aquatic FA (C_{12}, C_{14}, C_{16}) measured for the PLFA of DOM, FPOM and SEOM fractions suggest that allochthonous OM inputs accounted for little of the fresh matter in these systems. The PLFA $\delta^{13}C$ signatures in the FPOM fraction suggest that most of the living biomass was governed by bacterial communities (Figure 5-1).

Furthermore, the low abundances of PUFA in all fractions show that our aquatic systems were dominated by prokaryotic biomass (Guckert et al. 1985). Contrary to similar studies carried out in marine systems, algal PUFA (*e.g.* C20:5ω3; Azarus and Canuel, 2004) were not found in the FPOM and SEOM of the lacustrine systems

indicating that the contribution of algal biomass to both fractions was low. This suggests that the relative proportion of the coarse particulate OM fraction, which contains more algae (> 70-μm; not sampled in this study), was small compared the total POM fraction or that the algal biomass was actively degraded in the sediment. These results, as well as others presented in Chapter 3 (Figure 3-4B), suggest that the bacterial population dynamics and abundance are closely coupled to the algal biomass, whose growth is dependant on nutrients and light availability (Planas et al. 2000; Prepas et al. 2001; Karlsson et al. 2009, Chapter 3).

In lakes, the abundances of bacterial alkanes in the SEOM fraction were similar to those measured in the FPOM fraction (1 to 2.2 μmol mol OC^{-1}) and lower than those measured in the reservoirs (2.8 to 5 μmol mol OC^{-1}). Reservoirs thus appeared to harbour greater populations of bacteria in sediments compared to lakes. As previously reported (Chapter 4) the effects of wood harvesting did not translate into significantly higher bacterial proliferation in the sediment (Figures 5-2C and -2D). A considerable difference between reservoirs and lakes was also highlighted by the TAR index calculated for the SEOM fraction, which unambiguously shows higher autochthonous material inputs into the sediment. These findings are also supported by the lower lignin biomarker abundances measured in the sediments of reservoirs (Plouhinec et al. In preparation). Because only four sampling sites in two reservoirs were analyzed for lipid biomarkers, more samples from reservoirs must be analyzed before drawing broad conclusions on the higher bacterial biomass in sediments of old boreal reservoirs compared to those of natural lakes. We hypothesize here that the more dynamic hydrology in reservoirs (currents and water drawdown) results in the deepening or the absence of a clear

thermocline, which leads to a larger fraction of the sediment being in contact with warm and oxygen-rich epilimnetic water (Chapter 3 Table 3-1, Figure 3-3). Higher temperatures and oxic conditions would then translate into an increased bacterial proliferation and CO_2 production as shown in Figure 5-3 and Table 5-1.

Because the top three centimeters of the sediments were integrated before the lipid biomarker analysis, the SEOM samples analyzed in this work correspond to different average ages (see Chapter 4, Table 4-3 for sedimentation rates). When sedimentation rates cannot be measured because of hydroturbation (as for Decelles-1 and -2 cores), alkane biomarkers can still be elegantly used for understanding bioprocesses involved in the production of carbon dioxide. Alkane degradation rates, although slightly different between odd short and long-chain n-alkanes, are assumed to be consistent with the extent of bacterial respiration within an ecosystem (Yunker et al. 2005). For example, the lake sediments analyzed were between 7.7 and 88 years in age; Chapter 4 Table 4-3); however they were characterized by comparable relative biomarker distributions (Figures 5-2 and -3). Therefore, the relative contribution of specific alkanes relative to the total alkane fraction can still be exploited despite differences in sediment age. Sediments are integrators of past and present biomass inputs, therefore their link with CO_2 production also reflect longer time scales. Because factors other than total bacterial abundances are involved in methane cycling (O_2 depletion, T° and CH_4 oxidation to CO_2) and also because the differences in hydrology between reservoirs and lakes alter these water chemical properties, the methane concentrations measured in the surface waters could not be directly linked to bacterial biomarkers in the SEOM fraction. Results shown in Figures 5-3A and -3B suggest that greater bacterial biomass likely resulted in a more effective

degradation of terrestrially derived matter in the reservoirs, leading to higher CO_2 concentrations in the water column. While the causes and sources of carbon dioxide supersaturation in freshwater systems remain hotly debated (Del Giorgio and Peters, 1994; Carignan et al. 2000a; Dubois et al. 2009), our study strongly suggests that bacterial degradation of terrestrial OM is the major source of carbon dioxide production in boreal freshwater systems, along with DOM UV oxidation (which accounts for roughly 20-30% of total CO_2 production in the summer; Plouhinec et al. In preparation). Whether this finding applies to different seasons and to other regions remains to be investigated.

Chapter 6.

6 The processing of organic matter in freshwater aquatic systems: Looking inside the black box.

6.1 The carbon cycle in freshwater environments

This study aimed to understand the chemical, physical and biological processes controlling carbon (C) cycling in freshwater lakes. Anthropogenic perturbations such as long-term reservoir impoundment and wood harvesting were also studied to understand the effects of additional of organic matter (OM) inputs, degradation and sedimentation in freshwater ecosystems. Finally, we attempted to unravel the relationships between terrestrial carbon inputs and outputs, notably through the emission of greenhouse gases (GHG). To do this, a wide array of bulk water chemical parameters were analyzed along with the molecular characterization of amino acids (AA) and lipids from dissolved, fine particulate, and sedimentary OM (DOM, FPOM and SEOM, respectively) sampled in natural and perturbed systems. As part of this study, a team of collaborators based at the *Université du Québec à Montréal* (UQAM) assessed the bacterio- and photo-oxidation that take place in the photic zone of the same freshwater systems through *in situ* incubations of water samples in large quartz cells. This group also performed the analysis of lignin derivatives (terrestrial biomarkers) in all OM fractions from the same lakes and reservoirs; once fully integrated, their results and ours will offer a complete picture and contribute extensively to the understanding of the mechanisms controlling carbon cycling in freshwater environments. We briefly summarize in this section the major conclusions and scientific advancements derived from this research project.

6.1.1 Sample representativity

The study of the carbon cycle in freshwater systems is carried out using a variety of sampling device and analytical instruments. A tangential flow filtration reverse osmosis (TFF-RO) system allowed the sampling of the large quantity of DOM and FPOM necessary for the bulk and molecular analyses. While the calibration of some instruments is straightforward (*e.g.* pH meter, oxygen sensor), assessing the TFF-RO system for the representativity of the collected OM and for possible molecular or biochemical fractionation is essential; this was addressed in Chapter 2 (Ouellet et al. 2008). A multi-point sampling strategy was adopted and a high temperature catalytic oxidation total carbon analyzer was used to calculate the mass balance of the entire system, which is fitted with 0.45-μm (TFF) and 300-Dalton (RO) filters. By designing a meticulous method for rinsing both filters and the instrumental dead space, most of the sample carry-over was eliminated with total recoveries ranging between 96.4 and 106.9%. In addition, Fourier transform infrared spectroscopy (FTIR) and stable carbon isotope ratio mass spectrometry (IRMS) were used to evaluate sample fractionation during sampling. It was shown that using the TFF-RO systems, minimal sample fractionation occurred and the concentrated samples collected were representative of the initial material.

6.1.2 Organic matter sources in lakes and reservoirs

In most traditional limnology studies, a large number of water and OM chemical analyses are carried out to collect basic information on the studied systems. The results for the bulk chemical parameters presented in Chapter 3 are representative of such preliminary, yet essential data. Within the five lakes and two reservoirs sampled in this study, two lakes and one reservoir were partially wood harvested. Altogether, the non-

harvested systems displayed significantly lower levels of surface water dissolved organic carbon (DOC), total nitrogen (TN), and iron (Fe) complexed DOC compared to the perturbed systems. Bulk elemental and isotopic analyses of DOM, FPOM and SEOM as well as for the soil extracts and the dissolved inorganic carbon (DIC) provided additional clues that perturbed systems are characterized by higher inputs and degradation of terrestrial OM.

Although not usually used as proxies for OM sources, amino acids (AA) (Chapter 4) have revealed interesting trends with respect to OM diagenetic state which, in our case, is ultimately linked to its source. The relative contribution of AA to the total organic carbon ($\%T_{AA}C$) and total nitrogen ($\%T_{AA}N$) in DOM was low indicating that this fraction was more degraded than FPOM in all water bodies. This suggests that the majority of the terrestrial OM inputs were in the dissolved form while the FPOM fraction was composed of fresher, partly autochthonous, material. Higher and lower amounts of bacterial AA (D-AA) with respect to perturbation were measured in DOM and SEOM, respectively. This result, along with the output from a principal component analysis, showed that a strong relationship exists between OM sources and the extent of perturbation through reservoir operation or wood harvesting. Independently of wood harvesting, the reservoirs were characterized by more degraded (allochthonous) FPOM and fresher (autochthnous) SEOM fractions. This was later confirmed through lipid biomarker analyses.

Lipid biomarker (the fatty acids (FA) and the alkanes) data presented in Chapter 5 were used to pinpoint OM sources in all sampled water bodies. It was shown that higher quantities of terrigenous DOM are exported to the aquatic systems when they are

perturbed. In the FPOM fraction, the biomarker analyses suggested larger contributions from bacterially processed material in natural lakes whereas higher relative contributions from fresh bacterial biomass were observed along with greater inputs of fresh terrestrial OM in the perturbed systems. Little contribution from algal biomarkers was found in the FPOM and in the accumulating SEOM fractions suggesting that algae played a minor role in OM autochthonous production, or that the algal material is quickly degraded in the particulate fractions.

6.1.3 Organic matter cycling: Linking bacteria and GHG

Despite the small number of aquatic systems sampled in this study, the higher CO_2 concentrations and atmospheric fluxes measured in wood harvested freshwater systems demonstrate, for the first time, the direct relationship between terrestrial organic matter inputs and CO_2 production following wood harvesting. To a lower extent, similar results were obtained for the non-harvested Cabonga Reservoir, with higher terrestrial inputs resulting in greater CO_2 supersaturation levels compared to natural lakes. The results presented in Chapter 3 suggest that DOC and TN inputs are the major bacterial CO_2 production driving forces in the studied systems. In the wood harvested water bodies, a relationship between the DIC concentration and its stable carbon isotope signature ($\delta^{13}C$) suggests that terrestrial OM is more extensively degraded in these systems. Similarly, the bacterial AA and alkane biomarkers in DOM and SEOM, respectively, were related to the surface water GHG and showed that bacterial activity in freshwater systems is driving GHG production.

The extent of bacterial activity depends on several factors, most importantly nutrients availability. Higher terrestrial OM inputs coincided with greater relative

abundance of bacterially-derived biomarkers in FPOM. Furthermore, the SEOM fraction from reservoirs displayed lower abundances of terrestrially-derived biomarkers with systematically greater relative contributions from bacterial biomarkers. We believe that the higher water currents and drawdown in the reservoirs cause the epilimnetic layer to be deeper and sometimes missing, which results in warmer and more oxygenated waters just above the sediments. Higher temperatures and more oxic conditions would then increase bacteriological activity and GHG production. While such link still has to be unambiguously demonstrated, this data suggests that the degradation of terrestrial derived OM is ultimately linked to GHG production.

6.2 Forecoming contributions and future work

6.2.1 Articles in preparation

The full integration of the biomarker data presented in this study with the lignin biomarkers analyzed by our colleagues at UQAM is the main remaining task to fully exploit the huge dataset generated in this study. First, the lipid biomarker data must be better exploited and presented; as these results were compiled a few weeks prior to the first submission of this thesis, little time could be spent on the interpretation, including through advanced statistical methods, of the differences in the relative contributions from individual and families of lipid biomarkers. Only then will we be able to couple the lipid to the lignin datasets. Lignin is only found in terrestrial plants and represents the ultimate biomarker for land plants (Houel et al. 2006). The lignin oxidation analysis method produces 12 compounds that are also used to evaluate, among other things, the sources and freshness of terrestrial OM which, combined with our AA data, is essential to understand the effects of OM freshness on the dynamics of carbon and GHG production.

A manuscript presenting the integration of the lignin and lipid biomarkers will be prepared rapidly following the publication of individual results from both groups.

A few other manuscripts are being considered for publication using the data that has been accumulated during the seven consecutive seasonal sampling missions. In this thesis, very little water column chemistry data were presented (only those relevant to the biomarker analyses, *e.g.*, one out of the seven sampling missions). In fact, no limnological publication has ever reported the dynamics of GHG accumulation in the hypolimnion and their transfer to the epilimnion. Kim et al. (2006) suggested that the thermocline was permeable to DOC as increased hypolimnetic DOC concentrations were observed during the summer. In lakes such as those studied here, the thermocline deepens from the spring to late summer with little GHG accumulation in the hypolimnion. Significant CH_4 water surface concentrations were also observed at stations that contained a thermocline. Since lateral water currents in lakes are small (Marty et al. 2005) and because CH_4 is produced in anoxic conditions, the presence of CH_4 in the epilimnion suggests a constant transfer of GHG from the hypolimnion to the surface waters. This transfer would be driven by the deepening of the metalimnion combined with the accumulation and increase in GHG partial pressure in the hypolimnion (Åberg et al. 2010). As a constant flux of GHG was observed between the surface water and the atmosphere (characterized by contrasting densities and temperatures), we believe that a similar process occurs between the hypolimnion and the epilimnion. Calculating this process from our dataset is feasible and would help assessing the percentage of the atmospheric GHG fluxes that can be attributed to hypolimnetic GHG production processes. Noteworthy, we roughly estimated that hypolimnetic CO_2 accumulations

represented less than 7 % of the daily CO_2 atmospheric emissions (Chapter 3 and Table 6-1).

Table 6-1: Estimated hypolimnetic CO_2 storage in lakes (this study, Summer 2007)

Lake	Mean CO_2 emissions [a]	Hypolimnetic volume	Hypolimnetic CO_2 storage	Surface area of the lake	Equivalent CO_2 storage [b]
Units	**mmol CO_2 m^{-2} d^{-1}**	**Liters**	**mmol CO_2**	**m^2**	**days**
Brock	4.0 (0.9 – 8.9)	4.3×10^6	211×10^3	0.82×10^6	0.064
Jean	13.0 (2.9 – 55.0)	10.4×10^6	672×10^3	1.72×10^6	0.030
Clair	17.0 (5.8 – 30.2)	3.8×10^6	679×10^3	1.75×10^6	0.023

[a] Ranges of values in parenthesis. [b] Estimate based on the mean daily CO_2 emissions.

As the GHG transfer to the epilimnion would depend on its accumulation in the hypolimnion, such a low percentage fraction would not significantly influence the total GHG atmospheric fluxes presented in Chapter 3. Rather, very high flux events of a limited amount of GHG would be observed in the fall with lake water turnover and in the spring upon ice breakup. This publication will be prepared in fall 2010.

Finally, the last publication that will be generated through in this study will integrate the AA and lipids biomarkers from this project and from a sister project currently carried out in the St. Lawrence Estuary and Gulf by Karine Lalonde, a Ph.D. student from our laboratory. Because both types of biomarkers have very different reactivity, complementary information and corroboration of interpretation could be obtained by coupling both data sets. In this study alone, no conclusive trend was found between the AA and lipids biomarkers. More advanced statistical methods, principal component analysis and possibly self-organizing maps, should therefore be used to unravel and understand the relationships between both groups of biomarkers.

Noteworthy, our sampling effort has resulted in the collection of an impressive number of samples that will be exploited by other students in the close future. This bank

of samples will be used to assess seasonal variations in carbon cycling in natural and perturbed systems, which should nicely complement the current studies and address issues that could not be answered with the current dataset.

6.2.2 Future directions and environmental implications

The seasonal variations in bulk chemical parameters (water column and OM fractions) and lipid biomarkers (FA, alkanes and alcohols/sterols) in DOM and FPOM should be assessed to obtain additional information on the year-round carbon dynamics in freshwater ecosystems. By acquiring this data, changes in algal, bacterial and terrestrial sources and relative contributions could be monitored through time and specific seasonal events (*e.g.* ice breakup, algal blooms, water turnover, *etc.*). Using the already available data bank on water chemistry and the bulk OM characteristics (not exploited here except for the summer of 2007) will help understanding the controls on the bioprocesses responsible for GHG production. As seasonal sampling is often very difficult in northern boreal aquatic systems, most studies have been carried out during the summer; the samples collected as part of this study could help partly correct this bias.

In light of our findings, more work is needed to verify whether the contrasting results observed between lakes, reservoirs and the wood harvested systems are truly representative of the most of the water bodies from the boreal forest. Because only two reservoirs were visited in this study, additional sampling of old, stable and larger reservoirs (*e.g.* La Grande 2) should be targeted. Sampling prior to and for several years after wood harvesting events (during forest re-growth) should also be considered for estimating the total allochthonous OM loss as GHG to the atmosphere, which could be attributed to the perturbation. In addition to DOM, FPOM and SEOM, the sampling and

identification of the primary and secondary producers is essential to determine the biomass proportions and types (*e.g.* Gram positive and Gram negative bacteria) and how this translates to the AA and lipids biomarkers abundances. In freshwater aquatic systems, GHG measurements are rarely complemented with biomarker measurements and assessments of biological populations. Such diverse and complementary analyses are essential as GHG production in water bodies is closely linked to the aquatic algal, bacterial and terrestrial biomasses.

In this study. it was shown that anthropogenic perturbation, and more specifically wood harvesting, leads to greater GHG emissions to the atmosphere compared to natural lakes. This conclusion clearly indicates that the current forest management regulations are inappropriate; the forested protection bands around water bodies are too narrow (20 m) to buffer the export of large quantities of terrestrial OM to the aquatic systems. Based on a visual inspection of the sampling sites, we believe that a three fold increase in the width of the protective bands would substantially diminish the effects of wood harvesting practices on the aquatic system. A recent study carried out in Finland, where protective bands are 50-m wide, reported only modest differences in the aquatic bacterial populations between harvested and natural systems (Rask et al. 1998). Finally, the evaluation of OM degradation, reutilization and sedimentation following reservoir impoundment and wood harvesting is necessary to quantify the additional terrestrial carbon that is emitted to the atmosphere as GHG following anthropogenic perturbations. Such analysis becomes particularly important in the calculation of human GHG footprint upon perturbations of natural aquatic systems and for the development of sustainable environmental practices.

References

Åberg, J., M. Jansson and A. Jonsson. 2010. Importance of water temperature and thermal stratification dynamics for temporal variation of surface water CO_2 in a boreal lake. J. Geophys. Res. doi:10.1029/2009JG001085.

Adahcour M., J. Beens, R. J. J. Vreul and U. A. Th. Brinkman. 2006. Recent developments in comprehensive two-dimensional gas chromatography (GC × GC): I. Introduction and instrumental set-up. Trends Anal.Chem. **25:** 438-454.

Ahtiainen, M. and P. Huttunen. 1999. Long-term effects of forestry managements on water quality and loading in brooks. Boreal Environ. Res. **4:** 101-114.

Algesten, G., S. Sobek, A.-K. Bergström, A. Jonsson, L. J. Tranvik and M. Jansson. 2005. Contribution of sediment respiration to summer CO_2 emission from low productive boreal and subarctic lakes. Microb. Ecol. **50:** 529-535.

Al-Mutlaq, K. F., L. J. Standley and B. R. T. Simoneit. 2008. Composition and sources of extractable organic materr from a sediment core in Lake Kivu, East African rift valley. Appl. Geochem. **23:** 1023-1040.

Amon, R. M. W. and R. Benner. 1996. Bacterial utilization of different size classes of disslolved organic matter. Limnol. Oceanogr. **41:** 41-51.

Arzayus, K. M. and E. A. Canuel. 2004. Organic matter degradation in sediments of the York River estuary: Effects of biological vs. physical mixing. Geochim. Cosmochim. Ac. **69:** 455-463.

Aufdenkampe, A. K., J. I. Hedges, J. E. Richey, A. V. Krusche and C. A. Llerena. 2001. Sorptive fractionation of dissolved organic nitrogen and amino acids onto fine sediments within the Amazon Basin. Limnol. Oceanogr. **46:** 1921-1935.

_____, Mayorga, E., J. I. Hedges, C. Llerena, P. D. Quay, J. Gudeman, A. V. Krusche and J. E. Richey. 2007. Organic matter in the Peruvian headwaters of the Amazon: Compositional evolution from the Andes to lowland Amazon mainstem. Org. Geochem. **38:** 337-364.

Benner, R., J. D. Pakulski, M. M. McMarthy, J. I. Hedges and P. G. Hatcher. 1992. Bulk chemical characteristics of dissolved organic matter in the ocean. Science **255:** 1561-1564.

Berggren, M., H. Laudon and M. Jansson. 2007. Landscape regulation of bacterial growth efficiency in boreal freshwaters. Global Biogeochem. Cycles 21, GB4002, doi:10.1029/2006GB002844.

Böhlke, J. K., and T. B. Coplen. 1995. Interlaboratory comparison of reference materials for nitrogen-isotope-ratio measurements, in Reference and intercomparison materials for stable isotopes of light elements: Vienna, International Atomic Energy Agency, **IAEA-TECDOC-825:** 51-66.

Bjørnsen, P. K. 1988. Phytoplankton exudation of organic matter: Why do healthy cells do it? Limnol. Oceanogr. **33:** 151-154.

Bouillon, S., T. Moens and F. Dehairs. 2004. Carbon sources supporting benthic mineralization in mangrove and adjacent seagrass sediments (Gazi Bay, Kenya). Biogeosciences **1:** 71-78.

——, ——, N. Koedam, F. Dahdouh-Guebas, W. Baeyens and F. Dehairs. Variability in the origin of carbon substrates for bacterial communities in mangrove sediments. FEMS Microbial. Rev. **49:** 171-179.

Bourgoin, L.-H. and L. Tremblay. In press. Bacterial reworking of terrigenous and marine organic matter in estuarine water columns and sediments. Geochim. Cosmochim. Acta.

Canuel, E. A. and C. S. Martens. 1993. Seasonal variations in the sources and alteration of organic matter associated with recently-deposited sediments.Org. Geochem. **20:** 563-577.

Carignan, R., D. Planas and C. Vis. 2000a. Planktonic production and respiration in oligotrophic Shield lakes. Limnol. Oceanogr. **45:** 189-199.

——, P. D'Arcy and S. Lamontagne. 2000b. Comparative impacts of fire and forest harvesting on water quality in Boreal Shield lakes. Can. J. Fish. Aquat. Sci. **57:** 105-117.

—— and R. J. Steedman. 2000. Impacts of major watershed perturbations on aquatic ecosystems. Can. J. Fish. Aquat. Sci. **57:** 1-4.

Clair, T. A., J. R. Kramer, M. Sydor and D. Eaton. 1991. Concentration of aquatic dissolved organic matter by reserve osmosis. Water Res. **25:** 1033-1037.

Cole, J. J., N. F. Caraco, G.W. Kling and T.K. Kratz. 1994. Carbon dioxide supersaturation in the surface waters of lakes. Science **265:** 1568-1570.

—— and ——. 1998. Atmospheric exchange of carbon dioxide in a low-wind oligotrophic lake measured by the addition of SF_6. Limnol. Oceanogr. **43:** 647–656.

——, S. R. Carpenter, J. F. Kitchell and M.L. Pace. 2002. Pathways of organic carbon utilization in small lakes: Results from a whole-lake ^{13}C addition and coupled model. Limnol. Oceanogr. **47:** 1664-1675.

Coplen, T.B., W. A. Brand, M. Gehre, M. Groening, H. A. J. Meijer, B. Toman and R.M. Verkoutren. 2006. New guidelines for ^{13}C measurements. Anal. Chem., **78:** 2439-2441.

Cowie, G. L. and J. I. Hedges. 1992. Sources and reactivities of amino acids in a coastal marine environment. Limnol. Oceanogr. **37:** 703-724.

——— and ———. 1994. Biochemical indicators of diagenetic alteration in natural organic matter mixtures. Nature **369:** 304-307.

Cranwell, P. A., G. Eglinton and N. Robinson. 1987. Lipids of aquatic organisms as potential contributors to lacustrine sediments-II. Org. Geochem. **11:** 513-527.

Dauwe, B., J. J. Middelburg, P. M. Herman and C. H. R. Heip. 1999. Linking diagenetic alteration of amino acids and bulk organic matter reactivity. Limnol. Oceanogr. **44:** 1809-1814.

Davis, J., K. Kaiser and R. Benner. 2009. Amino acids and amino sugar yields and compositions as indicators of dissolved organic matter diagenesis. Org. Geochem. **40:** 343-352.

del Giorgio, P.A. and R.H. Peters. 1994. Patterns in planktonic P:R ratios in lakes: Influence of lake trophy and dissolved organic carbon. Limnol. Oceanogr. **39:** 772-787.

——— and R.L. France. 1996. Ecosystem-specific patterns in the relationship between zooplankton and POM or microplankton $\delta^{13}C$. Limnol. Oceanogr. **41:** 359-365.

———, J. J. Cole, and A. Cimbleris. 1997. Respiration rates in bacteria exceed phytoplankton production in unproductive aquatic systems. Nature **385:** 148-151.

——— and ———. 1998. Bacterial growth efficiency in natural aquatic systems. Ann. Rev. Ecol. Syst. **29:** 503-541.

———, ———, N. F. Caraco and R. H. Peters. 1999. Linking planktonic biomass and metabolism to net gas fluxes in northern temperate lakes. Ecology **80:** 1422-1431.

Demarty, M., J. Bastien, A. Tremblay, R. H. Hesslein and R. Gill. 2009. Greenhouse gas emissions from boreal reservoirs in Manitoba and Québec, Canada, measured with automated systems. Environ. Sci. Technol. **43:** 8908-8915.

De Schamphelaere, K. A. C., V. I. R. Unamuno, F. M. G. Tack, J. Vanderdeelen and C. R. Janssen. 2005. Reverse osmosis sampling does not affect the protective effect of dissolved organic matter on copper and zinc toxicity to freshwater organisms. Chemosphere **58:** 653-658.

Dittmar, T., K. Whitehead, E. C. Minor and B. P. Koch. 2007. Tracing terrigenous dissolved organic matter and its photochemical decay in the ocean by using liquid chromatography/mass spectrometry. Mar. Chem. **107:** 378-387.

Dubois, K., R. Carignan and J. Veizer. 2009. Can pelagic net heterotrophy account for carbon fluxes from eastern Canadian lakes? Appl. Geochem. doi :10.1016/j.apgeochem.2009.03.001.

Duchemin, E., M. Lucotte, R. Canuel and A. Chamberland. 1995. Production of the greenhouse gases CH_4 and CO_2 by hydroelectric reservoirs of the boreal region. Global Biogeochem. Cycles **9:** 529-540.

——, —— and ——. 1999. Comparison of static chamber and thin boundary layer equation methods for measuring greenhouse gas emissions from large water bodies. Environ. Sci. Technol. **33 :** 350-357.

——, ——, ——., A. G. Queiroz, D. C. Almeida, H. C. Pereira and J. Dezincourt. 2000. Comparison of greenhouse gas emissions from an old tropical reservoir with those from other reservoirs worldwide. Verb. Internat. Verein. Limnol. **27:** 1391-1395.

——, ——, —— and N. Soumis. 2006. First assessment of methane and carbon dioxide emissions from shallow and deep zones of boreal reservoirs upon ice break-up. Lakes Reserv. Res. Manage. **11:** 9-19.

Eglinton, G., P. M. Scott, T. Besky, A. L. Burlingame and M. Calvin. 1964. Hydrocarbons of biological origin from a one-billion-year-old sediment. Science **145:** 1322-1335.

—— and R. J. Hamilton. 1967. Leaf epicular waxes. Science **156:** 1322-1335.

Filley, T. R., K. H. Freeman, T. S. Bianchi, M. Baskaran, L. A. Colarusso and P. G. Hatcher. 2001. An isotopic biogeochemical assessment of shifts in organic matter input to Holocene sediments from Mud Lake, Florida. Org. Geochem. **32:** 1153-1167.

Ghaleb, B. 2009. Overview of the methods for measurement and interpretation of short-lived radioisotopes and their limits. Earth Env. Sci. **5:** doi:10.1088/1755-1307/5/1/012007.

Galimov, E.M. 2006. Isotope organic geochemistry. Org. Geochem. **37:** 1200-1262.

Gjessing, E. T., J. J. Alberts, A. Bruchet, P. K. Egeberg, E. Lydersen, L. B. McGown, J. J. Mobed, U. M. Nster, J. Pempkowiak, M. Perdue, H. Ratnawerra, D. Rybacki., M. Takacs and G. Abbt-Braun. 1998. Multi-method characterization of natural organic matter isolated from water: characterization of reverse osmosis-isolates from water of two semi-identical dystrophic lake basins in Norway. Water Res. **32:** 3108-3124.

González Pérez, M., L. Martin-Neto, S. C. Saab, E. H. Novotny, D. M. B. P. Milori, V. S. Bagnato, L. A. Colnago, W. J. Melo and H. Knicker. 2004. Characterization of Humic acids from a Brazilian Oxisol under different tillage systems by EPR, ^{13}C NMR, FTIR and fluorescence spectroscopy. Geoderma **118:** 181-190.

Guckert, J. B., C. P. Antworth, P. D. Nichols and D. C. White. 1985. Phospholipid, ester-linked fatty acid profiles as reproducible assays for changes in prokaryotic community structure of estuarine sediments. FEMS Microbial. Ecol. **31:** 147-158.

Halda-Alija, L. and T. C. Jonhson. 1999. Diversity of culturable heterotrophic aerobic bacteria in pristine stream bed sediments. Can. J. Microbiol. **45:** 879-884.

Hansell, D. and C. Carlson. 2002. Biogeochemistry of Marine Dissolved Organic Matter, Elsevier.

Harris, D.C. 2007. Quantitative Chemical Analysis. 7th ed. W. H. Freeman.

Hautevelle, Y., R. Michels, F. Malartre, M. Elie and A. Trouiller. 2007. Tracing of variabilities within a geological barrier by molecular organic geochemistry. Case of the Callovo-Oxfordian sedimentrary series in the East of the Paris Basin (France). Appl. Geochem. **22:** 736-759.

Hayes, J. M., K. H. Freeman, B. N. Popp and C. H. Hoham. 1990. Compound-specific isotopic analyses: A novel tool for reconstruction of ancient biogeochemical processes. Org. Geochem. **16:** 1115-1128.

Her, N., G. Amy, J. Chung, J. Yoon and Y. Yoon. 2008. Characterizing dissolved organic matter and evaluating associated nanofiltration membrane fouling. Chemosphere **70:** 495-502.

Hedges, J. I. and J. H. Stern. 1984. Carbon and nitrogen determinations of carbonate containing solids. Limnol. and Oceanogr. **29:** 657-663.

———, G. L. Cowie, J. E. Richey, P. D. Quay, R. Benner, M. Strom and B. R. Forsberg. 1994. Origins and processing of organic matter in the Amazon River as indicated by carbohydrates and amino acids. Limnol. Oceanogr. **39:** 743-761.

Hélie, J.-F. 2004. Geochemistry and fluxes of organic and inorganic carbon in aquatic systems of eastern Canada: examples of the St. Lawrence river and Robert-

Bourassa reservoir – isotopic approach. Ph.D. thesis. Univ. du Québec à Montréal.

Hertkorn, N., R. Benner, M. Frommberger, P. Schmitt-Kopplin, M. Witt, K. Kaiser, A. Kettrup and J. I. Hedges. 2006. Characterization of a major refractory component of marine dissolved organic matter. Geochim. Cosmochim. Ac. **70:** 2990-3010.

Hockaday, W. C., A. M. Grannas, S. Kim and P. G. Hatcher. 2006. Direct molecular evidence for the degradation and mobility of black carbon in soils from ultrahigh-resolution mass spectral analysis of dissolved organic matter from a fire-impacted forest soil. Org. Geochem. **37:** 501-510.

Homblette, N., F. Darchambeau, M. Heldal, S. Norland, P. Servais and J.-P. Descy. 2009. Stoichiometry of bacteria and algae in Lake Kivu. ASLO Conference.

Houel, S., P. Louchouarn, M. Lucotte, R. Canuel and B. Ghaleb. 2006. Translocation of soil organic matter following reservoir impoundment in boreal systems: Implications for in situ productivity. Limnol. Oceanogr. **51:** 1497–1513.

Houle, D., R. Carignan, M. Lachance and J. Dupont. 1995. Dissolved organic carbon and sulfur in southwestern Québec lakes: Relashionships with catchment and lake properties. Limnol. Oceanogr. **40:** 710-717.

Hu, L., Z. Guo, J. Feng, Z. Yang and M. Fang. 2009. Distributions and sources of bulk organic matter and aliphatic hydrocarbons in surface sediments of the Bohai Sea, China. Mar. Chem. **133:** 197-211.

Intergouvernmental Panel on Climate Change. 2001. Climate change 2001: Synthesis report. Summary for Policymakers.

———. 2007. Climate change 2007: Synthesis report.

Jedrysek, M. O. 1995. Carbon isotope evidence for diurnal variations in methanogenesis in freshwater lake sediments. Geochim. Cosmochim. Acta. **59:** 557-561.

Jørgensen, N. O. G., R. Stepanaukas, A.-G. U. Pederson, M. Hansen, and O. Nybroe. 2003. Occurrence and degragation of peptidoglycan in aquatic environments. Microb. Ecol. **46:** 269-280.

Kaiser, K. and R. Benner. 2005. Hydrolysis-induced racemization of amino acids. Limnol. Oceanogr. Met. **3**: 318-325.

——— and ———. 2008. Major bacterial contribution to the ocean reservoir of detrital organic carbon and nitrogen. Limnol. Oceanogr. **53**: 99-112.

Karlsson, J., M. Jansson and A. Jonsson. 2007. Respiration of allochthonous organic carbon in unproductive forest lakes determined by the Keeling plot method. Limnol. Oceanogr. **52:** 603-608.

——, P. Byström, J. Ask, P. Ask, L. Persson and M. Jansson. 2009. Light limitation of nutrient-poor lake ecosystems. Nature **460:** 506-509.

Kawasaki, N., and R. Benner. 2006. Bacterial release of dissolved organic matter during cell growth and decline: Molecular origin and composition. Limnol. Oceanogr. **51:** 2170-2180.

Kilduff, J. E., S. Mattaraj, A. Wigton, M. Kitis and T. Karanfil. 2004. Effects of reverse osmosis isolation on reactivity of naturally occurring dissolved organic matter in physicochemical processes. Water Res. **38:** 1026-1036.

Kim, C., Y. Nishimura and T. Nagata. 2006. Role of dissolved organic matter in hypolimnetic mineralization of carbon and nitrogen in a large, monomictic lake. Limnol. Oceanogr. **51:** 70–78.

Kim, S., A. J. Simpson, E. B. Kujawinski, M. A. Freitas and P. G. Hatcher. 2003 Non-invasive advanced spectroscopic methods (electrospray ionization mass spectrometry and 2D solution NMR) for analysis of DOM isolated by C18 solid phase disk extraction. Org. Geochem. **34:** 1325-1335.

Kitis, M., J. E. Kilduff and T. Karanfil. 2001. Isolation of dissolved organic matter (DOM) from surface waters using reverse osmosis and its impact on the reactivity of DOM to formation and speciation of disinfection by-products. Water Res. **35:** 2225–2234.

Kling, G. W., G. W. Kipphut and M.C. Miller. 1990. Arctic lakes streams as gas conduits to the atmosphere: Implications for tundra carbon budgets. Science **251:** 298-301.

Koprivnjak, J.F., E. M. Perdue and P. H. Pfromm. 2006. Coupling reverse osmosis with electrodialysis to isolate natural organic matter from fresh waters. Water Res. **40:** 3385-3392.

Kujawinski, E. B., M. A. Freitas, X. Zang, P. G. Hatcher, K. B. Green-Church and R. B. Jones. 2002. The application of electrospray ionization mass spectrometry (ESI MS) to the structural characterization of natural organic matter. Org. Geochem. **33:** 171-180.

Lambert, M. and J.-L. Fréchette. 2005. Analytical techniques for measuring fluxes of CO_2 and CH_4 from hydroelectric reservoirs and natural water bodies, p. 37-60. *In* A. Tremblay, L. Varfalvy, C. Rohem and M. Garneau [eds.], Greenhouse gas emissions – Fluxes and processes. Springer-Verlag, New York.

Lamontagne, S., R. Carignan, P. D'Arcy, Y. T. Prairie and D. Paré. 2000. Element export in runoff from eastern Canadian Boreal Shield drainage basins following forest harvesting and wildfires. Can. J. Fish. Aquat. Sci. **57:** 118-128.

Larson, J. H., P. C. Frost, Z. Zheng, C. A. Johnston, S. D. Bridgham, D. M. Lodge and G. A. Lamberti. 2007. Effects of upstream lakes on dissolved organic matter in streams. Limnol. Oceanogr. **52:** 60-69.

Leduc, L. G. and G. D. Ferroni. 1979. Quantitative ecology of psychrophilic bacteria in an aquatic environment and characterization of heterotrophic bacteria from permanently cold sediments. Can. J. Microbiol. **25:** 1433-1442.

Lehmann, M. F., S. M. Bernasconi and J. A. McKenzie. 2004. Seasonal variation of the $\delta^{13}C$ and $\delta^{15}N$ of particulate and dissolved carbon and nitrogen in Lake Lugano: Constraints on biogeochemical cycling in a eutrophic lake. Limnol. Oceanogr. **49:** 415-429.

Li, Y.-L., A. D. Peacock, D. C. White, R. Geyer and C. L. Zhang. 2007. Spatial patterns of bacterial signature biomarkers in marine sediments of the Gulf of Mexico. Chem. Geol. **238:** 168-179.

Loh, A. N., E. A. Canuel and J. E. Bauer. 2008. Potential source and diagenetic signatures of oceanic dissolved and particulate organic matter as distinguished by lipid biomarker distributions. Mar. Chem. **112:** 189-202.

Lomstein, B. A., J. Niggemann, N. O. G. Jørgensen and A. T. Langerhuus. 2009. Accumulation of prokaryotic remains during organic matter diagenesis in surface sediments off Peru. Limnol. Oceanogr. **54:** 1139-1151.

Marty, J., D. Planas, B. Pinel-Alloul and G. Méthot. 2005. Planktonic community dynamics over time in a large reservoir and heir influence on carbon budgets, p. 421-440. *In* A. Tremblay, L. Varfalvy, C. Rohem and M. Garneau [eds.], Greenhouse gas emissions – Fluxes and processes. Springer-Verlag, New York.

—— and ——. 2008. Comparison of methods to determine algal $\delta^{13}C$ in freshwater. Limnol. Oceanogr.: Methods **6:** 51-63.

Mackereth, F. J. H. 1958. A portable core sampler for lake deposits. Limnol. Oceanogr. **3:** 181–191.

McCallister, S. L., J. Bauer, J. E. Cherrier and H. W. Ducklow. 2004. Assessing sources and ages of organic matter supporting river and estuarine bacterial production: A multiple-isotope ($\Delta^{14}C$, $\delta^{13}C$, and $\delta^{15}N$) approach. Limnol. Oceanogr. **49:** 1687-1702.

——, —— and E. A. Canuel. 2006. Bioreactivity of estuarine dissolved organic matter: A combined geochemical and microbiological approach. Limnol. Oceanogr. **51:** 94-100.

—— and P. del Giorgio. 2008. Direct measurement of the $\delta^{13}C$ signature of carbon respired by bacteria in lakes: Linkages to potential carbon sources, ecosystem baseline metabolism, and CO_2 fluxes. Limnol. Oceanogr. **53:** 1204-1216.

McSween, H. Y., S. M. Richardson and M. E. Uhle. 2003. Geochemistry: Pathways and processes. 2nd ed. Columbia University.

Melillo, J.M., Nairman, R.J., Aber, J.D., Linkins, A.E., 1984. Factors controlling mass loss and nitrogen dynamics of plant litter decaying in northern streams. Bull. Mar. Sci. **35:** 341–356.

Meyers, P. A. 1997. Organic geochemical proxies of paleooceanographic, paleolimnologic, and paleoclimatic processes. Org. Geochem. **27:** 213-250.

——. 2003. Applications of organic geochemistry to paleolimnological reconstructions: a summary of examples from the Laurentian Great Lakes. Org. Geochem. **34:** 261-289.

Montgomery, S., M. Lucotte and L. Cournoyer. 2000. The use of stable isotopes to evaluate the importance of fine suspended particulate matter in the transfer of methylmercury to biota in boreal flooded environments. Sci. Total Environ. **261:** 33-41.

Nagata, T., B. Meon, and D. L. Kirchman. 2003. Microbial degradation of peptidoglycan in seawater. Limnol. Oceanogr. **48:** 745–754.

O'Driscoll, N. J., S. D. Siciliano, D. Peak, R. Carignan and D. R. S. Lean. 2006 The influence of forestry activity on the structure of dissolved organic matter in lakes: implications for mercury photoreactions. Sci. Total Environ. **336:** 880-893.

Ødegaard, H. and S. Koottatep. 1982. Removal of humic substances from natural waters by reverse osmosis. Water Res. **16:** 613-620.

Osburn, C. L., D. P. Morris, K. A. Thorn and R. E. Moeller. 2001. Chemical and optical changes in freshwater dissolved organic matter exposed to solar radiation. Biogeochem. **54:** 251-278.

Ouellet, A., D. Catana, J.-B. Plouhinec, M. Lucotte and Y. Gélinas. 2008. Elemental, isotopic and spectroscopic assessment of chemical fractionation of dissolved organic matter sampled with a portable reverse osmosis system. Environ. Sci. Technol. **42:** 2490-2495.

Pace, M. L., J .J. Cole, S .R. Carpenter, J. F. Kitchell, J. R. Hodgson, M. C. Van de Bogert, D. L. Bade, E. S. Kritzberg and D. Bastviken. 2004. Whole-lake carbon-13 additions reveal terrestrial support of aquatic food webs. Nature **427:** 240-243.

Peuravuori, J., A. Monteiro, L. Eglite and K. Pihlaja. 2005. Comparative study for separation of aquatic humic-type organic constituents by DAX-8, PVP and DEAE sorbing solids and tangential ultrafiltration: elemental composition, size-exclusion chromatography, UV-vis and FT-IR. Talanta **65:** 408-422.

Perdue E. M. and J.-F. Koprivnjak. 2007. Using the C:N ratio to estimate terrigenous inputs of organic matter to aquatic environments. Estuar. Coast Shelf Sci. **73:** 65-72.

Piirainen, S., L. Finér, H. Mannerkoski and M. Starr. 2007. Carbon, nitrogen and phosphorus leaching after site preparation at a boreal forest clear-cut area. Forest Ecol. Manag. **234:** 10-18.

Planas, D., M. Desrosiers, S.-R. Groulx, S. Paquet and R. Carignan. 2000. Pelagic and benthic algal responses in eastern Canadian Boreal Shield lakes following harvesting and wildfires. Can. J. Fish. Aquat. Sci. **57:** 136-145.

———, S. Paquet and A. Saint-Pierre. 2005. Production-consumption of CO_2 in reservoirs and lakes in relation to plankton metabolism. *In* A. Tremblay, L. Varfalvy, C. Rohem and M. Garneau [eds.], Greenhouse gas emissions – Fluxes and processes. Springer -Verlag, New York.

Prairie, Y. T., D. F. Bird and J. J. Cole. 2002. The summer metabolic balance in the epilimnion of southeastern Quebec lakes. Limnol. Oceanogr. **47:** 316-321.

———. 2009. Measurements of GHG emissions from the Eastmain-1 reservoir, Quebec, Canada. Unesco/Iha greenhouse gas (GHG) research project. Annex 7.

Prepas, E. E., B. Pinel-Alloul, D. Planas, G. Méthot, S. Paquet and S. Reedyk. 2001. Forest harvest impacts on water quality and aquatic biota on the Boreal Plain: introduction to the TROLS lake program. Can. J. Fish. Aquat. Sci. **58:** 421-436

Rask, M., K. Nyberg, S.-L. Markkanen and A. Ojala. 1998. Forestry in catchments: effects on water quality, plankton, zoobenthos and fish in small lakes. Boreal Environ. Res. **3:** 75-86.

Rindelberg, D. B., S. Sutton and D. C. White. 1997. Biomass, bioactivity and biodiversity: microbial ecology of the deep surface: analysis of ester-linked phospholipids fatty acids. FEMS Microb. Rev. **20:** 371-377.

Schindler, D. W., P. Jefferson Curtis, S. E. Bayley, B. R. Parker, K. G. Beaty and M. P. Stainton. 1997. Climate-induced changes in the dissolved organic carbon budgets of boreal lakes. Biogeochem. **36:** 9-28.

Serkiz, S. M. and E. M. Perdue. 1990. Isolation of dissolved organic matter from the Suwannee River using reverse osmosis. Water Res. **24:** 911-916.

Shiff, S. L., R. Aravena, S. E. Trumbore, M. J. Hinton, R. Elgood and P. J. Dillon. 1997. Export of DOC from forested catchments on the precambian shield of central Ontario: clues from ^{13}C and ^{14}C. Biogeochem. **36:** 43-65.

Simoneit, B. R. T. 2005. A review of current applications of mass spectrometry for biomarker/molecular tracer elucidations. Mass Spectrom. Rev. **24:** 719-765.

Sobek, S., G. Algesten, A.-K. Bergström, M. Jansson and L. J. Tranvik. 2003. The catchment and climate regulation of pCO_2 in boreal lakes. Global Change Biol. **9:** 630-641.

Soumis, N., E. Duchemin, R. Canuel and M. Lucotte. 2004. Greenhouse gas emissions from reservoirs of the western United States. Global Biogeochem. Cycles **18:** doi:10.1029/2003GB002197.

———, M. Lucotte, C. Larose, F. Veillette and R. Canuel. 2007. Photomineralization in a boreal hydroelectric reservoir : a comparison with natural aquatic ecosystems. Biogeochem. **86:** 123-135.

———, R. Canuel and M. Lucotte. 2008. Evaluation of two current approaches for the measurement of carbon dioxide diffusive fluxes from lentic ecosystems. Environ. Sci. Technol. **42:** 2964-2969.

Steinmann, P., B. Eilrich, M. Leuenberger and S. J. Burns. 2008. Stable carbon isotope composition and concentrations of CO_2 and CH_4 in the deep catotelm of a peat bog. Geochim. Cosmochim. Acta. **72:** 6015-6026.

Stepanauskas, R., H. Laudon, and N. O. G. Jørgensen. 2000. High DON bioavailability in boreal streams during a spring flood. Limnol. Oceanogr. **45:** 1298-1307.

Striegl, R. G., and C. M. Michmerhuizen. 1998. Hydrologic influence on methane and carbon dioxide dynamics at two north-central Minnesota lakes. Limnol. Oceanogr. **43:** 1519-1529.

St-Louis, V. L., C. A. Kelly, E. Duchemin, J. W. M. Rudd and D. M. Rosenberg. 2000. Reservoir surfaces as sources of greenhouse gases to the atmosphere: a global estimate. Bioscience **50:** 766-775.

Sun, L., E. M. Perdue and J. F. McCarthy. 1995. Using reverse osmosis to obtain organic matter from surface and ground waters. Water Res. **29:** 1471-1477.

Tadonléké, R. D., D. Planas and S. Paquet. 2005. Bacterial activity in the water column and its impact on the CO_2 efflux. *In* A. Tremblay, L. Varfalvy, C. Rohem and M. Garneau [eds.], Greenhouse gas emissions – Fluxes and processes. Springer - Verlag, New York.

Thérien, N. and K. Morrison. 2005. Production of GHG from the decomposition of in vitro inundated phytomass and soil. *In* A. Tremblay, L. Varfalvy, C. Rohem and M. Garneau [eds.], Greenhouse gas emissions – Fluxes and processes. Springer - Verlag, New York.

Tremblay, A., J. Therrien, B. Hamlin, E. Wichmann and L. J. LeDrew. 2005. GHG emissions from boreal reservoirs and natural aquatic ecosystems, p. 209-232. *In* A. Tremblay, L. Varfalvy, C. Rohem and M. Garneau [eds.], Greenhouse gas emissions – Fluxes and processes. Springer -Verlag, New York.

Tremblay, L. and R. Benner. 2006. Microbial contributions to N-immobilization and organic matter preservation in decaying plant detritus. Geochim. Cosmochim. Acta **70**: 133-146.

_____ and _____. 2009. Organic matter diagenesis and bacterial contributions to detrital carbon and nitrogen in the Amazon River system. Limnol. Oceanogr. **54:** 681-691.

Turkia, J., O. Sandman and P. Huttunen. 1998. Palaeolimnological evidence of forestry practices disturbing small lakes in Finland. Boreal Environ. Res. **3:** 45-61.

Vetter, T. A., E. M. Perdue, E. Ingall, J.-F. Koprivnjak and P. H. Pfromm. 2007. Combining reverse osmosis and electrodialysis for more complete recovery of dissolved organic matter from seawater. Sep. Purif. Technol. **56:** 383-387.

Vogt, R. D., J. Akkanen, D. O. Andersen, R. Brüggemann, B. Chatterjee, E. Gjessing, J. V. K. Kukkonen, H.E. Larsen, J. Luster, A. Paul, S. Pflugmacher, M. Starr, C. E. W. Steinberg, P. Schmitt-Kopplin and A. Zsolnay. 2004. Key site variables governing the functional characteristics of Dissolved Natural Organic Matter (DNOM) in Nordic forested catchments. Aquat. Sci. **66:** 195-210.

Volkman, J. K., A. T. Revill, P. I. Bonham, and L. A. Clementson. 2007. Sources of organic matter in sediments from the Ord River in tropical northern Australia. Org. Geochem. **38:** 1039-1060.

von Wachenfeldt, E. and L. J. Tranvik. 2008. Sedimentation in boreal lakes-The role of flocculation of allochthonous dissolved organic matter in the water column. Ecosystems **11:** 803-814.

Wakeham S. G. 1999. Monocarboxylic, dicarboxylic and hydroxy acids released by sequential treatments of suspended particles and sediments of the Black Sea. Org.Geochem. **30:** 1059-1074.

Wetzel, R. G. 2001. Limnology: lakes and river ecosystems. 3rd ed. Harcourt.

Winkler, G., V. Leclerc, P. Sirois, P. Archambault and P. Bérubé. 2009. Short-term impact of forest harvesting on water quality and zooplankton communities in oligotrophic headwater lakes of the eastern Canadian Boreal Shield. Boreal Environ. Res. **14:** 323-337.

Zimmerman, A. R. and E. A. Canuel. 2001. Bulk organic matter and lipid biomarker composition of Chesapeake bay surficial sediments as indicators of environmental processes. Estuar. Coast. Shelf S. **53:** 319-341.

Appendix A. Supplementary information to Chapter 1

Dissolved greenhouse gases concentrations and atmospheric fluxes calculations.

The GHG concentrations and fluxes calculations are fully described in Soumis et al. (2008). For information regarding the instrumental analysis, see the methods section in Chapter 3.

An example of carbon dioxide atmospheric fluxes calculation:

In this project, the boundary layer equation was used. It assumes the air-water interface behaves as a thin two-layer film. Each gaseous and aquatic phase is assumed to be well mixed so that the resistance to CO_2 flux from one phase to another is only the molecular diffusion. Therefore, Fick's law applies:

$$fCO_2 = kCO_2 \times ([CO_2]_{surf} - (pCO_{2atm} \times K_H)) \quad (1)$$

where fCO_2 is the atmospheric CO_2 flux which depends on the water surface CO_2 concentration ($[CO_2]_{surf}$) and the water CO_2 concentration at equilibrium with the atmosphere ($pCO_{2atm} \times K_H$). pCO_{2atm} is the atmospheric CO_2 partial pressure and K_H is Henry's law constant corrected for the water temperature. kCO_2 is the gas exchange coefficient and corresponds to the rate of the gas exchange through the air-water interface:

$$kCO_2 = k_{600} \times (600 / Sc_{CO2})^{0.67} \quad (2)$$

The gas exchange coefficient is normalized to the Schmidt number (Sc) of 600 (k_{600}):

$$Sc_{CO2} = 1911.1 - (118.11 T_{W°}) + (3.4527 T_{W°}^2) - (0.04132 T_{W°}^3) \quad (3)$$

$$k_{600} = 2.07 + (0.215 \times U_{10}^{1.7}) \quad (4)$$

Where $T_{W°}$ is the water temperature and U_{10} is the wind speed 10 meters above the water surface. The wind speed 1 meter above the water surface (U_1) was use in this study:

$$U_{10} = U_1 \times (Z_{10} / Z_1)^m \quad (5)$$

Where Z_1 and Z_{10} are the distances to the water surface in meters and m corresponds to the vertical extrapolation factor for wind speed, which depends on the terrain relief. In this case a value of 0.167 (1/6) was used.

Appendix B. Supplementary information to Chapter 5: Fatty acids and alkanes lipid biomarker data

Table B-1. Relative contribution (in mole percentages of total FA) of the branched (br), unsaturated and straight chain fatty acids to the total DOM fraction

Compound (mol%)	L. Mary	L. Jean	L. Clair	L. Bouleau	R. Cab. 6	R. Cab. 10	R. Dec. 1	R. Dec. 2
C8:0		3.14	17.46	8.15	5.49	6.44	7.11	21.78
C10:0	0.60	5.68	2.16	1.42	0.83	1.07	1.93	1.52
C11:1	0.76	0.80	1.88	1.06	1.05	1.07	1.82	2.05
C11:0	0.53	2.35	2.24	0.81	1.19	1.35	1.94	1.22
9-oxo-C9:0	0.19		1.25		0.60		0.53	0.58
C12:0	7.29	26.21	13.25	3.42	8.86	7.18	7.94	4.41
brC13:0	0.57	0.59	1.97	2.11	1.82	0.28	2.23	1.89
C13:1	0.61	0.54			0.56		0.45	0.66
C13:0	2.16	1.32	1.24	1.59	1.04	1.00	1.33	1.36
brC14:0	0.74	0.75	3.23	1.65	0.35	0.41	0.52	1.42
C14:1	0.45	0.00	2.08		0.09	0.18	0.54	0.96
C14:0	19.27	15.63	5.16	12.89	10.16	8.88	15.22	7.08
brC15:0	4.59	3.60	4.66	1.66	4.55	9.41	4.43	12.73
C15:1							0.31	0.23
C15:0	3.01	1.80	3.42	2.05	1.76	2.14	1.73	1.78
brC16	1.29	1.01	7.26	2.12	3.34	4.96	4.23	4.37
C16:1ω9c	0.85	1.29	2.41	0.13	1.11			1.86
C16:1ω7c	14.57	2.03	3.65	17.75	3.40	16.04	6.31	1.74
C16:1ω7t	0.33	0.22	1.53	0.08	0.93		1.14	0.36
C16:1ω?	0.10	0.05	4.56	0.00	1.71		4.24	1.67
C16:0	25.23	15.04	6.16	19.46	22.02	19.40	16.37	12.30
brC17:0	1.43	0.52	4.07		1.10	1.67	0.72	2.67
C17:1	0.16	0.14			0.27	0.68	0.00	0.39
C17:0	0.56	0.42	0.20	0.55	0.57	0.09	0.76	0.68
brC18:0	0.98	0.68		1.34	0.49	0.81	1.28	1.46
C18:2ω6,9	1.00	1.44	1.96	2.12	1.45	2.06	1.61	0.91
C18:1ω9c	1.86	1.67	2.68	1.11	1.16	2.12	1.45	0.55
C18:1ω7c C18:1ω9t	5.79	2.64	3.97	15.08	18.37	10.03	6.57	8.00
C18:1ω7t	0.32	0.07	0.07	0.06		0.13	0.08	0.11
C18:0	4.55	9.66	1.49	3.38	5.63	2.49	7.17	3.22
C20:X[a]	0.20	0.65						
C20:0	0.18	0.05			0.10	0.11	0.06	0.03
Sum (μmol FA mol OC^{-1})	39.6	37.5	18.6	10.0	19.7	18.0	11.5	10.7
Phospholipid derived (%)	48.0	96.7	98.6	97.9	94.3	96.0	97.2	97.1

[a] X corresponds to the sum of single and doubly unsaturated FA

Table B-2. Relative contribution (in mole percentages of total FA) of branched (br), unsaturated and straight chain fatty acids in the total FPOM fraction

Compound (mol%)	L. Mary	L. Jean	L. Clair	L. Bouleau	R. Cab. 6	R. Cab. 10	R. Dec. 1
C10:0		0.02	0.67	0.93	1.68	0.43	
C11:1			0.31	0.41	0.33	0.35	0.06
C11:0			0.68	1.10	0.69	0.89	0.37
9-oxo-C9:0			0.78	0.59		0.32	0.46
C12:0		1.76	2.34	4.17	3.19	2.84	2.14
brC13:0	2.65	0.50	0.43	0.46	0.53	0.40	0.30
C13:1			0.05	0.14		0.06	
C13:0	2.28	0.94	0.69	1.06	0.80	1.00	0.85
brC14:0		1.43	2.38	1.60	2.93	2.21	1.06
C14:1		0.17	2.02		1.70	1.58	0.31
C14:0	10.97	29.68	22.17	12.88	28.00	28.23	24.64
brC15:0	6.61	6.67	7.54	6.16	5.68	6.52	3.87
C15:1			0.22				
C15:0	3.19	3.31	1.54	2.07	1.57	1.44	1.52
brC16	6.43	1.42	1.21	1.09	1.17	1.50	1.21
C16:1ω9c		1.88	2.26	2.86	1.12	1.39	0.99
C16:1ω7c	7.00	7.34	12.20	9.89	12.70	14.63	21.10
C16:1ω7t	1.93	1.12	0.74	1.48	1.29	3.41	1.01
C16:1ω?			4.42	3.00	3.08	0.35	1.52
C16:0	5.18	28.36	21.35	31.10	21.98	19.37	26.07
brC17:0		1.98	1.56	1.58	1.66	1.68	1.33
C17:1		0.54	0.43	0.45	0.45	0.36	0.21
C17:0	2.18	0.73	0.53	0.55	0.42	0.34	0.37
brC18:0	12.17	0.76	1.63	1.73	0.86	1.19	1.20
C18:2ω6,9	2.74	0.59	0.68	1.06	0.48	0.80	0.66
C18:1ω9c	8.98	4.02	4.72	8.26	2.87	3.28	4.41
C18:1ω7c	15.01	2.59	3.88	2.47	2.65	3.13	2.13
C18:1ω7t	5.31	1.35		0.15	0.09		
C18:0		0.83	1.36	1.19	1.08	1.15	1.36
C20:X[a]	5.03	1.22	0.35	0.52	0.35	0.48	0.29
C20:0	2.35	0.54	0.28	0.27	0.26	0.29	0.20
C21:0				0.14	0.09	0.07	0.04
C22:0		0.24	0.48	0.49	0.22	0.21	0.24
C24:0			0.11	0.13	0.06	0.09	0.06
C26:0					0.03		
Sum (μmol FA mol OC^{-1})	8.2	61.1	146.3	203.7	290.6	374.1	278.6
Phospholipid derived (%)	67.2	82.6	88.6	89.1	87.2	91.4	82.6

[a] X corresponds to the sum of single and doubly unsaturated FA

Table B-3. Relative contribution of the branched (br), unsaturated and straight chain fatty acids to the total SEOM fraction

Compound (mol%)	L. Mary	L. Jean	L. Clair	L. Bouleau	R. Cab. 6	R. Cab. 10	R. Dec. 1	R. Dec. 2
C8:0		3.05	0.19	1.14	0.15	2.04	1.51	
C10:0	1.59	2.11	5.81	5.38	0.75	1.03	0.90	0.41
C11:1	0.87	0.58	0.41	0.54	0.15	0.70	0.63	0.44
C11:0	2.88	1.34	5.37	2.81	1.47	1.08	0.98	0.78
9-oxo-C9:0	0.73	0.47	0.23	0.59	0.15	0.94	1.20	1.11
C12:0	9.31	6.18	19.23	11.51	6.99	5.58	4.93	7.69
brC13:0	1.48	0.99	2.51	1.29	1.28	1.10	1.16	1.11
C13:1	0.32	0.61	4.06	0.26		0.63	0.21	0.74
C13:0	2.81	0.91	1.05	2.22	1.63	0.99	0.68	0.89
brC14:0	4.58	1.38	2.57	2.49	2.20	1.49	1.61	1.44
C14:1	0.25	0.14	0.04	0.24	2.89	0.04		0.21
C14:0	12.59	12.20	8.46	17.63	7.14	9.12	7.65	10.00
brC15:0	9.29	7.66	7.72	7.24	11.79	10.87	10.85	10.20
C15:1	0.60	2.58	0.29	0.24	0.35	0.62	0.54	1.08
C15:0	2.91	2.78	2.94	2.64	2.96	2.38	2.40	2.42
brC16	2.03	1.96	4.59	3.12	5.62	2.70	1.94	2.54
C16:1ω9c	1.11	0.36	0.30	0.25	0.31	1.15	0.61	0.74
C16:1ω7c C16:1ω9t	9.28	8.41	1.41	3.81	1.47	6.17	9.25	8.33
C16:1ω7t	2.83	0.91	0.34	0.93	0.11	0.94	1.77	1.30
C16:1ω?	2.78	0.69	0.38	0.68	0.15	1.57	2.74	1.88
C16:0	14.74	22.27	14.22	15.78	18.83	15.43	18.81	23.20
brC17:0	2.94	3.11	4.25	2.70	6.36	4.93	4.28	3.59
C17:1	0.66	0.33	0.39	0.25	1.07	0.53	0.55	0.49
C17:0	1.29	1.41	2.06	0.74	1.40	0.87	0.73	0.88
brC18:0	0.97	1.49	1.72	1.54	2.66	0.73	0.85	1.17
C18:2ω6,9	0.34	0.54	0.16	0.38	0.48	6.36	0.94	1.25
C18:1ω9c	2.13	2.20	0.48	1.38	0.86	3.93	3.22	3.41
C18:1ω7c C18:1ω9t	1.71	1.47	1.38	2.09	2.16	3.33	3.02	2.48
C18:1ω7t			0.23		0.41			
C18:0	1.80	2.74	1.45	1.45	4.06	2.45	2.82	2.64
C19:0		0.12	0.27	0.07	1.42		0.73	
C20:X	0.12	0.20	0.61	0.21	1.31	0.39	1.31	0.63
C20:0	0.15	0.34	0.55	0.43	1.14	0.35	1.15	0.36
C21:0	0.15	0.85	0.24	1.33	0.59	0.38	0.25	0.26
C22:X	0.02	0.06		0.06		0.14	1.55	0.27
C22:0	0.92	1.71	0.99	1.30	2.21	1.98	3.01	2.00
C23:0	0.12	0.25	0.20	0.17	0.64	0.46	0.46	0.29
C24:1	0.04	0.14	0.93	0.02		0.06		
C24:0	0.79	1.65	0.06	1.28	2.31	2.35	2.48	1.45
C25:0	0.17	0.24	0.15	0.18	0.50	0.57	0.37	0.26
C26:0	1.17	1.29	0.71	1.15	1.72	1.63	0.86	0.80
C27:0	0.19	0.29	0.11	0.19	0.28	0.28	0.13	0.16
C28:0	0.93	1.23	0.57	1.39	1.18	1.05	0.60	0.70
C29:0	0.11	0.18	0.08	0.15	0.22	0.20	0.11	0.12

C30:0	0.30	0.60	0.28	0.75	0.62	0.46	0.19	0.28
Sum (μmol FA mol OC^{-1})	167.6	117.3	392.3	218.4	139.0	127.8	132.8	165.0
Phospholipid derived (%)	74.3	86.6	46.8	83.2	79.8	81.2	85.2	65.3

X corresponds to the sum of single and doubly unsaturated FA

Table B-4. Compound-specific stable carbon isotope signatures for PLFA from the DOM and FPOM fractions

Compound	L. Mary	L. Jean	L. Clair	L. Bouleau	R. Cab. 6	R. Cab. 10	R. Dec. 1	R. Dec. 2
DOM								
C14:0	-23.8	-25.1	-21.5	-25.2	-24.4	-24.8	-25.8	-23.3
a-C15:0				-20.0	-17.1			-18.7
C15:0		-26.8		-27.2				
C16:1ω7c	-22.4	-22.3		-23.7	-20.9	-19.7	-27.0	-20.6
C16:0	-23.9	-25.3	-23.2	-24.3	-22.9	-24.1	-26.2	-23.1
C18:1ω9c	-17.7	-24.8		-20.4	-19.2	-19.2	-24.2	
C18:1ω7c	-26.8	-28.6		-26.8	-25.2	-24.5	-26.4	-26.8
C18:0	-25.7	-26.1		-25.7	-24.0	-24.7	-25.9	-24.9
LE	-27.9	-26.7	-28.8	-28.7	-28.7	-28.6	-28.6	-28.7
TOC	-26.3	-26.8	-27.1	-27.5	-27.1	-26.9	-27.2	-27.0
FPOM								
C14:0	-23.0	-28.4	-31.8	-36.0	-35.0	-33.7	-40.1	
i-C15:0			-23.8	-26.5	-24.6	-25.1	-26.1	
a-C15:0			-23.8	-19.3	-16.4			
C15:0			-27.1	-34.4	-27.6	-31.0	-29.8	
C16:1ω9c			-30.9	-35.9	-31.5	-31.0	-38.4	
C16:1ω7c			-32.8	-35.5	-37.6	-34.6	-43.4	
C16:0	-23.2	-26.2	-33.3	-42.0	-34.3	-33.0	-38.8	
C18:2ω6,9					-28.9	-23.2	-31.3	
C18:1ω9c	-24.3	-23.1	-27.3	-37.5	-30.1	-27.1	-32.9	
C18:1ω7c		-29.1	-34.7	-32.4	-35.8	-35.8	-39.8	
C18:0	-25.4	-28.1	-31.1	-33.4	-29.5	-28.5	-28.0	
LE	-29.9	-31.8	-30.6	-33.1	-31.6	-31.1	-32.2	
TOC	-27.7	-28.6	-28.6	-30.4	-29.4	-29.0	-28.3	

LE and TOC correspond to the total lipid extract and the total organic carbon isotopic signatures, respectively
i- and a- are the iso and anteiso branched FA
* A very high baseline (higher amounts unresolved complex mixture) at the end of the L. Clair sample GC-IRMS run have produced unreliable isotopic ratios which were not included in the trends discussed in the text.

Table B-5. Compound-specific stable carbon isotope signatures for PLFA from the SEOM fractions

Compound	L. Mary	L. Jean	L. Clair	L. Bouleau	R. Cab. 6	R. Cab. 10	R. Dec. 1	R. Dec. 2
C10:0	-30.1	-26.0	-30.8	-30.4		-29.7	-28.4	
C11:1		-23.0		-24.0	-26.7	-24.7	-24.6	
C11:0	-31.6	-30.0	-33.9	-31.9	-34.7	-33.9		
C12:0	-30.9	-28.4	-32.9	-33.4	-28.7	-29.2	-28.0	-28.8
i-C13:0	-34.4		-31.8	-33.9		-27.9	-28.4	
a-C13:0	-24.8			-26.3		-17.0	-32.0	
C13:1	-41.2			-39.2		-34.2	-29.7	-30.6
C13:0	-33.0	-28.6	-29.1	-35.5	-26.4	-33.2	-32.0	-32.1
i-C14:0	-32.0	-29.2	-31.3	-32.3	-30.3	-31.9	-29.3	-33.6
C14:0	-35.2	-36.6	-37.9	-47.4	-33.8	-33.4	-34.7	-34.0
brC15:0	-35.6	-31.9			-31.7			
i-C15:0	-35.5	-30.3	-31.8	-32.9	-29.9	-28.3	-29.0	-30.7
a-C15:0	-34.3	-32.2	-32.9	-32.2	-30.4	-27.2	-28.1	-30.6
C15:1	-46.2	-11.7	-46.4			-45.3	-76.1	-42.4
C15:0	-35.6	-33.9	-37.9	-36.3	-29.7	-30.5	-30.0	-30.6
i-C16:0	-34.6	-19.5	-41.8	-32.7	-36.0	-31.9	-26.5	-33.2
C16:1ω9c	-49.9	-38.9		-47.3		-36.5	-45.1	-43.4
C16:1ω7c	-66.7	-48.4		-59.7		-42.5	-54.8	-55.3
C16:1ω7t	-72.7							
C16:0	-35.9	-35.8	-38.7	-40.6	-31.7	-31.5	-32.1	-32.6
brC17:0	-38.3	-32.5	-32.3	-35.3	-29.1	-28.8	-29.6	-30.9
i-C17:0	-46.2	-26.8	-29.7	-35.7	-28.4	-34.6	-38.3	-32.9
a-C17:0	-31.9	-45.3	-30.4	-31.6	-28.2	-27.1	-22.9	-28.3
C17:1	-36.4	-29.6	-36.6		-34.3	-29.0	-26.6	-31.6
C17:0	-30.1	-35.0	-34.5	-31.3	-23.6	-30.1	-23.5	-36.0
C18:2ω6,9	-22.3	-32.1				-24.4	-20.5	-24.0
C18:1ω9c	-32.3	-32.9	-25.8	-34.0	-24.7	-30.0	-27.0	-28.7
C18:1ω7c	-46.0	-42.0	-51.2	-46.2	-43.2	-39.8	-37.7	-37.4
C18:0	-29.4	-29.3	-31.6	-30.5	-28.6	-29.7	-26.9	-23.4
C19:0		-19.9			-27.9	-33.6		-24.7
C20:0	-31.1	-24.7	-31.9	-28.5	-26.4	-37.4		-32.3
C21:0		-20.0		-25.7		-25.7		-25.8
C22:0	-33.7	-32.7	-29.8	-30.3	-30.4	-32.3	-29.9	-31.6
C24:0	-29.3	-29.2	-30.1	-29.9	-30.4	-23.3	-27.7	-29.7
C25:0	-32.2	-22.0	-29.2	-35.1	-30.7	-27.3	-25.2	
C26:0	-29.4	-30.1	-31.8	-32.7	-31.6	-27.9	-32.3	-31.4
C27:0	-29.7	-26.9	-31.4	-32.8	-30.8	-30.3		
C28:0	-27.5	-29.3	-31.9	-30.5	-32.3	-31.5	-31.7	-31.1
C29:0			-32.8	-30.7	-29.4	-33.2		
C30:0	-28.2	-31.1	-30.0	-31.6	-30.5	-31.3	-31.8	-33.1
LE	-33.2	-31.6	-33.5	-32.9	-31.7	-31.2	-30.5	-31.5
TOC	-28.1	-25.4	-29.2	-29.1	-27.6	-28.2	-28.0	-27.5

LE and TOC correspond to the total lipid extract and the total organic carbon isotopic signatures, respectively. i- and a- are the iso and anteiso branched FA

Table B-6. Relative contributions (in mole percentages of total alkanes) of branched (br) and straight chain (n) alkanes to the FPOM fraction

Compound mol%	L. Mary	L. Jean	L. Clair	L. Bouleau	R. Cab. 6	R. Cab. 10	R. Dec. 1
nC12:0							3.55
nC13	0.93	0.84	0.54	3.49	0.64	2.07	1.51
nC14	0.29	0.29	0.48	0.62		0.37	0.35
2brC16:0	4.21	12.18	18.47	4.12	3.99	6.78	6.29
brC15:0		0.11			0.10		
nC15:0	2.32	2.38		1.38		1.81	
nC16:0	11.46	20.49	32.44	5.57	27.00	30.67	37.48
brC18:0	9.40	1.65	4.04	10.98	12.23	9.61	5.93
nC17:0	44.62	31.57	9.49	10.70	15.48	11.73	5.44
Pristane	0.32						
nC18:0	0.63	0.47	0.67	2.10	0.48	0.46	0.71
Phytan	0.38	0.28			0.48	0.32	0.44
nC19:0	0.80			2.12	0.97		
nC20:0			0.85	2.78			
nC21:0	0.73	3.05	3.85	7.85	2.85	1.78	3.79
nC22:0	0.43	0.82	0.94	2.37	1.42	1.47	1.84
nC23:0	1.64	3.08	2.18	4.91	3.44	2.70	3.70
nC24:0					4.75		
nC25:0	1.32	2.54	2.89	4.45	3.78	2.11	3.31
nC26:0							0.88
nC27:0	2.02	2.67	2.69	5.34	3.42	1.51	2.86
nC29:0	7.46	7.65	7.95	13.93	6.36	8.84	8.39
nC31:0	1.35	2.09	1.44	2.31	1.98	1.94	1.34
nC32:0	0.60	0.53		0.78	1.46	0.73	0.47
nC33:0	0.73	0.64	1.25	1.81	1.60	1.33	1.16
nC34:0			1.13		1.24		
nC35:0		0.66	1.65	3.83	1.47	0.88	1.59
nC37:0	3.02	2.18	5.04	3.34	1.66	6.29	3.34
nC38:0	2.87	2.06	0.00	2.70	1.78	3.60	3.01
nC39:0	2.48	1.78	1.99	2.52	1.42	3.01	2.63
Sum (μmol Alk mol OC^{-1})	11.88	15.03	7.15	3.97	7.92	11.57	6.89

Table B-7. Relative contributions (in mole percentages of total alkanes) of branched (br) and straight chain (n) alkanes to the SEOM fraction

Compound mol%	L. Mary	L. Jean	L. Clair	L. Bouleau	R. Cab. 6	R. Cab. 10	R. Dec. 1	R. Dec. 2
nC12:0					0.66		0.78	
brC13:0	0.10		1.29	0.11	2.06	1.76	2.12	0.23
nC13	0.02	0.08	0.43	0.06	0.90	1.29	1.29	1.28
nC14	0.17	0.18	0.61	0.28	0.77	0.64	0.64	0.63
2brC16:0	0.37	0.53	3.66	0.43	4.81	7.21	12.31	2.39
brC15:0	0.09	0.15	0.68	0.06	0.94		2.14	0.25
nC15:0	0.17	0.35	0.59	0.32	1.22	0.99	2.35	0.49
nC16:0	0.10	0.38	0.33	0.23	0.49	0.51	0.72	0.20
brC18:0	7.76	3.39	10.06	14.46	17.98	22.59	15.07	19.32
nC17:0	2.15	1.46	1.87	1.79	1.61	1.70	1.49	1.17
Pristane (br)	0.03	0.12	0.28	0.11	0.36	0.87	0.38	0.23
nC18:0	0.36	0.68	0.63	0.58	0.58	0.62	0.57	0.66
Phytan (br)	0.70	0.65	0.23	0.66	0.27	0.21	0.18	0.40
nC19:0	1.39	1.73	1.57	1.66	1.46	1.70	1.69	1.68
nC20:0	1.30	11.00	2.51	1.37	1.48	1.89	1.80	1.87
nC21:0	6.21	5.45	6.18	3.96	4.58	5.08	3.82	4.59
nC22:0	2.33	2.74	3.08	1.65	2.04	2.43	1.45	1.69
nC23:0	9.08	8.53	8.45	7.77	7.34	7.20	10.80	8.32
nC24:0	3.36	4.74	2.30	2.04	2.48	2.31	2.20	2.24
nC25:0	13.40	11.00	8.97	9.75	8.40	6.97	6.74	11.70
nC26:0	3.90	4.98	2.46	2.56	2.50	1.98	2.03	2.29
nC27:0	17.71	15.76	13.84	16.16	9.47	7.74	9.05	14.85
nC28:0	2.32	3.07	1.98	1.96	2.04	1.91	1.89	1.67
nC29:0	12.54	10.45	12.59	16.33	8.10	6.87	5.12	7.68
nC30:0	1.21	1.81	1.03	1.07	1.23	1.07	1.65	0.88
nC31:0	4.91	5.73	5.77	7.45	6.20	5.27	3.53	5.23
nC32:0	1.79	0.92	0.69	0.94	0.00	0.86	1.95	1.72
nC33:0	2.50	2.47	3.30	3.01	5.98	4.71	3.04	3.04
nC34:0	2.69	1.17	2.49	1.72	1.58	1.58	2.00	2.09
nC35:0	1.29	0.37	1.75	1.51	2.31	2.01	1.19	1.18
nC38:0	0.06	0.10	0.03	0.03	0.03	0.02	0.01	0.04
nC39:0					0.03			
nC40:0			0.33		0.10			
Sum (μmol Alk mol OC^{-1})	23.21	16.58	10.94	13.82	18.52	12.79	13.23	12.69

Table B-8. Compound-specific stable carbon isotope signatures for alkanes from the FPOM and SEOM fractions

Compound	L. Mary	L. Jean	L. Clair	L. Bouleau	R. Cab. 6	R. Cab. 10	R. Dec. 1	R. Dec. 2
FPOM								
nC17:0	-38.9	-38.4	-36.5	-40.3	-36.0	-33.9	-34.9	
nC21:0		-38.5	-41.2	-35.5	-34.8		-37.4	
LE	-29.9	-31.8	-30.6	-33.1	-31.6	-31.1	-32.2	
TOC	-27.7	-28.6	-28.6	-30.4	-29.4	-29.0	-28.3	
SEOM								
nC17:0	-27.8	-27.4	-31.1	-32.7	-27.9	-26.8	-28.1	-28.2
nC19:0	-35.2	-31.3	-33.4	-35.0	-30.3	-28.3		-30.7
nC20:0	-35.6	-32.3	-33.3	-31.1	-31.0	-31.6		-30.3
nC21:0	-38.3	-32.3	-35.0	-31.4	-32.5	-33.5	-34.4	-31.6
nC22:0	-31.9	-27.2	-31.8	-28.8	-31.5	-30.1		-30.7
nC23:0	-31.5	-31.3	-34.9	-31.1	-35.1	-33.4	-34.4	-34.1
nC24:0	-31.9	-27.3	-31.8	-28.7	-31.3	-30.8		-29.5
nC25:0	-31.1	-31.6	-33.9	-32.6	-34.3	-33.7	-33.7	-32.4
nC26:0	-30.9	-28.4	-32.5	-29.5	-31.7	-30.7		-30.6
nC27:0	-30.3	-32.0	-32.3	-33.9	-32.6	-32.3	-32.5	-31.3
nC28:0	-29.0	-29.1	-32.3	-29.6	-30.8	-31.3	-32.4	-32.5
nC29:0	-30.2	-32.0	-32.4	-34.5	-32.9	-32.5	-33.0	-33.1
nC30:0	-28.9	-28.5	-32.4	-29.5	-31.1	-30.5		-31.2
nC31:0	-36.5	-30.9	-32.2	-32.9	-31.7	-31.3	-33.4	-33.1
nC32:0		-27.1	-33.5	-27.3	-34.9	-31.2		-29.1
nC33:0	-30.9	-31.8	-28.6	-27.8	-32.0	-30.4	-27.4	-28.0
nC34:0	-35.5		-35.3	-33.9	-35.6	-33.9		
nC35:0		-28.7	-30.1	-27.7	-28.4	-29.4	-29.4	
LE	-33.2	-31.6	-33.5	-32.9	-31.7	-31.2	-30.5	-31.5
TOC	-28.1	-25.4	-29.2	-29.1	-27.6	-28.2	-28.0	-27.5

LE and TOC correspond to the total lipid extract and the total organic carbon isotopic signatures, respectively.

Appendix C. Cover page of the published chapter 2

Environ. Sci. Technol. 2008, 42, 2490–2495

Elemental, Isotopic, and Spectroscopic Assessment of Chemical Fractionation of Dissolved Organic Matter Sampled with a Portable Reverse Osmosis System

ALEXANDRE OUELLET,[†] DRAGOSH CATANA,[†] JEAN-BAPTISTE PLOUHINEC,[‡] MARC LUCOTTE,[‡] AND YVES GÉLINAS*[,†]

GEOTOP and Department of Chemistry and Biochemistry, Concordia University, 7141 Sherbrooke Street West, Montréal, Québec, Canada, H4B 1R6 and GEOTOP, Université du Québec à Montréal, C.P. 8888, Succursale Centre-Ville, Montréal, Québec, Canada, H3C 3P8

Received October 4, 2007. Revised manuscript received December 26, 2007. Accepted January 8, 2008.

Portable reverse osmosis (RO) systems are increasingly being used for isolating dissolved organic matter (DOM) from freshwater aquatic systems because of their high volume processing capacity and high absolute DOM recoveries. However, obtaining complete recoveries implies the rinsing of the reverse osmosis system with a solution of dilute NaOH and combining the rinse solution and the DOM concentrate. Because of the potential chemical alterations that can affect the integrity of the organic pool leached from the RO system at high pHs, this approach is not compatible with studies based on the molecular-level analysis of DOM. The potential for elemental, isotopic, and chemical fractionation was thus evaluated on a series of freshwater DOM samples concentrated in the field with a portable RO system when the concentrate and the rinse solution are not combined. DOC recoveries in the concentrate varied between 81.6 and 88.8%, and total balance calculations showed total recoveries of dissolved and particulate organic carbon ranging between 96.4 and 106.9%. Despite similar $\delta^{13}C$ signatures, differences in N content and FTIR-based chemical composition between the concentrate and the rinse DOM solutions suggest some degree of chemical fractionation.

Introduction

Dissolved organic matter (DOM) is one of the largest and most dynamic pools of organic carbon on Earth (*1*). The number of studies on the bulk characteristics, chemical composition, and biogeochemical cycling of DOM has grown exponentially in the past decade. With the recent advances in the development of sophisticated analytical instrumentation to probe the molecular composition of the complex mixtures of organic macromolecules found in DOM (e.g., electrospray ionization mass spectrometry (*2*), ion cyclotron resonance mass spectrometry (*3*), liquid chromatography coupled to mass spectrometry (*4*), two-dimentional gas chromatography (*5*), multidimensional nuclear magnetic resonance (*6*), and others), an increasing emphasis is now being put on the collection of salt-free, chemically unaltered, and representative DOM samples. Different methods have been developed for this purpose, including resin adsorption chromatography (using synthetic polymeric resins such as polymethylmethacrylate or polyvinylpyrrolidone), tangential ultrafiltration (*7*), and more recently, solid-phase extraction disk (*8*) and reverse osmosis coupled to electrodialysis (*9, 10*). Although these methodologies have been applied with varying success in numerous studies, they are either tedious to use, unsuitable for extracting large quantities of DOM, and/or lead to chemical fractionation owing to the incomplete recovery of DOM.

Reverse osmosis (RO) is the only method available to rapidly concentrate DOM from large volumes of water (hundreds of liters) with minimal DOM losses. The industrial use of reverse osmosis emerged in the early 1970s to produce large volumes of clean water at a reasonable cost. Reverse osmosis has been exploited to concentrate freshwater DOM since the early 1980s and has since been routinely used in a broad range of freshwater environments (*11–20*). In particular, Serkiz and Perdue (*12*) have developed and commercialized a portable RO system that can be used in the field for concentrating large volumes of surface and groundwater DOM samples. Total dissolved organic carbon (DOC) recoveries greater than 90% are routinely reported with this system (*12, 14, 16, 17, 20*), which make this approach the most attractive for the bulk and molecular characterization of freshwater DOM samples.

Depending on the study, these recoveries either correspond to the DOC recovered in the concentrate only or they are calculated by combining the mass of DOC in the concentrated sample with the mass of carbon recovered upon rinsing the RO membranes following the concentration step, divided by the total mass of DOC in the initial, nontreated sample. The rinsing step is necessary because a fraction of the DOC pool, typically 10–20% of initial DOC, sorbs onto the membranes of the RO system and is not recovered in the permeate (water passing through the RO membranes) nor in the concentrate (volume of water containing the compounds rejected by the membrane). To completely recover this sorbed DOC fraction and to eliminate problems associated with cross contamination of samples from carry-over effects, the RO system is usually leached with a dilute NaOH leaching solution (10^{-2}–10^{-4} M), which is then neutralized and demineralized using a H^+-saturated cation exchange resin (*9*). Although such harsh chemical treatment might not significantly alter the bulk reactivity (*16, 17*) and trace metal complexation properties (*19*) of the concentrated DOM pool, it might not be suitable when probing DOM dynamics through the analysis of specific molecular biomarkers. Such molecular-level studies hinge on the preservation of the chemical integrity of a sample, as the slightest chemical alteration can result in the loss of a target molecule from the analytical window. It is, thus, important to evaluate the percentage of bulk DOM that remains sorbed onto the membranes of the RO system and to know whether the composition of the sorbed DOM fraction differs from that of bulk DOM. Knowing whether the incomplete recovery of DOM leads to significant chemical fractionation upon sampling would also be useful in studies where only the DOM concentrate is used (see for instance refs (*15*) and (*18*)). Despite the fact that RO systems have been exploited for more than 15 years to collect and concentrate DOM from

* Corresponding author phone: 514-848-2424, extension 3337; fax: 514-848-2868; e-mail: ygelinas@alcor.concordia.ca.
† Concordia University.
‡ Université du Québec à Montréal.

10.1021/es702523w CCC: $40.75
Published on Web 02/20/2008